해양 방선균 *Streptomyces bacillaris* MBTC38 유래 대사물질의 항균활성 및 작용기전 연구

Studies on Antimicrobial Activity and Mode of Action of Metabolites from Marine-derived *Streptomyces bacillaris* MBTC38

2021 년 8 월

서울대학교 대학원

농생명공학부 응용생명화학전공

정 범 구

A Dissertation for the Degree of Doctor of Philosophy

Studies on Antimicrobial Activity and Mode of Action of Metabolites from Marine-derived *Streptomyces bacillaris* MBTC38

August 2021

Beomkoo Chung

Applied Life Chemistry Major

Department of Agricultural Biotechnology

Seoul National University

해양 방선균 *Streptomyces bacillaris* MBTC38 유래 대사물질의 항균활성 및 작용기전 연구

Studies on Antimicrobial Activity and Mode of Action of Metabolites from Marine-derived *Streptomyces bacillaris* MBTC38

지도교수 오 기 봉

이 논문을 농학박사학위논문으로 제출함
2021 년 6 월

서울대학교 대학원
농생명공학부 응용생명화학전공

정 범 구

정범구의 박사학위논문을 인준함
2021 년 7 월

위 원 장		이 상 기
부 위 원 장		오 기 봉
위 원		신 종 헌
위 원		이 희 승
위 원		권 용 훈

Studies on Antimicrobial Activity and Mode of Action of Metabolites from Marine-derived *Streptomyces bacillaris* MBTC38

Advisor: Ki-Bong Oh

A Dissertation Submitted in Partial Fulfillment
of the Requirement for the Degree of

DOCTOR OF PHILOSOPHY

to the Faculty of
Applied Life Chemistry Major,
Department of Agricultural Biotechnology

at

SEOUL NATIONAL UNIVERSITY

by

Beomkoo Chung

Date Approved

July 2021

Sangkee Rhee

Ki-Bong Oh

Jongheon Shin

Hyi-Seung Lee

Yonghoon Kwon

Abstract

Actinobacteria are attractive phylum to produce various secondary metabolites with promising biological activities. Especially, marine-derived actinobacteria have been expected to produce metabolites with novel structure and mechanisms due to their unique circumstances. The present thesis evaluates biological activities of natural products from marine *Streptomyces* and investigates action mechanism of those compounds.

The first part deals with estimation of antibacterial activities of four lactoquinomycins and identification of their mode of action. Lactoquinomycin A (LQM-A) (compound **1**) and its derivatives (**2**–**4**) showed potent antibacterial activities against Gram-positive bacteria. Especially, LQM-A exhibited the most significant inhibitory activity against methicillin-resistant *Staphylococcus aureus* (MRSA), with a low incidence of resistance. An in vivo dual-reporter assay designed to distinguish between compounds that inhibit translation and those that induce DNA damage was employed to assess the mode of action of LQM-A. Consequently, LQM-A-induced DNA damage via DNA intercalation, which was verified by reduced fluorescence based on the ethidium bromide displacement assay. Moreover, LQM-A dramatically reduced expression of *grlA* and *grlB* encoding topoisomerase IV in MRSA. These data suggest that LQM-A exhibited promising antibacterial activity based on the intercalation into double-stranded DNA and transcriptional inhibition of essential genes.

The second part of this research describes structure elucidation of alkaloid-type compounds and confirmation of significant inhibitory activity against isocitrate lyase (ICL). ICL, a key enzyme of glyoxylate cycle, plays an important

role in the infection and pathogenesis of microorganisms. Based on the spectroscopic data, two compounds were identified and named as bacillimide (**5**) and bacillapyrrole (**6**). Absolute configuration (3R, 6S, 7S) of novel compound, bacillimide was determined through NOESY and ECD measurements with benzoyl bacillimide. The bacillimide and bacillapyrrole exhibited significant (IC$_{50}$ = 44.24 μM) and moderate (IC$_{50}$ = 190.45 μM) ICL inhibitory activity, respectively. The kinetics assay showed bacillimide behaved as a mixed type inhibitor. The growth phenotype assay using *icl*-deletion mutant showed that bacillimide inhibited the growth of *Candida albicans* under C$_2$ carbon utilizing condition. Moreover, bacillimide resulted in dramatically reduced expression of *icl* gene encoding ICL.

Contents

Part I. Antibacterial Activity and Mode of Action of Lactoquinomycin A from *Streptomyces bacillaris* MBTC38

iv

Part II. Isocitrate Lyase Inhibitory Activity of Bacillimide and Bacillapyrrole from *Streptomyces bacillaris* MBTC38

List of Figures

List of Tables

List of Abbreviations

ATCC	American Type Culture Collection
CIP	Ciprofloxacin
CLSI	Clinical & Laboratory Standards Institutes
COSY	Correlation spectroscopy
DMAP	4-Dimethylaminopyridine
gDNA	Genomic DNA
HMBC	Heteronuclear multiple-bond correlation spectroscopy
HSQC	Heteronuclear single-quantum correlation spectroscopy
HRMS	High resolution mass spectrometry
MIC	Minimum inhibitory concentration
m/z	Mass-to-charge ratio
NCBI	National Center for Biotechnology Information
NMR	Nuclear magnetic resonance
NOESY	Nuclear overhauser effect spectroscopy
OD	Optical density
PCR	Polymerase chain reaction
TFA	Trifluoroacetic acid
TMS	Tetramethylsilane
t_R	Retention time
Tris	Tris(hydroxymethyl)aminomethane

Part I

Antibacterial Activity and Mode of Action of Lactoquinomycin A from *Streptomyces bacillaris* MBTC38

Introduction

Antibiotics and resistant microorganisms

Antibiotics which are either cytostatic or cytotoxic to the microorganisms allow human immune system to combat them (Zaman et al., 2017). They often inhibit synthesis of fundamental components such as deoxyribonucleic acid (DNA), ribonucleic acid (RNA), protein, cell wall for bacterial existence and act as breaking a membrane potential (Levy, 2004). Apodictically, antibiotics contributed health of mankind and advance of human civilization, which ushered in an antibiotic era (Levy, 1992). Numerous classes of antibiotics have been produced for last several decades on increased demand for them, while paradoxically excessive popularization of antibiotics caused the advent of resistant microorganisms (Aminov, 2010). Since sulfonamide-resistant *Streptoccoccus pyogenes* first emerged in the 1930s, resistant strains such as penicillin-resistant *Staphylococcus aureus* and streptomycin-resistant *Mycobacterium tuberculosis* have been rapidly soared (Barber and Rozwadowsk-Dowzenko, 1948; Crofton and Mitchison, 1948; Levy, 1982). What was worse, resistant strains against multiple drugs were reported in late 1950s to early 1960s (Watanabe, 1963). According to CDC (Centers for Disease Control and Prevention) reports, more than 2.8 million infectious diseases caused by antibiotic-resistant microorganisms occur and over 35,000 people die only in USA every year (Centers for Disease Control and Prevention, 2019). Furthermore, it is monitored that at least 70,000 worldwide deaths happen annually and 10 million people face death due to resistant infections in 2050, which becomes serious threats in various fields such as public health, food supply and medical service (O'Neill, 2016).

Methicillin-resistant *S. aureus* (MRSA) together with vancomycin-resistant *enterococci* (VRE) are known as representative drug-resistant bacteria. The

resistance of methicillin result from horizontal transfer of mobile genetic element named staphylococcal cassette chromosome *mec* (SCC*mec*) (Katayama et al., 2000; Turner et al., 2019). SCC*mec* consists of two fundamental components, *ccr* gene and *mec* gene complex, and other functional genes. Cassette chromosome recombinase (ccr) genes mediate the integration of SCC*mec* into chromosome and elimination of it from chromosome. The *mec* gene complex contains *mecA*, *mecR1* encoding the signal transducer and inducer protein MecR1 and *mecI* encoding the repressor protein MecI. The *mecA* encodes penicillin-binding protein 2a (PBP2a), a modified form of PBP which is involved in reactions of synthesizing cross-linked peptidoglycan in bacterial cell wall. β-lactam antibiotics bind PBP and inhibit formation of cell wall while PBP2a has a low affinity for them resulting in resistance against β-lactam drugs (Hartman and Tomasz, 1984). MRSA has been widely diffused since it was initially observed from hospital patients in the 1960s. Even decades later, MRSA remains one of the hazardous bacteria with high mortality because the symptoms of MRSA are various and fatal depending on infection site (Tenover et al., 2006; Van Hal et al., 2012). Although therapeutic methods were improved and effective drugs such as ceftaroline and ceftobiprole, derivatives of cephalosporin, were discovered due to ongoing effort for treatment against MRSA, continuous development and comprehension of antibiotics are definitely needed (Kisgen and Whitney, 2008; Arshad et al., 2017).

Natural products and actinobacteria

Natural products are chemical substances that originate from living organisms such as plants, animals and microorganisms. They have been focused as a variety of pharmacological activities and lead compounds in drug discovery fields (Shepard, 2007). Unfortunately, development of medicine based on natural sources declined as

3

the number of novel natural products was continuously decreased since 1970s and organic synthesis technology was advanced. However, natural products are still valuable chemical groups because their structural complexity and diversity provide useful scaffolds for pharmaceutical fields. To make up for the weak points of natural products, several researchers paid attention to understudied marine environments because previous studies about natural products were restricted in terrestrial circumstances (Fenical and Jensen, 2006).

The ocean environment covers 70% of the Earth's surface and has more diverse conditions than the terrestrial environment, such as low oxygen, lack of light and high pressure (Tyler, 2003; Tortorella et al., 2018). Under these conditions, biosynthesis of secondary metabolites typically involves mechanisms modified for physiological adaptation, which increases the probability that unusual natural products might be present (Bull et al., 2000; Wright et al., 2003). Rapid technological development allow researchers to collect marine organisms and their biological activities and structural uniqueness were monitored in earnest since late 1990s. In the last decade, numerous natural products have been discovered in the marine environment; notably, thousands of those compounds exhibit new structures, and three-fourths of them demonstrate diverse bioactivities (Blunt et al., 2018).

Actinobacteria are a phylum of Gram-positive bacteria with high contents of guanine and cytosine in chromosome. They have an importance due to their ability to produce bioactive secondary metabolites with unique structures. Since they were researched for discovering novel compounds in the early 1950s, a number of metabolites have been identified and applied to anticancer (daunorubicin, mitomycin), immunosuppressive (rapamycin) and antimicrobial (erythromycin, amphotericin B) drugs (Zotchev, 2012). Especially, most antibiotics were produced and utilized from metabolites of *Streptomyces*, major genus in actinomycetes. The

representative antibiotics such as tetracycline, streptomycin and vancomycin were discovered from *S. aureofaciens*, *S. griseus* and *S. orientalis*, respectively (Procopio et al., 2012) Recently, marine-derived *Streptomyces* species have been identified as major producers of novel antibiotics, such as branimycins B and C; ansalactams B, C, and D; desotamide B; and lobophorin H (Pan et al., 2013; Song et al., 2014; Le et al., 2016; Brana et al., 2017) Thus, marine-derived *Streptomyces* species could be attracted as outstanding sources of novel antimicrobial agents.

Polyketides and lactoquinomycin A

Polyketides are large family of secondary metabolites containing modified carbonyl groups or precursors with those. These natural products are attracted attention as anticancer, antimicrobial and antiparasitic drugs (Naught et al., 2006). Polyketides are bio-synthesized by stepwise condensation of acetyl-coenzyme A (CoA) or propionyl-CoA in plants, microorganisms and even some marine animals. They are generally classified into three groups, type I, II, and III depending on the involved enzyme type (Wang et al., 2020). Type I polyketide synthases (PKSs), multifunctional peptides, are separated into modular type I PKSs (mPKSs) playing a role similar to non-ribosomal peptide synthase in mainly bacteria and iterative type I PKSs (iPKSs) catalyzing multiple elongation in fungi. Type II PKSs consist of multi-enzyme complexes with mono-functional proteins and produce various aromatic polyketide mainly in bacteria. Type III PKSs, simple homodimers, are predominantly found in plants and feature exploiting CoA rather than acyl carrier protein for chain extension (Hertweck et al., 2007; Keatinge-Clay, 2012; Shimizu et al., 2017). Although type II PKSs and their representative substances, aromatic polyketides, remain obscurer than other type PKSs and compounds derived from them, they contribute our life with attractive therapeutical properties. Tetracylcine

(Tet) and anthracycline-type doxorubicin (Dox) are typical examples of pharmacological aromatic polyketides (Katz and Baltz, 2016; Fang et al., 2018). The mechanisms of them are completely different despite their structure similarity. Tet binds the 30S and 50S subunit of ribosome and inhibits protein synthesis by interfering attachment of aminoacyl-transfer ribonucleic acid (aminoacyl-tRNA) to the A-site on the ribosome (Wilson, 2014). Contrastively, Dox intercalates with DNA and inhibits macromolecular biosynthesis such as DNA replication and RNA transcription (Agudelo et al., 2016a). Both compounds are clinically recognized and especially Dox has been used as one of the most effective anticancer drugs (Agudelo et al., 2016b). Therefore, researches of aromatic polyketides are well worth enough for development of anticancer and antimicrobial agents.

Lactoquinomycin A (LQM-A), a member of pyranonaphthoquinone family synthesized via type II PKSs, was first reported from *Streptomyces tanashiensis* and showed significant anticancer and antibacterial activities (Takano et al., 1976; Okabe et al., 1985). The structure of LQM-A was revised that D-angolosamine is attached at C-8 of naphthoquinone ring based on the two-dimensional ROESY experiment (Williamso et al., 2002). The biosynthetic gene cluster of LQM-A (about 36 kb) was identified, 34 complete open reading frames (ORFs) with incomplete ORFs at both ends (Ichinose et al., 2003). While the derivatives of LQM-A have been continuously identified, mechanisms of those compounds are not clearly characterized. LQM-A was known to inhibit the serine/threonine kinase, AKT by binding T-loop cysteines in cancer cell whereas mode of action remains uncertain in bacteria (Toral-Barza, 2007).

During the search for bioactive secondary metabolites from marine-derived actinomycetes, four lactoquinomycins (**1**–**4**) were identified from *Streptomyces bacillaris* strain MBTC38, which was collected from marine sediment of Jeju Island,

Republic of Korea. It has been reported that *S. bacillaris* isolated from terrestrial and marine habitats produce structurally unique natural compounds with diverse biological activities (Hu and Macmilan, 2012; Wahaab and Subramaniam, 2018; Pagmadulam et al., 2020). *S. bacillaris* strain RAM25C4 was isolated from marine sediments for controlling MRSA and multidrug-resistant bacteria. In HPTLC (high-performance thin-layer chromatography) analysis, the presence of macrolides, terpenoids, and quinolones was identified in the ethyl acetate extract of RAM25C4 culture (Hu and Macmilan, 2012). In addition, *S. bacillaris* strain SNB-019 isolated from Galveston Bay, Texas produced bafilomycin analogs that were responsible for the autophagy inhibitory activity (Wahaab and Subramaniam, 2018). However, to the best of my knowledge, lactoquinomycins are the first to be reported from *S. bacillaris*. These lactoquinomycins showed significant activities and a low incidence of resistant strains among Gram-positive bacteria including MRSA. An in vivo dual-reporter assay indicated that LQM-A does not inhibit protein synthesis, but instead induces DNA damage, similar to Dox. Furthermore, LQM-A was found to intercalate DNA based on the ethidium bromide displacement assay. The intercalation effect of LQM-A changed the form of plasmid DNA from supercoiled to relaxed. Real-time quantitative PCR analysis exhibited that LQM-A dramatically reduced expression of essential genes; *grlA* and *grlB* encoding topoisomerase IV. Moreover, LQM-A showed a synergetic effect with ampicillin at a specific concentrations.

Material and Methods

General experimental procedures

^{1}H, ^{13}C, and 2D (COSY, HSQC, HMBC) nuclear magnetic resonance (NMR) spectra were measured in methanol-*d4* using Bruker Avance 600 MHz spectrometers (Bruker, Billerica, MA, USA) at the National Instrumentation Center for Environmental Management (NICEM) of Seoul National University. Liquid chromatography/mass spectrometry (LC/MS) data were obtained with an Agilent Technologies 6130 quadrupole mass spectrometer (Agilent Technologies, Santa Clara, CA, USA) coupled with an Agilent Technologies 1200 series high-performance liquid chromatography (HPLC) instrument. High-resolution fast atom bombardment (HR-FAB) mass spectra were recorded on a Jeol JMS-700 high-resolution mass spectrometer (Jeol, Tokyo, Japan) at the National Center for Inter-University Research Facilities (NCIRF) of Seoul National University. HPLC was performed using a Gilson 321 HPLC pump with a Gilson UV/VIS-151 detector (Gilson, Middleton, WI, USA). All solvents used were of spectroscopic grade or were distilled prior to use.

Taxonomic identification of the lactoquinomycin-producing microorganism

Marine sediment samples were collected from the shoreline of Jeju Island, Korea. The air-dried sediment (1 g) was mixed with 10 mL of sterilized artificial seawater and shaken at 150 rpm for 30 min at 25°C. The suspension was serially diluted with sterilized artificial seawater and 0.1 mL volumes of three appropriate dilutions were spread onto actinomycete isolation agar (HIMEDIA, Mumbai, India) plates supplemented with 100 µg/mL cycloheximide, 50 µg/mL nalidixic acid (Sigma-

Aldrich, St. Louis, MO, USA) and artificial seawater. Plates were incubated at 28℃ for 2 to 3 weeks. To obtain single strains, colonies were transferred several times on fresh agar plates by streaking.

The isolated bacterial strain MBTC38 was identified using standard molecular biologi- cal protocols, including DNA amplification and sequencing of the 16S rDNA region (Janda and Abbott, 2007). Briefly, genomic DNA was prepared from MBTC38 mycelium using the i-Genomic BYF DNA Extraction Mini Kit (Intron Biotechnology, Seoul, Korea) according to the manufacturer's protocol. Polymerase chain reaction (PCR) amplification using the primers 27F (5J-AGAGTTTGATCCTGGCTCAG-3J) and 1429R (5J-GGTTACCTTGTTACG ACTT-3J) was performed under the following conditions: pre-denaturation (95℃, 5 min); 30 cycles of denaturation (95℃, 15 s), annealing (52℃, 30 s), and extension (72℃, 1 min 30 s); and final extension (72℃, 5 min). The nucleotide sequence was deposited in GenBank under accession number MK402083.1 and aligned according to the nucleotide basic logic alignment search tool (BLAST, version 2.10) of the National Center for Biotechnology Information (NCBI).

Cultivation, extraction, and isolation of compounds

Streptomyces bacillaris strain MBTC38 was sporulated on colloidal chitin agar plates (4 g chitin, 0.7 g K_2HPO_4, 0.5 g $MgSO_4 \cdot 7H_2O$, 0.3 g KH_2PO_4, 0.01 g $FeSO_4 \cdot 7H_2O$, 0.001 g $MnCl_2 \cdot 4H_2O$, 0.001 g $ZnSO_4 \cdot 7H_2O$, 20 g agar and 17 g sea salt in 1 L distilled water) at 28℃ for 10 days. Mature spores were inoculated into 500 mL colloidal chitin liquid medium and incubated at 28 ◦C for 7 days on a rotatory shaker. The entire culture (60 L) was filtered through filter paper and extracted with an equal volume of ethyl acetate twice. The organic solvents were evaporated to dryness under reduced pressure to obtain 2.4 g of total extracts. Based on the results

of the antibacterial activity assay, the entire extract (2.4 g) was separated through reversed-phase HPLC (Agilent Eclipse XDB-C18, 5 µm, 9.4×250 mm) under gradient solvent conditions ranging from 20% aqueous methanol to 100% methanol with 0.1% trifluoroacetic acid (ultraviolet detection at 254 nm, flow rate: 2 mL/min). After separation of compounds 1-4, each compound was further purified through reversed-phase HPLC under isocratic conditions to obtain compounds **1** (tR: 23 min, 8.4 mg), **2** (tR: 21 min, 3.8 mg), **3** (tR: 24 min, 11.6 mg), and **4** (tR: 25 min, 5.1 mg).

Lactoquinomycin A (**1**): ^{1}H NMR (CDCl$_3$) δ_H 12.27 (1H, br s), 7.91 (1H, d, J = 7.8 Hz), 7.73 (1H, d, J = 7.8 Hz), 5.25 (1H, d, J = 2.9 Hz), 5.07 (1H, q, J = 7.0 Hz), 4.90 (1H, br d, J = 9.6 Hz), 4.69 (1H, dd, J = 4.9, 3.0 Hz), 3.63 (1H, m), 3.54 (1H, m), 3.43 (dd, J = 9.1, 9.1 Hz), 3.14 (dd, J = 17.8, 5.2 Hz), 2.97 (1H, dd, J = 17.6, 5.1 Hz) 2.9 (3H, br s), 2.76 (3H, br s), 2.69 (1H, d, J = 17.6 Hz), 2.54 (1H, m), 1.56 (3H, d, J = 6.9 Hz), 1.47 (3H, d, J = 6.1 Hz), 1.29, (1H, m); ^{13}C NMR (CDCl$_3$) δ_C 188.5 (C), 181.1 (C), 173.9 (C), 157.7 (C), 149.6 (C), 136.5 (C), 135.5 (C), 133.8 (CH), 130.5 (C), 119.9 (CH), 114.3 (C), 77.7 (CH), 71.1 (CH), 70.4 (CH), 68.5 (CH), 68.0 (CH), 66.4 (CH), 66.2 (CH), 40.1 (CH$_3$), 39.6 (CH$_3$), 36.9 (CH$_2$), 29.3 (CH$_2$), 18.6 (CH$_3$), 18.1 (CH$_3$); HRFABMS m/z 458.1811 [M + H]$^+$ (calcd for C$_{24}$H$_{28}$NO$_8$, 458.1811).

Lactoquinomycin B (**2**): ^{1}H NMR (MeOH-d_4) δ_H 7.97 (1H, d, J = 7.9 Hz), 7.68 (1H, d, J = 7.9 Hz), 5.48 (1H, d, J = 4.3 Hz), 5.01 (1H, q, J = 7.2 Hz), 4.71 (1H, m), 4.62 (1H, dd, J = 6.2, 4.2 Hz), 3.60 (1H, m), 3.45 (1H, m), 3.04 (1H, dd, J = 18.4, 6.2 Hz), 2.91 (3H, br s), 2.80 (3H, br s), 2.64 (1H, m), 2.52 (1H, ddd, J = 12.4, 3.8, 2.2 Hz), 2.43 (1H, d, J = 18.4 Hz), 1.67 (1H, m), 1.62 (3H, d, J = 6.8 Hz), 1.41 (3H, d, J = 6.1 Hz); ^{13}C NMR (MeOH-d_4) δ_C 195.2 (C), 187.3 (C), 175.8 (C), 157.6 (C), 136.6 (C), 133.3 (CH), 130.8 (C), 119.1 (C), 114.0 (C), 77.2 (CH), 71.0 (CH), 70.3 (CH), 69.8 (CH), 67.1 (CH), 65.0 (CH), 64.4 (C), 64.3 (CH), 60.5 (C), 40.7 (CH$_3$),

36.0 (CH$_2$), 34.9 (CH$_2$), 28.9 (CH$_2$), 16.8 (CH$_2$), 13.3 (CH$_2$); HRFABMS m/z 474.1761 [M + H]$^+$ (calcd for C$_{24}$H$_{27}$NO$_9$, 474.1759).

N-Methyl lactoquinomycin A (**3**): ^{1}H NMR (MeOH-*d*$_4$) δ_H 7.93 (1H, d, *J* = 7.8 Hz), 7.73 (1H, d, *J* = 7.8 Hz), 5.34 (1H, d, *J* = 3.0 Hz), 5.08 (1H, q, *J* = 6.8 Hz), 5.02 (1H, br d, *J* = 10.5 Hz), 4.79 (1H, dd, *J* = 5.1, 2.7 Hz), 3.57 (1H, dq, *J* = 9.1, 6.1 Hz), 3.40 (1H, m), 3.28 (1H, m), 3.14 (1H, dd, *J* = 17.8, 5.1 Hz), 2.75 (3H, s), 2.65 (1H, ddd, *J* = 12.0, 4.2, 2.0 Hz), 2.54 (1H, d, *J* = 17.8 Hz), 1.58 (3H, d, *J* = 6.8 Hz), 1.42 (3H, d, *J* = 6.2 Hz); ^{13}C NMR (MeOH-*d*$_4$) δ_C 188.7 (C), 181.5 (C), 175.9 (C), 157.5 (C), 149.6 (C), 136.5 (C), 135.4 (C), 133.2 (CH), 130.8 (C), 118.7 (CH), 114.6 (C), 77.1 (CH), 72.2 (CH), 71.0 (CH), 69.5 (CH), 66.8 (CH), 66.4 (CH), 60.7 (CH), 36.3 (CH$_2$), 32.6 (CH$_2$), 29.2 (CH$_3$), 17.2 (CH$_3$), 16.9 (CH$_3$); HRFABMS m/z 444.1645 [M + H]$^+$ (calcd for C$_{23}$H$_{26}$NO$_8$, 444.1653).

Menoxymycin A (**4**): ^{1}H NMR (CDCl$_3$) δ_H 12.21 (1H, br s), 7.89 (1H, d, *J* = 7.5 Hz), 7.70 (1H, d, *J* = 7.5 Hz), 5.27 (1H, d, *J* = 2.7 Hz), 5.06 (1H, q, *J* = 6.2 Hz), 4.91 (br d, *J* = 9.8 Hz), 4.70 (1H, dd, *J* = 4.7, 2.5 Hz), 4.12 (1H, ddd, *J* = 11.5, 8.3, 3.0 Hz), 3.93 (1H, dd, *J* = 9.1, 9.1 Hz), 3.67 (1H, dd, *J* = 8.8, 6.1 Hz), 3.63 (3H, s), 3.58 (3H, s), 2.98 (1H, dd, *J* = 16.2, 4.8 Hz), 2.76 (1H, ddd, *J* = 11.5, 3.0, 2.0), 2.70 (1H, d, *J* = 16.2 Hz), 1.54 (3H, d, *J* = 6.5 Hz), 1.48 (1H, m), 1.47 (3H, d, *J* = 5.6 Hz); ^{13}C NMR (CDCl$_3$) δ_C 188.4 (C), 181.1 (C), 174.0 (C), 157.7 (C), 149.6 (C), 136.3 (C), 135.5 (C), 133.8 (CH), 130.6 (C), 119.8 (CH), 114.3 (C), 78.5 (CH), 77.3 (CH), 71.2 (CH), 71.0 (CH), 68.6 (CH), 66.5 (CH), 66.2 (CH), 56.6 (CH$_3$), 55.5 (CH$_3$), 36.9 (CH$_2$), 32.2 (CH$_2$), 18.5 (CH$_3$), 17.9 (CH$_3$); HRFABMS m/z 474.1757 [M + H]$^+$ (calcd for C$_{24}$H$_{28}$NO$_9$, 474.1759).

Antibacterial activity assays

Antibacterial activity assays were carried out according to the methods of the Clinical and Laboratory Standard Institute (CLSI) (Clinical and Laboratory Standards Institute, 2018). Microorganisms obtained from the American Type Culture Collection (ATCC) and the stock Culture Collection of Antimicrobial Resistant Microorganisms (CCARM; clinical isolates; Seoul Women's University, Seoul, Republic of Korea) were used for antibacterial activity assays: Gram-positive bacteria (*Staphylococcus aureus* ATCC25923, *Enterococcus faecalis* ATCC19433, and *E. faecium* ATCC19434), Gram-negative bacteria (*Salmonella enterica* ATCC14028, *Klebsiella pneumoniae* ATCC10031, and *Escherichia coli* ATCC25922), methicillin-sensitive *S. aureus* (MSSA; strains CCARM0027, 0204, 0205, and 3640), and methicillin-resistant *S. aureus* (MRSA; strains CCARM3089, 3090, 3634, 3635, and ATCC43300). Each bacterium was cultured overnight in cation-adjusted Mueller Hinton broth (MHBc; BD Difco, Sparks, MD, USA) at 37℃, collected via centrifugation, diluted in MHBc, and adjusted to match the turbidity of a 0.5 McFarland standard at 625 nm wavelength [approximately 5×10^6 colony forming units (cfu)/mL of the test bacterium]. Stock solutions of the compound were prepared in dimethyl sulfoxide (DMSO) at 12.8 mg/mL. Each stock solution was diluted in MHBc to concentrations ranging from 0.03 to 32 µg/mL. The final DMSO concentration was maintained at 1% by adding DMSO to the medium, according to CLSI guidelines. In each well of a 96-well plate, 90 µL of MHBc containing the test compound was mixed with 10 µL of broth containing the test bacterium (final concentration: 5×10^5 cfu/mL). The plates were incubated for 24 h at 37℃. The minimum inhibitory concentration (MIC) value was defined as the lowest concentration of test compound that prevented cell growth. Ampicillin (Duchefa, Amsterdam, Netherlands), tetracycline, daptomycin, vancomycin, platensimycin, linezolid, and ciprofloxacin (Sigma-Aldrich, St. Louis, MO, USA) were used as positive controls.

Multi-step resistance development assay

To identify drug susceptibility and the appearance of strains resistant to lactoquinomycin A and its analogs, multi-step resistance development experiments were carried out based on methods described previously (Friedman et al., 2006) with minor modifications. Each test compound, including compounds 1-4 and ciprofloxacin (Cip; dissolved in DMSO at 12.8 mg/mL), was serially 2-fold diluted in MHBc based on previously determined MIC values. Overnight cultures of MRSA strain ATCC43300 were prepared at 10^6 cfu/mL in MHBc based on the 0.5 McFarland standard. Next, 50 µL of bacterial solution was inoculated into 50 µL dilution series of each compound in a 96-well plate (final concentration: 5×10^5 cfu/mL). Following incubation at 37°C for 24 h, the MIC was determined. The cultures were passaged daily for 30 days, using 50 µL inocula (10^6 cfu/mL) from wells of the highest antibiotic concentration showing bacterial growth from the previous passage to inoculate a fresh series of dilutions.

Time-kill kinetics assay

A time-kill kinetics assay of lactoquinomycin A was conducted according to the following procedures (Tsuji et al., 2008). A single colony of overnight-cultured MRSA strain ATCC43300 was inoculated into fresh MHBc medium and incubated to the turbidity of the 0.5 McFarland standard. Additions of 8× the MICs of lactoquinomycin A (MIC = 0.25 µg/mL), tetracycline (MIC = 0.25 µg/mL), ciprofloxacin (MIC = 0.25 µg/mL), and vancomycin (MIC = 1 µg/mL) were made to MHBc containing 5×10^5 cfu/mL of ATCC43300. These mixtures were incubated at 37°C, and 200 µL aliquots of medium were collected at 0, 1, 2, 4, 8, and 24 h and inoculated on MHBc agar plates. The cfu values of the tested samples were

determined following overnight incubation at 37°C. The assay was conducted for three independent experiments and $\log_{10}$ (cfu/mL) was plotted against time.

Membrane permeabilization assay

Membrane potential was monitored using the fluorescent dye $DiSC_3$ (5) (3,3'-dipropylthiadicarbocyanine iodide) (Anaspec, Fremont, CA, USA) according to the following procedures (Wu and Hancock, 1999). *S. aureus* ATCC25923 was grown to mid-logarithmic phase (0.5 to 0.6 optical density at 600 nm) in MHBc at 37°C. Cells were collected through centrifugation (5500 × g, 10 min) and washed with buffer (5 mM HEPES, 5 mM glucose, pH 7.2). Following resuspension in the same buffer (optical density of 0.05 at 600 nm), $DiSC_3$ (5) and KCl were added to final concentrations of 0.4 µM and 100 mM, respectively. The mixture was incubated until stabilization of fluorescence and treated with 4× the MICs of lactoquinomycin A (MIC = 0.06 µg/mL) and nisin (MIC = 4 µg/mL), using the latter as a positive control and DMSO as a negative control. Fluorescence was measured using a microplate reader FLx800 (BioTek, Winooski, VT, USA) at wavelengths of 622 nm for excitation and 670 nm for emission.

Detection of the mode of action with the dual-reporter system

To assess the mode of action of LQM-A, an in vivo dual-reporter assay designed to distinguish between compounds that inhibit translation and those that induce DNA damage was employed (Osterman et al., 2016; Osterman et al., 2020). The plasmid, pDualrep2, was kindly provided by Prof. Ilta A. Osterman (Lomonosov Moscow State University, Moscow, Russia). To construct the dual-reporter system, pDualrep2 was transformed into E. coli DH5α with the heat-shock method (42°C, 90

s) (Froger and Hall, 2007). Tested antibiotic solutions at the MIC (doxorubicin = 4 µg/mL, erythromycin = 4 µg/mL, lactoquinomycin A = 4 µg/mL, and tetracycline = 0.25 µg/mL) were dropped onto an MHBc agar plate that already contained a lawn of the reporter strain. The agar plate was analyzed using the Chemi-Doc (Bio-Rad, Hercules, CA, USA) imaging system in Cy3 mode for red fluorescent protein (RFP) and Cy5 mode for Katushka2S after incubation overnight at 37℃.

Ethidium bromide (EtBr) displacement assay

To confirm whether lactoquinomycin A interacts with DNA, an EtBr displacement assay was performed according to previously reported procedures (Tse and Boger, 2004). First, *S. aureus* strain ATCC25923 was selected, and its DNA was rapidly extracted using the Tris-EDTA- NaCl-Triton X100 (TENT) method (Hassanzadeh et al., 2016). The strain was cultured in 100 mL tryptic soy broth (TSB) at 37℃ for 16 h and then centrifuged (11,000 × g, 10 min). The pellets were suspended in 1 mL TENT buffer containing 10 mM Tris-Cl, 0.1 M NaCl, 1 mM EDTA, and 5% [v/v] Triton X100 at pH 8.0. Then, the cell suspension was boiled at 100℃ for 5 min. Following centrifugation, the supernatant was mixed with cold 95% ethanol and stored at 20℃ for 20 min. The DNA pellet was dissolved in distilled water after the solution was re-centrifuged and air-dried. The DNA concentration was measured using a NanoDrop spectrophotometer (ACTGene, Piscataway, NJ, USA). 20-mers of poly-AT and poly-GC double-stranded DNA synthesized by Cosmogenetech (Seoul, Korea) were employed. Next, 70 µL of 8.57 µM EtBr solution containing 0.1 M Tris-Cl and 0.1 M NaCl at pH 8.0 (final EtBr concentration: 6 µM) was added to 96-well black plates, and 10 µL of 1 mg/mL prepared DNA solution was mixed with the EtBr solution. Then, 20 µL of Tris buffer containing up to 125 µM of lactoquinomycin A was added to each well and equilibrated at room temperature for

30 min. The intensity of fluorescence was read (excitation: 545 nm, emission: 595 nm) using a BioTek FLx800 microplate reader. The procedure was conducted in triplicate and a graph of relative fluorescence intensity against the concentrations of test compounds was plotted.

DNA mobility shift assay

The rapid and sensitive DNA mobility shift assay was performed using previously described procedures (Furlan et al., 2002). The plasmid pUC 19 (2.7 kb) was used for double-strand DNA intercalation. Plasmid DNA was isolated using the DNA-maxi SV Plasmid DNA Purification Kit (Intron Biotechnology, Seoul, Korea), and the concentration was measured using a NanoDrop spectrophotometer. The assay was conducted using 1 µL (100 ng/µL) plasmid DNA mixed with various concentrations of lactoquinomycin A solution (from 0 to $8 \times$ MIC). The total volume of each reaction was brought to 10 µL with Tris buffer (0.1 M Tris-Cl, 0.1 M NaCl, pH 8.0). For time-dependent experiments, lactoquinomycin A was added at the MIC value and incubated for 0 to 120 min. To assess intercalation activity, the gel was stained with EtBr for 30 min after electrophoresis, using a 1% (w/v) agarose gel without EtBr and 0.5 Tris-Borate-EDTA (TBE) buffer at 50 V for 2 h. The gel was monitored using the Chemi-Doc imaging system with ultraviolet light.

Real-time quantitative PCR and reverse transcription (RT) PCR assays

To confirm transcriptional inhibition by lactoquinomycin A, RT-PCR was conducted with following procedures. Total RNA of MRSA ATCC43300 was extracted using easy-BLUE™ Total RNA Extraction Kit (Intron Biotechnology, Seoul, Korea). After the bacterial strain was cultured in mid-log phase (OD = 0.5 at 600 nm), 0, 1/2,

16

1 and 2 × MIC of lactoquinomycin A were treated for 40 min (Real-time PCR) and 1 × MIC of lactoquinomycin A was treated for 0, 20, 40 and 80 min (RT-PCR). Cells were centrifuged (11,000 × g, 1 min) and resuspended with 1 mL of easy-BLUE™ reagent. The mixtures were transferred into the 2 mL Safe-Lock tube containing the acid-washed beads (Sigma-Aldrich, St. Louis, MO, USA). The bacterial cells were disrupted in the Precellys 24 tissue homogenizer (Bertine Technologies, Rockville, Washington, DC, USA) for 5 min at maximum speed. 200 µL chloroform was added into lysates and mixtures were centrifuged at 4℃ (11,000 × g, 10 min). After upper aqueous fractions were transferred to a clean tube, 400 µL isopropanol was added and centrifuged at 4℃ (11,000 × g, 10 min). The supernatants were removed and 1 mL of 75% ethanol was mixed with pellets and centrifuged at 4℃ (11,000 × g, 10 min). RNA pellets were dissolved in RNase free water followed by air-drying. For mRNA enrichment, MICROB*Express*™ kit was employed with manual instructions. 200 µL of binding buffer, 4 µL of Capture oligo mix and total RNA were mixed and incubated under the below conditions (70℃ for 10 min for denaturing secondary structures in RNA and 37℃ for 15 min for annealing). Supernatants of oligo MagBeads were removed using magnetic stand and resuspended with binding buffer. 50 µL of oligo MagBeads were added in RNA/Capture oligo mix and incubated at 37℃ for 15 min. The supernatants containing enriched mRNA were separated from mixtures using magnetic stand. After the volume of mRNA, 1/10th volume 3 M sodium acetate and 1/50th volume glycogen were mixed, ethanol precipitation was performed. Subsequently, DNase I (Enzynomics, Daejeon, KOREA) was treated at 37℃ for 10 min for removing residual DNA. The concentration of RNA was measured using a NanoDrop spectrophotometer.

The complementary DNA (cDNA) was synthesized using SuperScript III cDNA synthesis kit (Enzynomics, Daejeon, KOREA) with following methods. Same concentration of RNAs was mixed with 1 µL random hexamers and dNTPs and

17

RNase free water was added up to 10 µL. Following incubation at 65℃ for 5 min, mixture was place on ice for at least 3 min. cDNA synthesis mix (4 µL of 25 mM MgCl$_2$, 2 µL of 10 × RT buffer, 2 µL of 0.1 M DTT, 1 µL of RNase inhibitor and 1 µL of SuperScript III reverse transcriptase) was added and incubated at 25℃ for 10 min. Additional incubation at 50℃ for 50 min was followed by incubation at 85℃ for 5 min for terminating reaction. For eliminating residual RNA, RNase H was treated at 37℃ for 20 min. Real-time PCR was performed with cDNA of samples treated with 0, 1/2, 1 and 2 × MIC of lactoquinomycin A for 40 min, various primers listed on the Table 1.1, fast SYBR™ green master mix (Thermo Fisher scientific, Waltham, MA, USA) and MicroAmp™ fast optical 96-well reaction plate (Thermo Fisher scientific, Waltham, MA, USA) using 7500 fast real-time PCR instruments (Thermo Fisher scientific, Waltham, MA, USA) under the following conditions: activation of fast DNA polymerase (95℃, 20 s); 40 cycles of denaturation (95℃, 3 s), annealing and extension (60℃, 30 s).

RT-PCR was carried out with cDNA of samples treated with 1 × MIC of lactoquinomycin A for 0, 20, 40 and 80 min and three genes (two reduced genes; *grlA* and *grlB*, one control gene; *gyrB*) under the conditios: pre-denaturation (95℃, 5 min); 35 cycles of denaturation (95℃, 10 s), annealing (52℃, 30 s), and extension (72℃, 20 s); and final extension (72℃, 5 min).. The 1% agarose gel electrophoresis was conducted with PCR products and 10× loading buffer at 100 V for 20 min. Agarose gel was detected using Chemi-Doc imaging system with ultraviolet light.

Table 1.1. List of used oligonucleotides on real-time PCR of essential genes

Primer	Gene	Sequence (5'-3')
dnaART-F	*dnaA*	CTGGTAACCGCTTTCCACAT
dnaART-R		GACCAATGGCATGCATTAAA
dnaCRT-F	*dnaC*	GCCGATATCGTTGCATTCTT
dnaCRT-R		GCCTGTTGGACCATTACGTT
dnaERT-F	*dnaE*	GCCGAGAAAAGGTCATTCAG
dnaERT-R		CCCATAATTCGTCCAACGTC
dnaXRT-F	*dnaX*	GGGCACAACGTTTTGATTTT
dnaXRT-R		ATACCCCCTTCAGACGCTTT
grlART-F	*grlA*	GCGTGACGCTAAAGAAAACC
grlART-R		GCGTGACGCTAAAGAAAACC
grlBRT-F	*grlB*	TGAATACGCTTGGACAGACG
grlBRT-R		GTCTGGGTTCATCGTCGTTT
gyrART-F	*gyrA*	CGTGACAAGAAAATTGACGG
gyrART-R		TGACACTAGCATTTGCATCC
gyrBRT-F	*gyrB*	ATGAAAATCCACAAGTCGCA
gyrBRT-R		TCTAACGCTGATTTACGACG
ligART-F	*ligA*	AACGGCAAAACGAAAGCTAA
ligART-R		CGCGCGCTCTATTTTTATTC
polCRT-F	*polC*	CCTCGAATTCCACGTTCATT
polCRT-R		CTTGATAAAGTGCCGGTGGT
rpoART-F	*rpoA*	TGGTTCAATCACACCACAAGA
rpoART-R		TCATGATTTCAGCGTTTTGC
rpoBRT-F	*rpoB*	AATTACATGCGCGTTCAACA
rpoBRT-R		ACCTCCATCTCACCAAAACG
rpoCRT-F	*rpoC*	CCGCACCATCTGGTAAGATT

rpoCRT-R		ATCGGCAAGACCTTTACGTG
rpoDRT-F	*rpoD*	CAAGCAATCACTCGTGCAAT
rpoDRT-R		GGTGCTGGATCTCGACCTAA

Checkerboard assay

To confirm synergetic effect of lactoquinomycin A with other antibiotics, checkerboard assay was carried out according to the previous reported procedures (Bajaksouzian et al., 1997). Stock solutions of each antibiotic were prepared in DMSO. Ampicillin, vancomycin, tetracycline and ciprofloxacin was vertically diluted in MHBc to concentrations ranging from 0.25 to 16 µg/mL, 1 to 64 µg/mL, 0.5 to 32 µg/mL and 0.25 to 16 µg/mL respectively. Lactoquinomycin A was horizontally diluted in same media to concentration ranging from 0.03 to 2 µg/mL in an each 96-well plate. 45 µL of MHBc containing each antibiotic was mixed in a new 96-well plate and 10 µL of broth containing MRSA ATCC43300 was added (final concentration: 5×10^5 cfu/mL). The final DMSO concentration was maintained at 1% by adding DMSO to the medium, according to CLSI guidelines. The plate was incubated for 16 h at 37°C and absorbance of each well was measured with Multi-Reader SpectraMAX M5 (Molecular Devices, San Jose, CA, USA). The percentages of inhibition were shown as the absorbance of each well, divided by that of a well with no compounds, multiplied by 100. Fractional inhibitory concentration (FIC) value was calculated as the sum of two components, MIC value of ampicillin in combination divided by MIC value of ampicillin and that of LQM-A in combination divided by that of LQM-A. If FIC index is over 4, LQM-A show an antagonistic effect with ampicillin. If FIC index is between 0.5 to 4, then two compounds are in indifference relationship. FIC index below 0.5 is tagged as a synergetic effect.
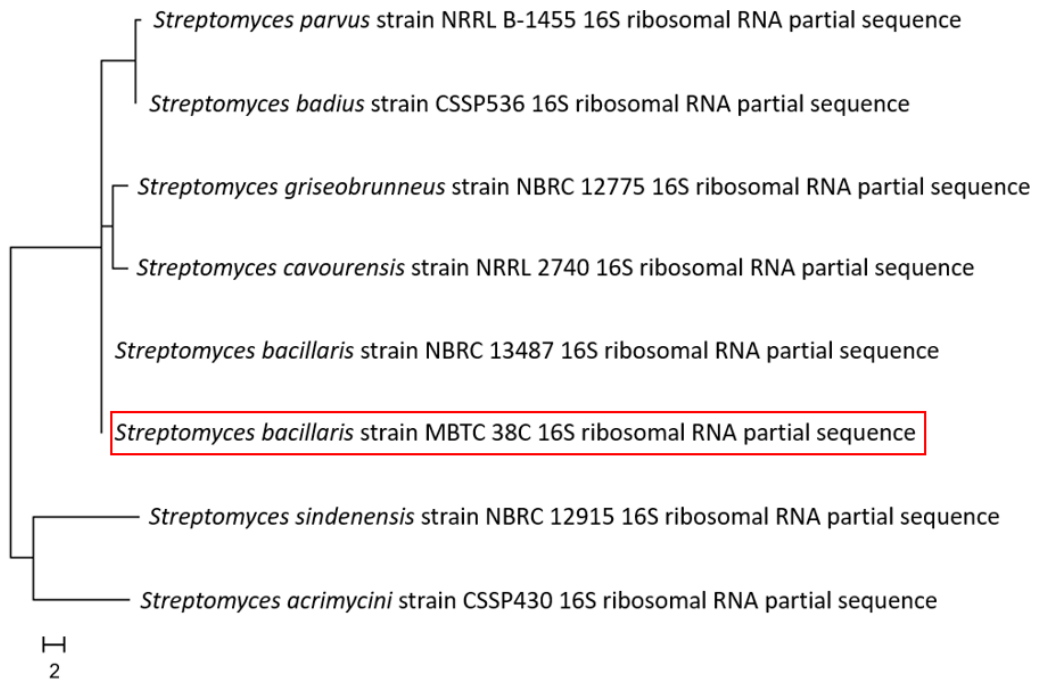
Results

Taxanomy of strain MBTC38

The 16S rDNA of strain MBTC38 was amplified using PCR and sequenced. After a BLAST sequence comparison, strain MBTC38 showed 100% identity to *Streptomyces bacillaris* strain NBRC13487 (type strain, GenBank accession number: NR041146.1) and ATCC15855 (type strain, GenBank accession number: CP029378.1). Thus, this strain was designated *S. bacillaris* strain MBTC38 (GenBank accession number: MK402083.1). The phylogenetic tree of *S. bacillaris* strain MBTC38 was drawn with maximum likelihood methods based on the *Tamura 3-parameter* model, which showed evolutionary relationships between strain MBTC38 and other *Streptomyces* species (Fig. 1.1).

Figure 1.1. Phylogenetic tree of *Streptomyces bacillaris* strain MBTC38

The phylogenetic tree was constructed based on the *Tamura 3-prameter* model and maximum likelihood methods using the neighbor-joining program of MEGA-X software. According to the 16S rDNA sequence alignments of NCBI blast, MBTC38 strain has the highest similarity with *S. bacillaris* species.

Streptomyces parvus strain NRRL B-1455 16S ribosomal RNA partial sequence

Streptomyces badius strain CSSP536 16S ribosomal RNA partial sequence

Streptomyces griseobrunneus strain NBRC 12775 16S ribosomal RNA partial sequence

Streptomyces cavourensis strain NRRL 2740 16S ribosomal RNA partial sequence

Streptomyces bacillaris strain NBRC 13487 16S ribosomal RNA partial sequence

Streptomyces bacillaris strain MBTC 38C 16S ribosomal RNA partial sequence

Streptomyces sindenensis strain NBRC 12915 16S ribosomal RNA partial sequence

Streptomyces acrimycini strain CSSP430 16S ribosomal RNA partial sequence

2

Isolation and structural elucidation of compounds 1-4

S. bacillaris strain MBTC38 was cultured in colloidal chitin liquid medium at 28℃ for 7 days with shaking and filtrated with filter paper. 100 L of filtrate was fractionated twice with equal volumes of ethyl acetate and evaporated. Based on the results of the antibacterial activity assay, the entire extract (2.4 g) was separated through semi-preparative HPLC (Agilent Eclipse XDB-C18, 5 µm, 9.4×250 mm) under gradient solvent conditions ranging from 20% aqueous methanol to 100% methanol with 0.1% TFA (ultraviolet detection at 254 nm, flow rate: 2 mL/min) to yield four compounds; compound **1** (t_R: 23 min, 8.4 mg), **2** (t_R: 21 min, 3.8 mg), **3** (t_R: 24 min, 11.6 mg), and **4** (t_R: 25 min, 5.1 mg) (Fig. 1.2).

Based on combined spectroscopic analyses including 1D (^{1}H and ^{13}C)·2D (COSY, HSQC, HMBC) NMR , ultraviolet (UV), and high resolution mass spectrometry, compounds **1**–**4** were identified as lactoquinomycin A (**1**) (Okabe etal., 1985), lactoquinomycin B (**2**) (Okabe et al., 1986), *N*-methyl lactoquinomycin A (**3**) (Huang et al., 2018), and menoxymycin A (**4**) (Hayakawa et al., 1994) (Fig. 1.3). The spectroscopic data for these compounds were in good agreement with those in the literature (Tables 1.2-1.5, Figs. S1-S22).

Figure 1.2. Flow chart of extraction and separation of metabolites from *Streptomyces bacillaris* MBTC38

Filtrate of strain MBTC38 culture was extracted by ethyl acetate and separated by reversed-phase HPLC after evaporation.

Streptomyces bacillaris MBTC38 culture (60L)

Colloidal chitin medium, 28℃, 7days

Mycelium   Filtrate

Liquid-liquid extraction

Ethyl acetate (2.4g)

Revered-phase HPLC
20% to 100% (v/v) aq. MeOH + 0.1% TFA

| **1** | **2** | **3** | 4 |
| (8.4 mg) | (3.8 mg) | (11.6 mg) | (5.1 mg) |
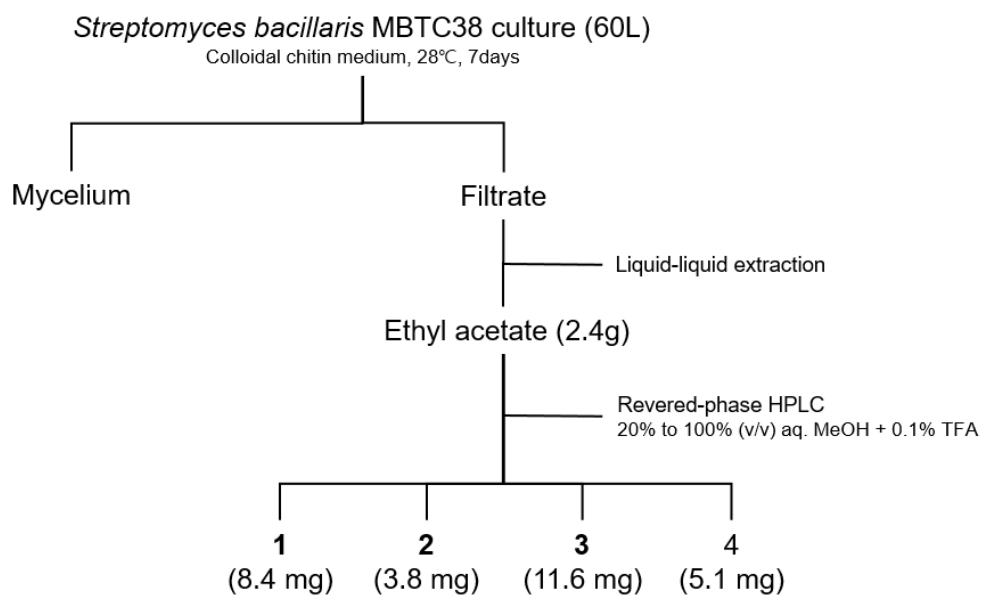
Figure 1.3. Structures of compounds 1-4

1) lactoquinomycin A; 2) lactoquinomycin B; 3) *N*-methyl lactoquinomycin A; 4) menoxymycin A

31
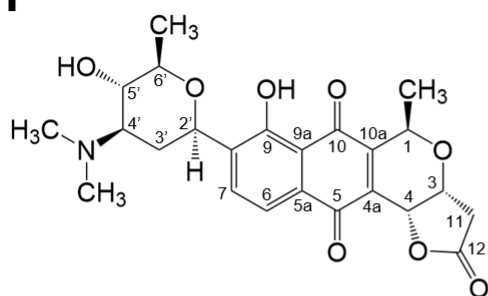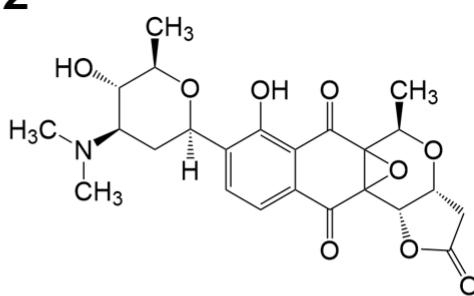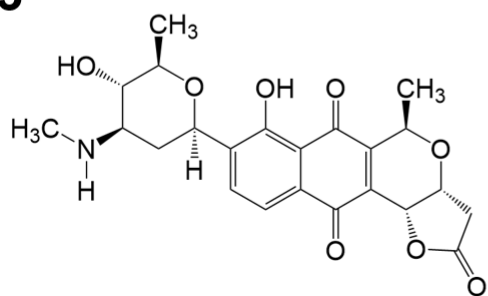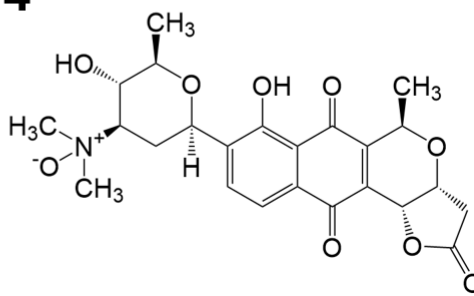
Table 1.2. Comparison of ^{13}C NMR data of compound 1 with lactoquinomycin A in CDCl₃

Position	1	Lactoquinomycin A
	δ_H, ppm	
1	66.2	66.3
3	66.4	66.5
4	68.5	68.7
4a	135.5	134.9
5	181.1	180.8
5a	130.5	129.7
6	119.9	119.6
7	133.8	133.5
8	136.5	138.6
9	157.7	157.7
9a	114.3	114.0
10	188.5	187.8
10a	149.6	149.2
11	36.9	37.0
12	173.9	173.5
1-CH₃	18.1	18.8
2'	71.1	72.2
3'	29.3	28.2
4'	68.0	67.2
5'	70.4	71.5
6'	77.7	77.6
4'-N(CH₃)₂	40.1	40.3
6'-CH₃	18.6	18.9

Sample was dissolved in chloroform-*d*.

Table 1.3. Comparison of ^{13}C NMR data of compound 2 with lactoquinomycin B in MeOH-d_4, CDCl$_3$, respectively

Position	2	Lactoquinomycin B
	δ_H, ppm	
1	64.3	64.2
3	65.0	64.8
4	67.1	69.2
4a	60.5	60.0
5	187.3	187.6
5a	130.8	129.7
6	119.1	120.0
7	133.3	134.2
8	136.6	139.1
9	157.6	157.8
9a	114.0	113.5
10	195.2	193.9
10a	64.4	64.4
11	36.0	35.6
12	175.8	173.3
1-CH$_3$	13.3	15.2
2'	71.0	72.4
3'	28.9	28.1
4'	69.8	67.2
5'	70.3	71.5
6'	77.2	77.6
4'-N(CH$_3$)$_2$	40.7	40.3
6'-CH$_3$	16.8	19.0

Sample was dissolved in methanol-d_4 and chloroform-d.

Table 1.4. Comparison of ^{13}C NMR data of compound 3 with *N*-methyl lactoquinomycin A in MeOH-*d*$_4$

Position	3	*N*-methyl lactoquinomycin A
	δ_H, ppm	
1	66.4	67.7
3	66.8	68.1
4	69.5	70.8
4a	135.4	136.7
5	181.5	182.8
5a	130.8	132.2
6	118.7	120.0
7	133.2	134.4
8	136.5	137.9
9	157.5	158.8
9a	114.6	116.0
10	188.7	190.1
10a	149.6	151.0
11	36.3	37.7
12	175.9	177.3
1-CH$_3$	17.2	18.5
2'	71.0	72.3
3'	32.6	34.0
4'	60.7	62.0
5'	72.2	73.6
6'	77.1	78.4
4'-N-CH$_3$	29.2	30.6
6'-CH$_3$	16.9	18.2

Sample was dissolved in methanol-*d*$_4$.

Table 1.5. Comparison of ^{13}C NMR data of compound 4 with menoxymycin A in CDCl$_3$

Position	4	Menoxymycin A
	δ_H, ppm	
1	66.2	66.2
3	68.6	68.5
4	66.5	66.4
4a	136.3	135.4
5	181.1	181.1
5a	130.6	130.4
6	119.8	119.8
7	133.8	133.8
8	135.5	136.9
9	157.7	157.8
9a	114.3	114.3
10	188.4	188.4
10a	149.6	149.6
11	36.9	36.9
12	174.0	173.9
1-CH$_3$	17.9	17.8
2'	71.2	72.9
3'	32.2	29.7
4'	77.3	75.9
5'	71.0	71.3
6'	78.5	77.8
4'-NO(CH$_3$)$_2$	56.6, 55.5	58.4, 52.7
6'-CH$_3$	18.5	18.5

Sample was dissolved in chloroform-*d*.

Antibacterial activities of compounds 1-4

The antimicrobial activities of compounds **1-4** were evaluated against pathogenic bacterial strains including MRSA. These compounds displayed significant antibacterial activities against the Gram-positive strains tested (*S. aureus*, *E. faecium*, and *E. faecalis*), with MIC values of 0.06-4 µg/mL (Table 1.6). However, the tested compounds exhibited weak to no inhibitory activity against Gram-negative bacteria such as *E. coli* (MIC = 16-32 µg/mL) and *K. pneumoniae* (MIC = 32 µg/mL), although they were effective against *S. enterica* (MIC = 0.03-1 µg/mL) when ampicillin and tetracycline were used as positive controls. These compounds also showed significant inhibitory activities against all MSSA and MRSA strains (Table 1.7). In particular, LQM-A (**1**) had significant and broad antibacterial effects on MRSA, with MIC values of 0.25-0.5 µg/mL, indicating that it is more potent than important antibiotics such as daptomycin (MIC = 32 µg/mL), platensimycin (MIC = 4-8 µg/mL), linezolid (MIC = 1-2 µg/mL), and ciprofloxacin (MIC = 0.25->32 µg/mL).

Table 1.6. Antibacterial activity assays

Microorganisms	MIC (μg/mL)					
	1	**2**	**3**	**4**	**Amp**	**Tet**
Staphylococcus aureus *ATCC25923*	0.06	2	0.5	1	0.06	0.25
Enterococcus faecalis *ATCC19433*	2	>32	2	4	0.5	0.5
Enterococcus faecium *ATCC19434*	2	32	2	4	0.5	0.5
Salmonella enterica *ATCC14028*	0.03	1	0.25	0.13	0.03	0.13
Klebsiella pneumonia *ATCC10031*	>32	>32	32	>32	>32	0.25
Escherichia coli *ATCC25922*	16	>32	32	>32	8	0.5

Amp (ampicillin) and Tet (tetracycline) were used as positive controls. DMSO (1%) was used as a negative control.

Table 1.7. MICs against MRSA strains

Microorganisms	MIC (μg/mL)								
	Dap	Van	Pla	Lin	Cip	1	2	3	4
CCARM0027	4	0.5	4	2	0.25	0.25	2	1	1
CCARM0204	1	0.5	4	1	0.25	0.13	1	0.25	0.5
CCARM0205	0.5	0.5	2	1	0.25	0.06	1	0.25	0.5
CCARM3640	8	0.25	4	2	0.25	0.13	2	1	1
CCARM3089	>32	0.5	8	2	>32	0.25	4	1	2
CCARM3090	32	0.06	8	1	>32	0.5	8	1	2
CCARM3634	32	0.25	8	2	>32	0.25	4	1	1
CCARM3635	>32	0.06	8	2	>32	0.25	4	0.5	0.5
ATCC43300	>32	1	4	2	0.25	0.25	4	0.5	1

MSSA strains (CCARM0027, 0204, 0205 and 3640) and MRSA strains
(CCARM3089, 3090, 3634, 3635 and ATCC43300) were used in antibacterial
assays. Dap (daptomycin), Van (vancomycin), Pla (platensimycin), Lin (linezolid)
and Cip (ciprofloxacin) were used as positive controls. DMSO (1%) was used a
negative control.

Multi-step resistance development and time-kill kinetics

Resistance development profiles for compounds **1–4** against MRSA strain ATCC43300 were determined (Fig. 1.4a). In the present study, resistance was defined as a > 4-fold increase in the initial MIC (Clark etal., 2009; Kosowska-Shick et al., 2009). For compounds **1**, **3**, and **4**, 4-fold increases in the MIC (from 0.25 to 1 µg/mL, from 0.5 to 2 µg/mL, and from 1 to 4 µg/mL, respectively) were observed, indicating that resistance against compounds **1**, **3**, and **4** did not develop over 30 passages. Conversely, for compound **2** and ciprofloxacin, 8- and 256-fold changes relative to the initial MIC values (compound **2** = 2 µg/mL; ciprofloxacin = 0.25 µg/mL), respectively, were observed during the passage experiment.

To confirm the time-dependent antibacterial effects of LQM-A (**1**), which showed the strongest antibacterial activity, a time-kill kinetics experiment was conducted from 0 to 24 h. The time-kill profile of LQM-A showed a reduction in the number of viable cells for the first 8 h followed by a gradual increase up to 24 h, indicating that the inhibitory effect of LQM-A is much greater than those of the control antibiotics, tetracycline, and ciprofloxacin, which reduced the number of viable cells for the first 4 h. Meanwhile, vancomycin showed a bactericidal effect of decreasing the total number of viable cells at 24 h (Fig. 1.4b).

Figure 1.4. Antibacterial activities of lactoquinomycins (1-4) against MRSA strain ATCC43300

(**a**) The multi-step resistance development assay was conducted for 30 days with sub-MIC levels of four lactoquinomycins and ciprofloxacin. (**b**) The time-kill kinetics experiment was performed for 24 h with 8× MIC levels of LQM-A (MIC = 0.25 µg/mL), tetracycline (MIC = 0.25 µg/mL), ciprofloxacin (MIC = 0.25 µg/mL), and vancomycin (MIC = 1 µg/mL). Each point indicates the mean ± standard deviation (SD) of three independent experiments.

(a)
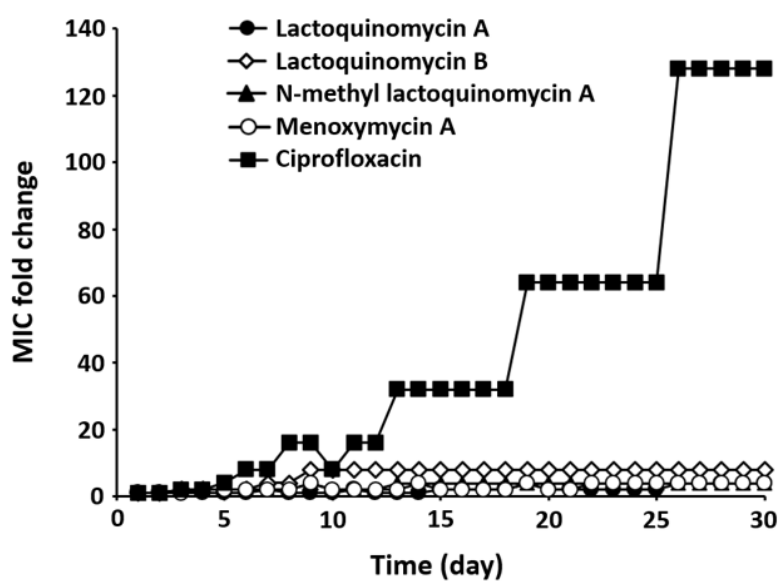
(b)
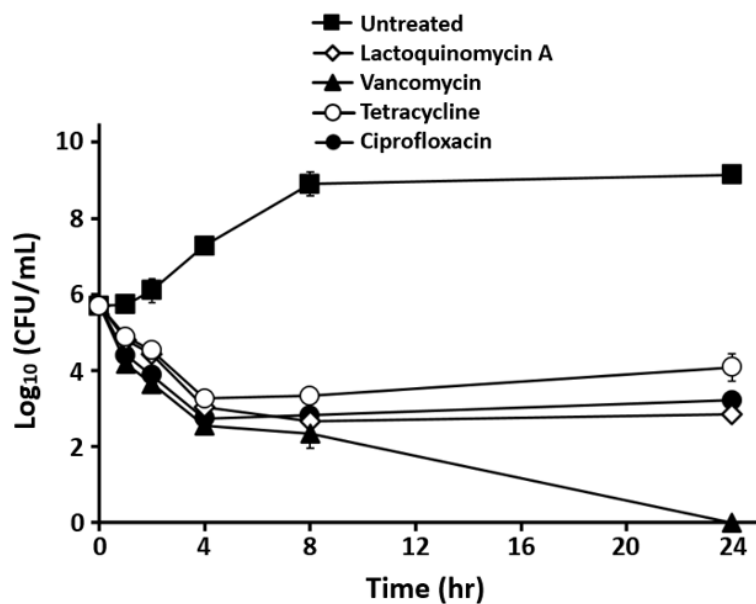
Mode of action of LQM-A

To assess the mode of action of LQM-A (**1**), I employed an in vivo dual-reporter assay, which was designed to identify mechanisms of inducing DNA damage or inhibiting translation (Osterman et al., 2016; Osterman et al., 2020). This system operates on the principle that compounds inducing DNA damage cause the SOS response and activate the sulA promoter by inactivating LexA, which leads to the expression of RFP (shown in green pseudo-color). Meanwhile, compounds that inhibit translation trigger ribosome stalling at a tryptophan operon leader sequence mutated with two alanines (trpL-2Ala) and Katushka2S (far-red fluorescent) protein is expressed, as shown in red. LQM-A, the representative translation inhibitors Tet and erythromycin (Ery), and the typical DNA replication inhibitor Dox were spotted onto an agar plate already containing a lawn of the reporter strain. In contrast to Tet and Ery, LQM-A led to the appearance of pseudo-green fluorescence similar to that of Dox, indicating that LQM-A induces DNA damage rather than inhibiting translation (Fig. 1.5a).

The mechanisms of LQM-A (**1**) and γ-actinorhodin, which share their main tetracyclic structure, are related to bacterial membrane potential (Nomoto et al., 1988; Nass et al., 2017). Thus, I confirmed whether LQM-A increased membrane permeabilization with the membrane-associated fluorescent dye $DiSC_3$ (5). In the present study, however, no change was observed in LQM-A-treated cell membranes, whereas nisin, which is known to generate pores in the cell membrane, led to enhanced fluorescence intensity over time (Fig. 1.5b).

Figure 1.5. Modes of action of LQM-A

(**a**) The dual-reporter system employed MIC levels of LQM-A, Ery, Tet, and Dox (4 µg/mL, 4 µg/mL, 4 µg/mL, and 0.25 µg/mL, respectively). The reporter strain was spread on an MHBc agar plate; then, MICs of each compound were dropped onto it and incubated overnight at 37°C. The plate was analyzed with the Chemi-Doc imager in Cy3 mode for red fluorescent protein (RFP) and Cy5 mode for Katushka2S. (**b**) The membrane permeabilization assay was performed with 4× the MICs of LQM-A (MIC = 0.06 µg/mL) and nisin (MIC = 4 µg/mL), using the latter as a positive control and DMSO as a negative control against *S. aureus* ATCC25923. Fluorescence was applied at wavelengths of 622 nm for excitation and 670 nm for emission.

(a)
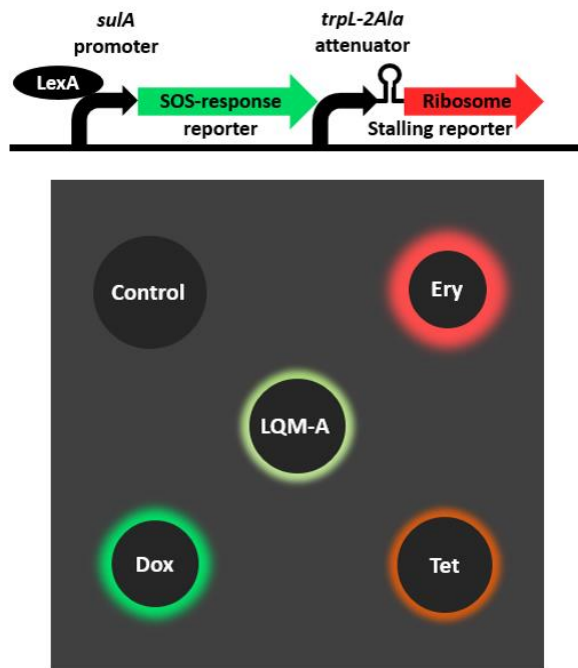
(b)
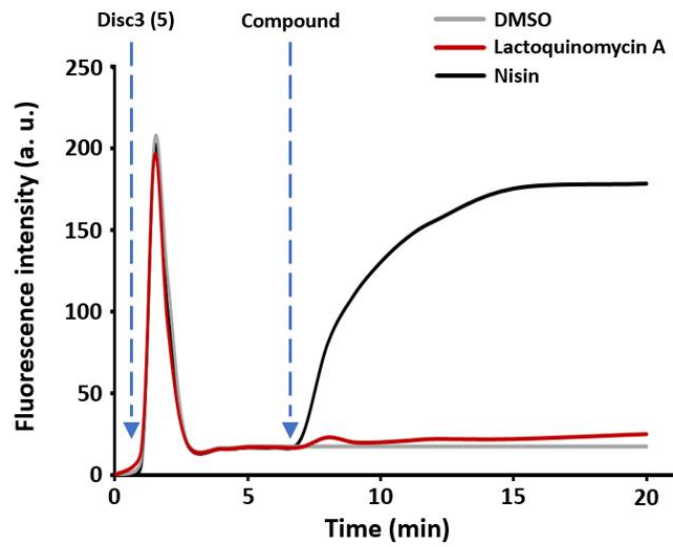
DNA intercalation effects of LQM-A

Based on its structural similarity to Dox, it was expected that LQM-A intercalates into DNA, and therefore an EtBr displacement assay was conducted. EtBr, a fluorescent DNA intercalator, tends to be inserted between base pairs of the DNA double helix. This assay uses the reduction of fluorescence caused by compounds intercalated in DNA due to displacement of EtBr (Tse and Boger, 2004). LQM-A (**1**) reduced fluorescence intensity by 36% as the concentration increased, similar to Dox. By contrast, Cip, which is known to act as a gyrase inhibitor, scarcely affected fluorescence intensity (Fig. 1.6a). Additionally, 20-mers of poly- AT and poly-GC DNA were prepared to determine whether LQM-A prefers AT- or GC-rich regions of DNA. The poly-GC and LQM-A system showed a fluorescence reduction of 33%, while fluorescence was reduced by 42% in the poly-AT and LQM-A system (Fig. 1.6b). The gel mobility shift assay was also performed to ascertain the intercalation activity of LQM-A. The plasmid pUC 19 switched from the supercoiled form to the relaxed form as time progressed. The relaxed form of the plasmid performed better than the supercoiled form at 4× the MIC value in the concentration-dependent experiment (Fig. 1.7).

Figure 1.6. EtBr displacement assay based on fluorescence spectroscopy

(**a**) The fluorescence intensity of the EtBr and *S. aureus* ATCC25923 DNA complex was measured at wavelengths of 545 nm for excitation and 595 nm for emission with increasing concentrations of LQM-A. Cip and Dox were used as control antibiotics. (**b**) 20-mers of poly-AT and poly-GC DNA were applied to identify preference among DNA intercalation regions. All experiments were conducted independently in triplicate and each point represents the mean ± SD.

(a)
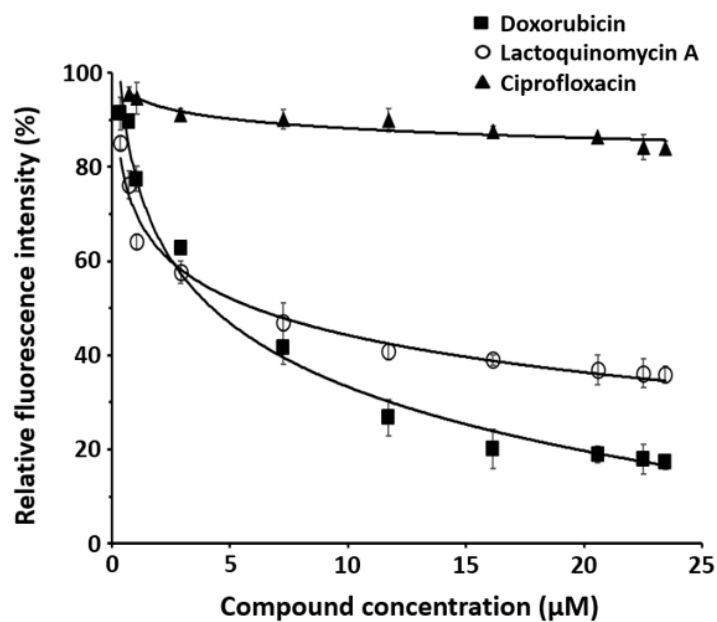
(b)
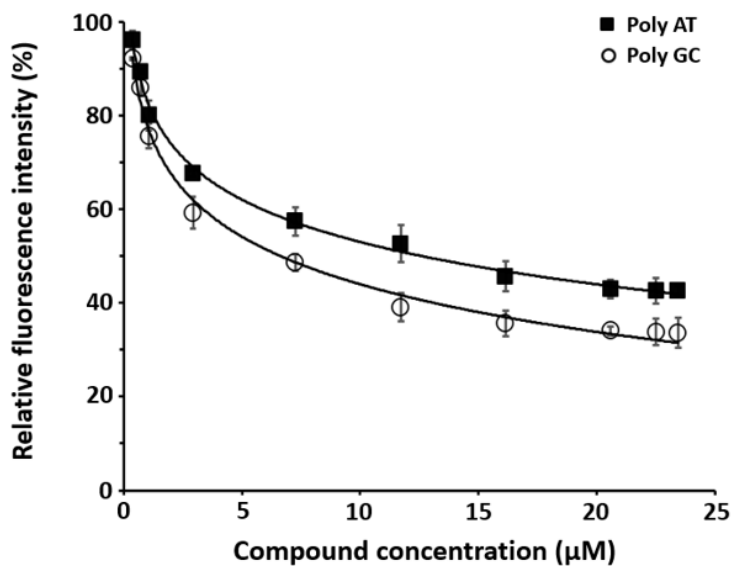
Figure 1.7. Gel mobility shift assay in the presence of LQM-A.

The assay was performed with pUC 19 plasmid (**a**) at various time points (0, 10, 30, 60, 90, and 120 min) and (**b**) with different concentrations of LQM-A from 0× to 8× MIC. C: untreated pUC 19.

(a)

C   0   10   30   60   90   120 (min)

Relaxed form
Supercoiled form

(b)

C   1x MIC   2x MIC   4x MIC   8x MIC

Relaxed form
Supercoiled form

51
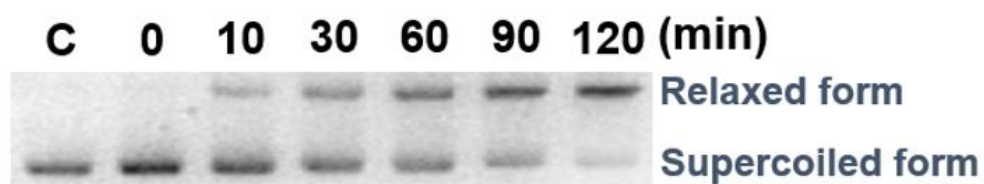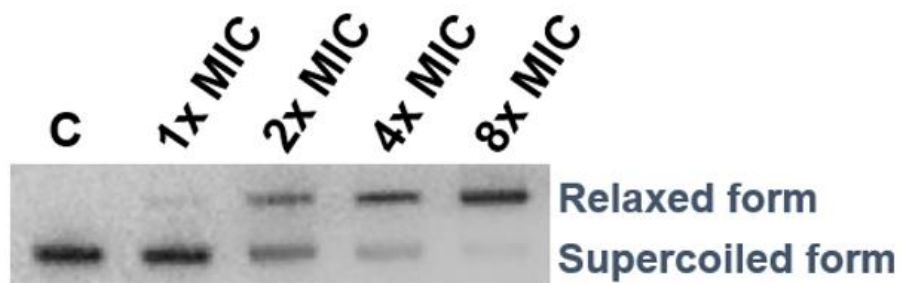
Transcriptional inhibition of LQM-A on essential genes of *S. aureus*

The effects of LQM-A on gene expression of *S. aureus* were examined by real-time PCR. Interestingly, expressions of *gylA* and *gylB* encoding topoisomerase IV subunit A and B were dramatically decreased as concentrations of treated LQM-A were increased. Two genes were expressed at the 20% of the normal level when $2 \times$ MIC of LQM-A was treated (Table 1.8). Moreover, time-dependent RT-PCR showed expression of *grlA* and *grlB* were constantly decreased from 0 to 80 min. The expression of *gyrB* encoding gyrase subunit B in *S. aureus* was uniformly detected in all treatments regardless of LQM-A and it was used as a positive control (Fig. 1.8).

Table 1.8. Real-time PCR analysis with 14 essential genes of *S. aureus*

Gene	Function	Relative gene expression			
		0× MIC	1/2× MIC	1× MIC	2× MIC
dnaA	Chromosomal replication initiator	1.00	0.96	1.16	0.66
danC	Replicative DNA helicase	1.00	1.14	0.94	0.73
dnaE	DNA polymerase III alpha subunit	1.00	0.96	0.75	0.54
dnaX	DNA polymerase III gamma and tau subunits	1.00	0.90	0.87	0.93
grlA	DNA topoisomerase IV subunit A	1.00	0.72	0.44	0.23
grlB	DNA topoisomerase IV subunit B	1.00	0.75	0.41	0.19
gyrA	DNA gyrase subunit A	1.00	1.13	1.25	1.20
gyrB	DNA gyrase subunit B	1.00	0.95	1.01	0.93
ligA	DNA ligase	1.00	1.31	1.07	0.52
polC	DNA polymerase III PolC type	1.00	1.23	0.95	0.59
rpoA	DNA-directed RNA polymerase alpha chain	1.00	1.2	0.73	0.40
rpoB	DNA-directed RNA polymerase beta chain	1.00	0.90	1.00	1.13
rpoC	DNA-directed RNA polymerase beta' chain	1.00	1.29	1.08	0.93
rpoD	RNA polymerase sigma factor	1.00	1.03	0.96	1.02

14 essential genes related to DNA and RNA metabolisms were employed in real-time PCR assay to confirm transcriptional inhibition of LQM-A. $0 \times$ to $2 \times$ MIC of LQM-A was treated. Real-time PCR was carried out under following conditions:

DNA polymerase activation stage (95℃, 20 s); 40 cycles of denaturation stage (95℃

3 s) and annealing & extension stage (60℃, 30 s).

Figure 1.8. Time-dependent RT-PCR analysis of *grlA* and *grlB*

Mid log-phase *S. aureus* cells were incubated in the absence or presence of 0.25 µg/mL of LQM-A at 37°C in MHBc. Cells were harvested at various time points (0, 20, 40 and 80 min) after incubation. *gyrB* was used a positive control.

.

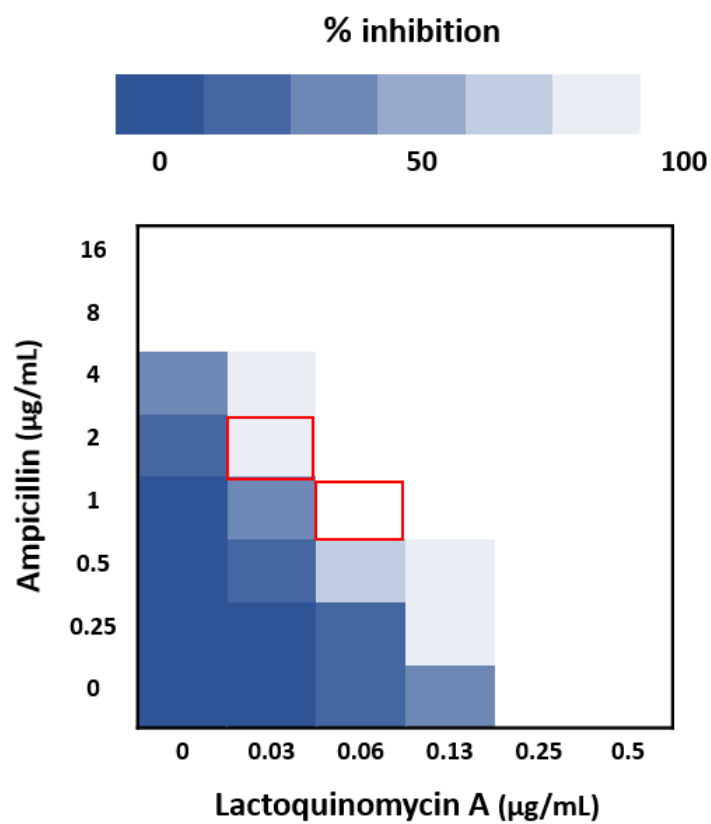|	Lactoquinomycin A (0.25 μg/mL)							
	(-)				(+)			
Time (min)	0	20	40	80	0	20	40	80
grlA								
grlB								
gyrB								

Synergetic effect of LQM-A with ampicillin

To confirm synergetic effects between LQM-A and other representative antibiotics such as ampicillin, vancomycin, tetracycline and ciprofloxacin, checkerboard assay was carried out and MIC value was defined as over 90% growth inhibition in present study. FIC value is less than 0.5 in two fields when 0.06 µg/mL of LQM-A and 1 µg/mL of ampicillin; 0.03 µg/mL of LQM-A and 2 µg/mL of ampicillin were treated, which showed synergetic effect between two antibiotics (Fig. 1.9). Additional synergetic effects of LQM-A with other three antibiotics were not detected.

Figure 1.9. Heat plots showing synergy of lactoquinomycin A and ampicillin

Heat plots showed percentage inhibition on the combined effect of LQM-A and ampicillin against MRSA ATCC43300. Various concentrations of two antibiotics were treated and strain was incubated at 37℃ for 16 h. Red boxes exhibited the sections with synergetic effect between LQM-A and ampicillin.

% inhibition

0   50   100

Ampicillin (µg/mL): 16, 8, 4, 2, 1, 0.5, 0.25, 0

Lactoquinomycin A (µg/mL): 0, 0.03, 0.06, 0.13, 0.25, 0.5

Discussion

Polyketides are a large family of secondary metabolites containing modified carbonyl groups or their precursors (McNaught, 1997). They are generally classified into three groups, types I, II, and III, depending on the enzyme types involved. Among them, aromatic polyketides, which are type II polyketides, have been reported to exhibit fascinating biological activities (Katz and Baltz, 2016). Numerous research groups have focused on aromatic polyketides with pharmacological potential, as they have advantages for clinical application including structural diversity, a broad range of therapeutic effects, and potential for genetic engineering (Shen B, 2000). In this study, four lactoquinomycins, which are a type of aromatic polyketides, were isolated from marine-derived *S. bacillaris* strain MBTC38 through activity-guided separation procedures and identified as LQM-A, lactoquinomycin B, *N*-methyl lactoquinomycin A, and menoxymycin A. These compounds showed potent inhibitory activities against pathogenic bacteria. Among these substances, known as compounds **1–4**, LQM-A exhibited the most significant antibacterial activity against Gram-positive bacteria including MRSA (MIC = 0.06–2 µg/mL). I also observed that the 4a,10a-epoxide structure played an important role in reducing biological activity; therefore, lactoquinomycin B unlike showed weak antibacterial activity (from 1 µg/mL to > 32 µg/mL) (Table 1.6).

LQM-A have been isolated from various species of *Streptomyces* as it was initially discovered from a soil actinomycete *S. tanashiensis* (Tanaka et al., 1985; Jiang et al., 2015; Jiang et al., 2018). Furthermore, LQM-A has been reported to exhibit antimicrobial activities against Gram-positive strains (*S. aureus* FDA209, *Bacillus subtilis* PCI219, *Corynebacterium xerosis*) with MIC values of 1.55–3.13 µg/mL. However, the compound showed weak to no inhibitory activity against Gram-negative bacteria, such as *Pseudomonas aeruginosa* IFO3455 (MIC = 100

µg/mL), *Proteus vulgaris* (MIC = 100 µg/mL), and *E. coli* K12 (MIC = 100 µg/mL) (Tanaka et al., 1985). In the present study, I isolated LQM-A from a marine actinomycete *S. bacillaris* and confirmed the antibacterial activities of LQM-A against *S. aureus* ATCC25923 and *E. coli* ATCC25922, with MIC values of 0.06 µg/mL and 16 µg/mL, respectively, which were ten times higher than those reported previously (Table 1.6). These differences may be attributed to distinctions among strains or the purity of the compound. The potential for the development of resistance to compounds **1–4** in the MRSA strain *S. aureus* ATCC43300 was also investigated. As shown in Table 1.7, ciprofloxacin showed potent antibacterial activities against MRSA strain *S. aureus* ATCC43300 (MIC = 0.25 µg/mL). However, based on multi-step (30-passage) resistance selection studies in the presence of ciprofloxacin, a steady increase in MIC for ciprofloxacin against *S. aureus* ATCC43300 was observed during the passage experiment. Reportedly, topoisomerase IV is the primary target of fluoroquinolones in *S. aureus*, which may be due to the greater sensitivity of topoisomerase IV to these agents (Ng et al., 1996). Furthermore, resistance from an altered DNA gyrase requires resistant topoisomerase IV for expression (Ferrero et al., 1995; Ng et al., 1996). By contrast, during the passage experiment, MIC values for compounds **1**, **3**, and **4** showed no more than a 4-fold increase from the starting MIC value, indicating that no resistance was detected over the 30 passages (Fig. 1.4a).

LQM-A is known as an inhibitor of the serine/threonine kinase AKT, which binds to T-loop cysteines in cancer cells, but its mechanism has not been well characterized in bacteria (Toral-Barza et al., 2007). The mechanism of LQM-A is generally assumed to be related to the bacterial cell membrane based on previous research (Nomoto et al., 1988; Nass et al., 2017). However, LQM-A did not affect membrane potential in membrane permeabilization assay (Fig. 1.5b). Thus, the mode of action of LQM-A appears to be the induction of DNA damage or inhibition of

protein synthesis due to its structural similarities with Dox and Tet. In the present study, it was demonstrated that the mode of action of LQM-A approximates that of Dox using a dual-reporter system. LQM-A-induced expression of RFP (shown in green pseudo-color), indicating that it caused the SOS response to DNA damage (Fig. 1.5a). This result indicated that the tetracyclic structure of LQM-A, containing three six-membered rings and one five-membered ring, is relatively flat, like that of Dox. The mechanism of inducing DNA damage was identified as intercalation into DNA using the fluorescence intercalator EtBr. However, the preference of DNA base pairs for intercalation was minor (Fig. 1.6).

The anthracyclines which containing planar four-ring with quinone chromophore and one, two or three sugar moieties have received attention as promising antibiotics. They have been reported to exhibit two representative cellular effects; inhibition of nucleic acid metabolism and disruption of phospholipid membranes (Lown, 1983). Because LQM-A did not affect membrane potential in Fig. 1.5b, transcriptional inhibition of LQM-A on nucleic acid metabolism was monitored. 14 essential genes of *S. aureus* involved in DNA and RNA metabolism were employed in Real-time PCR and RT-PCR analysis and *grlA* and *grlB* related to topoisomerase IV were dramatically reduced in a dose-and time-dependent manner (Table 1.8, Fig. 1.8). LQM-A did not cause resistant *S. aureus* for 30 days in Fig. 1.4a, which may be resulted from inhibitory mechanism of LQM-A on expression of essential genes. Furthermore, synergetic effect with valuable antibiotic; ampicillin and remarkable antibacterial activity exhibited potential of LQM-A as an infectious disease drug. The preference of LQM-A among DNA regions for intercalation should be studied further via docking simulation and DNase I footprinting assay to clearly characterize the correlation between DNA base pairs and LQM-A.

Part II

Isocitrate Lyase Inhibitory Activity of Bacillimide and Bacillapyrrole from *Streptomyces bacillaris* MBTC38

Introduction

Isocitrate lyase and its potential of antifungal agents

Glyoxylate cycle is an anaplerotic pathway of tricarboxylic acid (TCA) cycle and occurs in plants, bacteria, fungi and nematodes. The primary function of glyoxylate cycle is conversion of acetyl-CoA to succinate and malate for synthesis of carbohydrates (Vanni et al., 1990). Isocitrate lyase (ICL) and malate synthase (MS), key enzyme of this cycle cleaves isocitrate to glyoxylate and succinate and converts glyoxylate and acetyl-CoA to malate, respectively. In microorganisms, glyoxylate cycle plays an essential role in utilizing C_2 carbon sources such as fatty acid, acetate and ethanol when available simple sugars such as glucose do not exist in host environment (Dunn et al., 2009). Several pathogenic microorganisms such as *Candida albicans* and *Mycobacterium tuberculosis* were monitored to up-regulate glyoxylate cycle and employ C_2 carbon source during host infection (Kunze et al., 2006; Strijbis and Distel, 2010). In particular, virulence and persistence of *C. albicans* mutant strain lacking ICL enzyme are remarkably decreased in a mouse model of systemic candidiasis (Goldstein and McCusker, 2001; Lorenz and Fink, 2001; Ramirez and Lorenz, 2007). Moreover, ICL is considered as a promising target for development of antimicrobial agents since this metabolic cycle is absent in mammalian cells,

Alkaloids and their biological activities

Alkaolid is one of the extensive groups of natural products and characterized by a nitrogen atom in a heterocyclic ring structure (Ziegler and Facchini, 2008). They are produced by various organisms including plants, microorganisms and animals

(Roberts, 1998). These compounds have been focused in pharmaceutical fields due to their high structural complexity and diverse types of promising biological activities (Cordell et al., 2001). In recent years, a number of marine-derived novel alkaloids such as marinamide, penicitrinine A and veranamine were reported with remarkable structural complexity (Zhu and Lin, 2006; Liu et al., 2015; Kochanowska-Karamyan et al., 2020). The evaluation of biological activity showed that marine alkaloids and their analogs have potential as therapeutic agents containing anti-tumor, anti-depressant and anti-malarial activities (Gul and Hamann, 2005; Ang et al., 2000). Nitrosporeusine A and B were described as a unprecedented thioester-bearing alkaloids from marine *Streptomyces nitrosporeus* and exhibited inhibitory activity against influenza virus (Yang et al., 2013). Novel *N*-hydroxypyrroles, surugapyrroles A and B were reported from *Streptomyces* sp. and showed DPPH (2,2-diphyenyl-1-picrylhydrazyl) radical-scavenging activity (Yasumasa et al., 2009).

In continuous study for novel inhibitors of *C. albicans* ICL, I discovered extract of *Streptomyces bacillaris* MBTC38, collected from marine sediment in Jeju island, Republic of Korea. Based on the activity-guided separation of organic extract of MBTC38 strain, two compounds with ICL inhibitory activity were identified as bacillimide (compound **5**) bacillapyrrole (compound **6**) (Fig. 2.1). Absolute configuration of novel compound, bacillimide was determined based on NOESY and ECD measurements. Bacillimide exhibited potential inhibitory activity against ICL of *C. albicans* (IC_{50} = 44.24 µM) with mixed type of inhibition. Furthermore, the compound significantly reduced expression of *icl* genes in a dose-dependent manner under C_2-carbon-utilizing condition.

Material and Methods

General experimental procedures

^{1}H, ^{13}C, and 2D (COSY, HSQC, HMBC, NOESY) nuclear magnetic resonance (NMR) spectra were measured in MeOD-*d4,* DMSO-*d6* using Bruker Avance 600 MHz spectrometers (Bruker, Billerica, MA, USA) at the National Instrumentation Center for Environmental Management (NICEM) of Seoul National University. Liquid chromatography/mass spectrometry (LC/MS) data were obtained with an Agilent Technologies 6130 quadrupole mass spectrometer (Agilent Technologies, Santa Clara, CA, USA) coupled with an Agilent Technologies 1200 series high-performance liquid chromatography (HPLC) instrument. High-resolution electrospray ionization (HR-ESI) mass spectra were recorded on a Jeol JMS-700 high- resolution mass spectrometer (Jeol, Tokyo, Japan) at the National Center for Inter-University Research Facilities (NCIRF) of Seoul National University. HPLC was performed using a Gilson 321 HPLC pump with a Gilson UV/VIS-151 detector (Gilson, Middleton, WI, USA). All solvents used were of spectroscopic grade or were distilled prior to use.

Cultivation, extraction, and isolation of compounds

Streptomyces bacillaris strain MBTC38 was sporulated on colloidal chitin agar plates (4 g chitin, 0.7 g K_2HPO_4, 0.5 g $MgSO_4 \cdot 7H_2O$, 0.3 g KH_2PO_4, 0.01 g $FeSO_4 \cdot 7H_2O$, 0.001 g $MnCl_2 \cdot 4H_2O$, 0.001 g $ZnSO_4 \cdot 7H_2O$, 20 g agar and 17 g sea salt in 1 L distilled water) at 28°C for 10 days. Mature spores were inoculated into 500 mL colloidal chitin liquid medium and incubated at 28°C for 7 days on a rotatory shaker. The entire culture (160 L) was filtered through filter paper and extracted with

an equal volume of ethyl acetate twice. The organic solvents were evaporated to dryness under reduced pressure to obtain 4.4 g of total extracts. Based on the result of the ICL inhibitory activity, the entire extract (4.4 g) was separated through reversed-phase HPLC (Agilent Eclipse XDB-C18, 5 µm, 9.4×250 mm) under 18% ACN with 0.1% trifluoroacetic acid condition (ultraviolet detection at 254 nm, flow rate: 2 mL/min). Compounds **5** and **6** were further purified through reversed-phase HPLC under isocratic conditions with MeOH to obtain 9.1 mg (t_R: 15 min) and 7.8 mg (t_R: 14 min), respectively.

Benzoylation of compound 5

For absolute structural configuration of compound **5**, benzoylation was performed. Compound **5** (0.7 mg, 0.0035 mmol) in pyridine (200 µl) was added dropwise to a solution of benzoic anhydride (2.2 mg, 0.0097 mmol) and dimethylaminopyridine (DMAP, 0.1 mg, 0.00081 mmol) in pyridine (200 µl). The mixture was stirred at room temperature for 8 h. The reaction was diluted with ethylacetate and slowly added with 1 N HCl until pH turned acidic. The crude reaction mixture obtained upon concentrating in vacuo was further purified by analytical HPLC (YMC-ODS column, 4.6×250 mm; 0.7 mL/min; H_2O-ACN gradient from 80:20 to 10:90 in 40 min), yielding benzoyl compound **5** (0.9 mg, 0.0029 mmol, 85 %).

Electronic circular dichroism (ECD) calculation

Based on the density functional theory (DFT) calculations, the geometries were optimized to the ground-state energy level by computer software, Turbomole. The basis parameter sets, def-SVP and the B3-LYP functional for all atoms were employed. The calculated ECD data were measured based on the optimized

structures obtained with TDDFT at the B3-LYP functional. The ECD spectra were obtained by overlapping Gaussian functions for each transition, where σ is the width of the band at height 1/e. Values ΔE_i and R_i represent the excitation energy and rotatory strength for transition i, respectively. In this work, the value of σ was 0.10 eV.

$$\Delta\varepsilon(E) = \frac{1}{2.297 \ \times 10^{-39}} \frac{1}{\sqrt{2\pi\sigma}} \sum \binom{A}{i} \Delta E_i R_i e^{[-(E-\Delta E_i)^2/(2\sigma)^2]}$$

Preparation of recombinant isocitrate lyase of *C. albicans*

Expression and purification of recombinant ICL protein from *C. albicans* ATCC10231 were performed using following procedures with minor modifications (Shin et al., 2005). The gene encoding ICL was amplified by PCR (initial denaturation 94℃ for 3 min, 30 cycles of   94℃ for 1 min, 56℃ for 1 min and 72℃ for 1.5 min and final extension at 72℃ for 10 min) using two primers (forward primer; 5'-AGAATTCCTACCATGCCTTACACTCC-3', reverse primer; 5'-CTTCGTCGACTCAAAATTAAGCCTTG-3'). The PCR product was ligated into pBAD/TOPO-Thio expression vector (Invitrogen, Carlsbad, CA, USA) and transformed into *E. coli* Top10. Following protein expression was induced with 2% arabinose (Sigma-Aldrich, St. Louis, MO, USA) at 25℃ for 8 h, cells were centrifuged (5500 × g, 10 min) and washed with 25 mM MOPs (Duchefa, Amsterdam, Netherlands) buffer. Then cells were lysed with lysozyme treatment (Sigma-Aldrich, St. Louis, MO, USA) and vibra cell sonicator (SONICS, Newtown, CT, USA). After centrifuged (8000 × g, 10 min) for removal of cell debris, the recombinant ICL protein was purified using a Ni-NTA affinity column (Qiagen, Hilden, Germany). The column was washed by MOPs buffer containing 10 mM imidazole (Sigma-Aldrich, St. Louis, MO, USA) and eluted by same buffer with 250 mM imidazole. Imidazole was removed through centrifugation at 5500 × g for 30

min using 50 K Amicon ultra centrifugal filters (Merck, Kenilworth, NJ, USA). The concentration of protein was determined by the Bradford assay using the Bio-Rad protein assay kit (Bio-Rad, Hercules, CA, USA) and bovine serum albumin as a control (Bradford, 1976).

ICL inhibitory activity assay

The ICL inhibitory activity assay was carried out according to the methods previously described (Dixon and Kornberg, 1959; Hautzel et al., 1990). Compound **5**, **6** and 3-nitropropionate (Sigma-Aldrich, St. Louis, MO, USA) known for an ICL inhibitor were dissolved in DMSO at 12.8 mg/mL. The 772 (first cuvette) and 390 (other cuvettes) µL of reaction MOPs buffer containing 3.75 mM $MgCl_2$ (Duchefa, Amsterdam, Netherlands), 1.27 mM of DL-isocitric acid and 4.1 mM phenlhydrazine (Sigma-Aldrich, St. Louis, MO, USA) was mixed with 8 µL of tested samples and serially diluted (final DMSO concentration, 1%). Then, 10 µL of purified ICL (concentration = 2.5 µg/mL) was added and incubated at 37°C for 30 min. The absorbance at 324 nm was measured by UV mini 1240 spectrophotometer (Shimadzu, Kyoto, Japan) at 0 min and 30 min after incubation. The ICL inhibitory effect of each compound was calculated as an absorbance percentage relative to that of sample treated with only DMSO. A half maximal inhibitory concentration, IC_{50} was measured by non-linear regression analysis (Graph Pad ver. 8.0, Prism). 3-Nitropropionate was used as a positive control (Sharma et al., 2000).

Kinetics analysis

Dixon plot is a graphical method to determine the type of enzyme inhibition (Burlingham and Widlanski, 2003). Various concentrations of DL-isocitric acid (0.32, 0.43, 0.64, 1.27 and 2.54 mM), substrate for ICL and $0 \times$ to $2 \times$ MIC of

71

compound **5** were employed for kinetic analysis. Velocity was measured with increased absorbance at 324 nm per minute. Each data point was calculated with the mean of three independent experiments and a graph of inverse velocity against the inverse concentrations of substrate was plotted.

In vitro growth assay

In vitro growth assay was performed under following procedures with minor modifications (Clinical and Laboratory Standards Institute, 2017). Wild-type *C. albicans* SC5314, ATCC10231, ATCC10259, ATCC11006, and ATCC18804 were employed. Five wild-type strains were cultured overnight at 28℃ in yeast nitrogen base (YNB; BD Difco, Sparks, MD, USA) media with 2% glucose and 2% acetate respectively, diluted and adjusted to match the turbidity of a 0.5 McFarland standard at 530 nm wavelength. Stock solutions of the compound **5** and amphotericin B (Sigma-Aldrich, St. Louis, MO, USA) were prepared in DMSO at 25.6 mg/mL. Each stock solution was diluted in YNB media to concentrations ranging from 0.25 to 256 µg/mL. The final DMSO concentration was maintained at 1% by adding DMSO to the medium according to CLSI guidelines. In each well of a 96 well plate, 90 µL of YNB media containing two compounds was mixed with 10 µL of broth with the test strain *C. albicans* (final concentration : 2.5×10^3 cfu/mL). The plates were incubated for 2 days at 28℃ and amphotericin B was used as a positive control. MIC value was defined as the lowest concentration of test compound that prevented cell growth.

Grow phenotype and *icl* expression analysis

C. albicans SC5314 (wild-type strain), MRC10 (Δ*icl*) (*icl*-deletion strain) and MRC11 (Δ*icl* + ICL) (*icl*-complementary strain) were used for confirmation of

growth phenotype. Prof. Michael C. Lorenz (University of Texas Health Science Center, Houston, TX, USA) kindly provided the ICL mutant strains (Ramirez and Lorenz, 2007). Three strains were cultured in YNB broth containing 2% glucose and 2% acetate, respectively at 28℃ for 24 h. Cells were centrifuged (8000 × g, 2 min) and washed with distilled water. The harvested cells were streaked on YNB agar plates containing 2% glucose, 2% acetate and 2% acetate plus 256 µg/mL of compound **5** and incubated at 28℃ for 2 days.

For *icl* expression analysis, overnight cultured *C. albicans* SC5314 was diluted with YNB media containing 2% glucose or 2% acetate and incubated to mid-log phase. Various concentrations of compound **5** (64, 128, or 256 µg/mL) were treated to media containing 2% acetate and incubated at 28℃ for 4 h. Total RNA extraction was carried out based on following procedures. Cells were resuspended with 1 mL of easy-BLUE™ reagent (Intron Biotechnology, Seoul, Korea) and mixtures were transferred into the 2 mL Safe-Lock tube containing the 425 – 600 µm acid-washed glass beads (Sigma-Aldrich, St. Louis, MO, USA). Then cells were disrupted in the Precellys 24 tissue homogenizer (Bertine Technologies, Rockville, Washington, DC, USA) for 5 min at maximum speed. 200 µL chloroform was added into lysates and centrifuged at 4℃ (11,000 × g, 10 min). Following upper aqueous fractions were transferred to a new tube, 400 µL isopropanol was added and centrifuged at 4℃ (11,000 × g, 10 min). The supernatants were removed and 1 mL of 75% ethanol was mixed with pellets and centrifuged at 4℃ (11,000 × g, 10 min). Air dried RNA pellets were dissolved in RNase free water and DNase I (Enzynomics, Daejeon, KOREA) was treated at 37℃ for 10 min for removing residual DNA. The concentration of RNA was measured using a NanoDrop spectrophotometer (ACTGene, Piscataway, NJ, USA).

The complementary DNA (cDNA) was synthesized using SuperScript III cDNA synthesis kit (Enzynomics, Daejeon, KOREA) with following methods. Same concentration of RNAs was mixed with 1 µL oligo dT and dNTPs and RNase free water was added up to 10 µL. Following incubation at 65℃ for 5 min, mixture was placed on ice for at least 3 min. cDNA synthesis mix (4 µL of 25 mM $MgCl_2$, 2 µL of 10× RT buffer, 2 µL of 0.1 M DTT, 1 µL of RNase inhibitor and 1 µL of SuperScript III reverse transcriptase) was added and incubated at 50℃ for 50 min. Following incubation at 85℃ for 5 min for terminating reaction, RNase H was treated at 37℃ for 20 min for eliminating residual RNA. RT-PCR was performed with cDNA and various primers listed on the Table 2. 1 under the conditions: initial denaturation at 95℃ for 5 min, 30 cycles of denaturation at 95℃ for 20 s, annealing at 55℃ for 30 s and elongation at 72℃ for 1 min and final extension at 72℃ for 5 min. The 1% agarose gel electrophoresis was conducted with PCR products and 10× loading buffer at 135 V for 15 min. Agarose gel was detected using Chemi-Doc (Bio-Rad, Hercules, CA, USA) imaging system with ultraviolet light.

Table 2.1. Lists of used oligonucleotides on RT-PCR

Primer	Sequence (5'-3')
ICL-F	ATGCCTTACACTCCTATTGACATTCAAAA
ICL-R	TAGATTCAGCTTCAGCCATCAAAGC
GAPDH-F	ATCACCATCTTCCAGGAG
GAPDH-R	ATGGACTGTGGTCATGAG

Results

Isolation and structural elucidation of compound 5-6

S. bacillaris strain MBTC38 was cultured in colloidal chitin liquid medium at 28°C for 7 days with shaking and filtrated with filter paper. 160 L of filtrate was fractionated twice with equal volumes of ethyl acetate and evaporated. Based on the results of the ICL inhibitory activity assay, the entire extract (4.4 g) was separated through semi-preparative HPLC (Agilent Eclipse XDB-C18, 5 µm, 9.4×250 mm) under isocratic solvent conditions; 18% aqueous acetonitrile with 0.1% TFA (ultraviolet detection at 254 nm, flow rate: 2 mL/min) to yield two compounds; compound **5** (t_R: 15 min, 9.1 mg) and **6** (t_R: 14 min, 7.8 mg) (Fig. 2.2). Structure elucidation of two compounds was assisted by lab of natural products and structure determination in SNU.

The compound **5** was isolated as a pale yellow gum. The molecular formula of this compound was deduced to be $C_8H_{11}NO_3S$ with 4 unsaturation degree, from HRESIMS analysis (*m/z* 200.0385 [M - H]$^-$). The ^{13}C NMR data of compound **5** (MeOH-d_4) showed signals of two carbonyl carbons at δ_C 181.6 and 177.9 (Fig. S24). In conjunction with a strong absorption band at 1775, 1740 cm^{-1} in the IR data, both carbonyl carbons were thought to be amides. Then the presence of single nitrogen inherent from the MS data indicated the presence of an imide group connecting these amide carbonyls by nitrogen.

Aided with the ^1H NMR and HSQC NMR data, the other NMR signals were also diagnosed to be a non-protonated carbon (δ_C 58.7) and two methines (δ_C/δ_H 76.6/4.43, 64.4/2.95), two methylenes (δ_C/δ_H 35.2/2.37 and 2.25, 35.0/1.92 and 1.67), and a methyl (δ_C/δ_H 13.3/2.24) groups (Figs. S25-S26). Based upon the characteristic

76

NMR chemical shifts, the remaining oxygen and sulfur were placed at a methine (δ_C/δ_H 76.6/4.43) and a methyl group, respectively. Thus, compound **5** was thought to be a bicyclic compound.

The planar structure of compound **5** was determined by a combination of ^{1}H-^{1}H COSY and HMBC experiments in MeOH-d_4 and DMSO-d_6 (Figs. S27-S28). First, the COSY data revealed a linear array of two methylenes (CH$_2$-4 and CH$_2$-5) and an oxymethine (CH-6) group that was supported by the mutual HMBC correlations among these: H$_2$-4/C-5 and C-6, H$_2$-5/C-4 and C-5 and H-6/C-4 and C-5 (Fig. 2.3). Despite the weak vicinal H-H coupling ($J_{H-6,H-7}$ = 1 Hz), a methine (δ_C/δ_H 64.4/2.95) was placed at C-7 by the HMBC correlations at H$_2$-5/C-7 and H-7/C-5 and C-6. This interpretation as well as the designation of oxygenated functionality at C-6 was decisively confirmed by the HMBC correlation of a hydroxyl proton (δ_H 5.29, OH-6) with C-5, C-6 and C-7 in DMSO-d_6. The extension of this four carbon system (C-4-C-7) constructing a 5-membered ring was also accomplished by the HMBC correlations of a nonprotonated carbon (δ_C 58.7, C-3) with all of H$_2$-4, H$_2$-5, H-6, H-7. The remaining HMBC correlation at H$_2$-4/C-7 was also supportive of 5-membered ring. In addition, the sulfur-bearing methyl proton (δ_C/δ_H 13.3/2.24, C-9) was secured at C-3 by the crucial 3-bond HMBC correlation.

The preliminary interpretation of spectroscopic data revealed the presence of an imide group (NH-1, C-2 and C-8). The incorporation of this moiety to 5-membered ring system (C-3-C-7) was only available by the simultaneous linkages of the carbonyl carbons to the open ends of ring system: C-2/C-3 and C-7/C-8. This interpretation was also supported by a series of HMBC correlations: H$_2$-4/C-2, H-6/C-8, and H-7/C-2 and C-8. Thus, the last cyclic moiety of compound **5** was determined as a pyrrolidine-2,5-dione.

The molecular formula of pale red compound **6** was estimated as $C_8H_{12}N_2O_2S$, with 4 degrees of unsaturation, by positive HRESIMS analysis (*m/z* 201.0687 [M + H]$^+$). The ^{13}C NMR data of compound **6** showed signals of a amide carbon (δ_C 160.8) and four sp^2 carbons (δ_C 126.0-108.6) (Fig. S35). Based on the combined ^1H NMR and HSQC data, the chemical shifts and splitting patterns (δ_H 6.85-6.07) of corresponding protons were indicative of aromatic moieties. The NMR data of **6** also contained two methylenes (δ_C/δ_H 32.6/3.60 and 3.52, 53.8/3.00 and 2.86), of which the former carbon would bear nitrogen according to their carbon and proton chemical shifts. The remaining methyl signal in the NMR data, the carbon and proton chemical shifts indicated the presence of a thiomethyl (δ_C/δ_H 38.1/2.58) (Figs. S36-S37).

The gross structure of **6** was determined by combined ^1H-^1H COSY and HMBC experiments (Figs. S38-S39 and 2.3). First, the COSY data showed the proton spin couplings of a pyrrole group (δ_C/δ_H 121.4/6.85, 110.0/6.74, and 108.6/6.07; CH-2-CH-4), which was confirmed by the HMBC correlations among these. The COSY data also showed a linear array of two methylenes and a nitrogeous proton (δ_C/δ_H 32.6/3.60 and 3.52, 53.8/3.00 and 2.86, and 8.26; CH$_2$-8, CH$_2$-9 and NH-7). Aided by their ^1H and ^{13}C NMR chemical shifts and the crucial HMBC correlation at H$_2$-8/C-6, an amide moiety was identified for C-6 – CH$_2$-8. Similarly, the CH$_3$-10 methyl was connected to the CH$_2$-9 methylene by a sulfoxide linkage according to the HMBC correlation at H$_3$-10/C-9. Thus, the overall structure of compound **6** was determined to be a pyrrole bearing alkaloid and correlated with the compound designated as CAS number 1928723-80-1. Based on the combined spectroscopic analyses, compounds **5**–**6** were identified and named as bacillimide (**5**) bacillapyrrole (**6**).

Bacillimide: ^1H NMR (DMSO-*d6*) δ_H 11.44 (1H, br s), 5.29 (1H, s), 4.27 (1H, br s), 2.86 (1H, dd, *J* = 1.0, 1.0 Hz), 2.25 (1H, dd, *J* = 13.0, 6.0 Hz), 2.19 (1H, ddd,

$J = 13.0$, 6.5, 1.5 Hz), 2.15 (3H, s), 1.76 (1H, ddd, $J = 13.5$, 6.5, 1.5 Hz), 1.47 (1H, ddd, $J = 13.0$, 7.0, 2.5 Hz); ^{13}C NMR (DMSO-$d6$) δ_C 180.6 (C), 177.9 (C), 75.0 (CH), 63.3 (CH), 57.8 (C), 34.6 (CH$_2$), 34.4 (CH$_2$), 13.3 (CH$_3$); HRESIMS m/z 200.0385 [M - H]$^-$ (calcd for C$_8$H$_{10}$NO$_3$S, 200.0385).

Bacillapyrrole: ^{1}H NMR (DMSO-$d6$) δ_H 11.45 (1H, br s), 8.26 (1H, t, $J = 4.5$ Hz) 6.85 (1H, d, $J = 1.5$ Hz), 6.74 (1H, d, $J = 1.5$ Hz), 6.07 (1H, t, $J = 2.0$ Hz), 3.60 (1H, ddd, $J = 13.0$, 7.0, 1.5 Hz), 3.52 (1H, ddd, $J = 13.0$, 6.0, 1.5 Hz) 3.00 (1H, ddd, $J = 13.5$, 6.0, 1.5 Hz), 2.86 (1H, ddd, $J = 12.5$, 6.0, 1.0 Hz), 2.58 (3H, s); ^{13}C NMR (DMSO-$d6$) δ_C 160.8 (C), 126.0 (C), 121.4 (CH), 110.0 (CH), 108.6 (CH), 53.8 (CH$_2$), 38.1 (CH$_3$), 32.6 (CH$_3$); HRESIMS m/z 201.0687 [M + H]$^+$ (calcd for C$_8$H$_{13}$N$_2$O$_2$S, 201.0687).

Figure 2.1. Structures of compounds 5-6

5) Bacillimide; 6) bacillapyrrole.

5
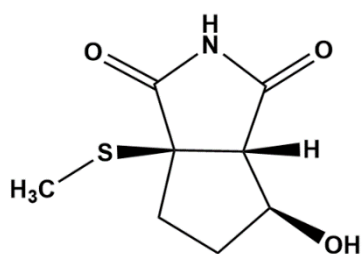
6
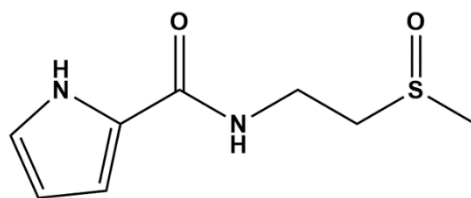
Figure 2.2. Isolation procedures of compounds 5-6

Streptomyces bacillaris MBTC38 culture (160L)

Colloidal chitin medium, 28℃, 7days

Mycelium

Filtrate

Liquid-liquid extraction

Ethyl acetate (4.4g)

Revered-phase HPLC
18% (v/v) aq. ACN + 0.1% TFA

5
(9.1 mg)

6
(7.8 mg)
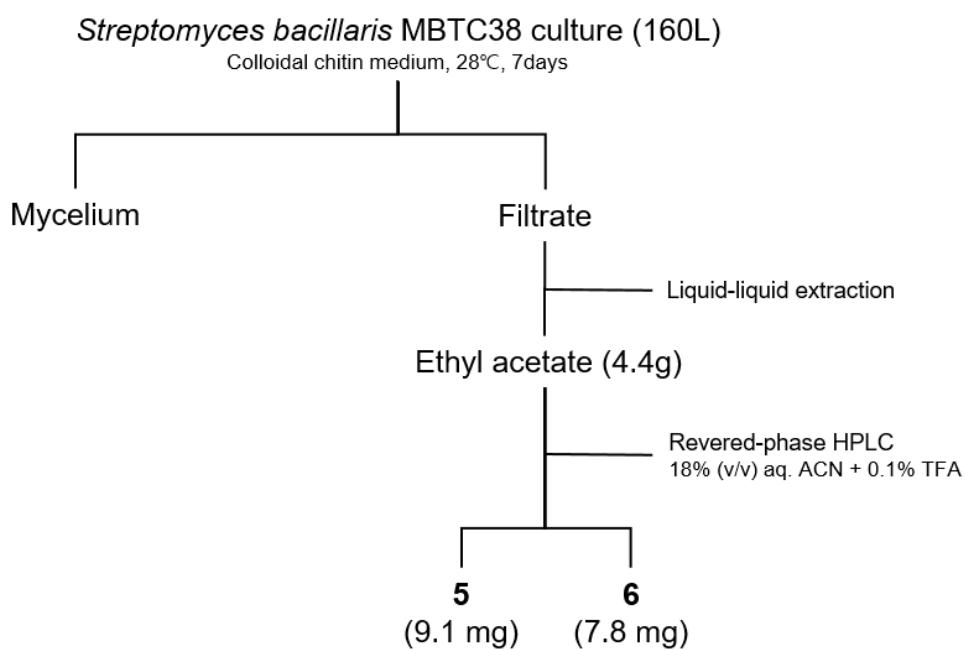
Figure 2.3. COSY and HMBC correlations of compounds 5-6

Thick black lines represented COSY correlations and black arrows symbolized HMBC signals.

5
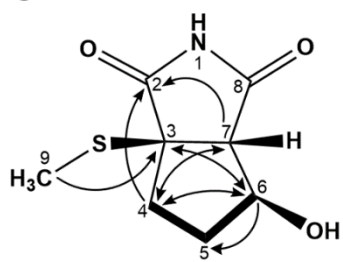
6
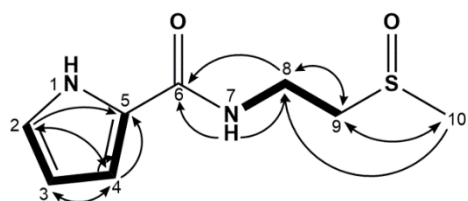
━━━━ COSY ───▶ HMBC

Absolute configuration of bacillimide

The bacillimide bears three stereogenic centers at C-3, C-6, and C-7. The conspicuous NOESY cross-peak at H-7/H$_3$-9 assigned the 3R* and 7S* configurations. However, the configuration at C-6 was unassigned, because there were no reliable NOESY correlations of either H-6 or 6-OH with the bridgehead protons H-7 or H$_3$-9, despite a number of cross-peaks with neighboring ring protons (Fig. S29). This problem was solved by constructing a more-rigid space-filling derivative of bacillimide. Thus, a benzoyl analog was prepared by the treatment of bacillimide with benzoic anhydride (yield 85 %) (Scheme 2.1). Beside the pre-described cross-peak at H-7/H$_3$-9, additional NOESY cross-peak signals H-3′/H$_3$-9 (H-7′/H$_3$-9) were detected in benzoyl bacillimide (Fig. 2.4). Thus, the relative configurations of benzoyl bacillimide assigned as 3R*, 6S* and 7S*. Given these configurations, the calculated ECD profile for benzoyl bacillimide with the 3R, 6S and 7S configurations matched well with the observed profile in both the intensity and wavelength of the signals (Fig. 2.5a). In this way, the absolute configurations of bacillimide (**5**) at C-3, C-6, and C-7 were assigned as the 3R, 6S and 7S. Thus, compound **5**, designated bacillimide, was determined to be a new cyclopenta[*c*]pyrrole-1,3-dione class compound (Fig. 2.5b).

Benzoyl bacillimide: ^{1}H NMR (DMSO-d_6, 800 MHz) δ_H 7.98 (2H, d, J = 8.0 Hz), 7.51 (1H, t, J = 7.5 Hz), 7.55 (2H, t, J = 7.5 Hz), 5.46 (1H, d, J = 3.8 Hz), 3.28 (1H, overlap), 2.31 (1H, dd, J = 13.1, 7.1 Hz), 2.13 (3H, s), 2.10 (1H, m), 2.02 (1H, J = 14.3, 6.9 Hz), 1.78 (1H, m); ^{13}C NMR (DMSO-d_6, 800 MHz) C-2 (C), C-8 (C), δ_c 164.8 (C), 133.5 (CH), 129.6 (C), 129.2 (CH), 128.8 (CH), 78.0 (CH), 60.2 (CH), 57.9 (C), 34.3 (CH$_2$), 31.2 (CH$_2$), 12.6 (CH$_3$); HRMS (ESI) *m/z:* [M+Na]$^+$ Calcd for 328.06140; found 328.06124.

Scheme 2.1. Benzolyation reaction of bacillimide

Reagents and conditions: a) benzoic anhydride, DMAP, pyridine, rt, 8 h, 85 %
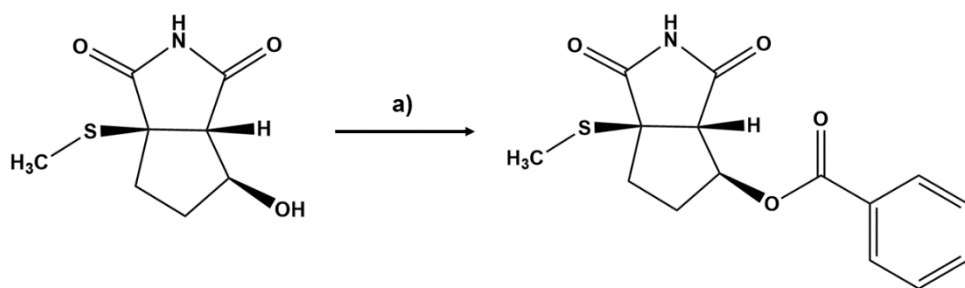
Figure 2.4. Key NOE correlations of benzoyl bacillimide

NOE (800 MHz) spectra of benzoyl bacillimide was analyzed in DMSO-*d6*

NOESY

91
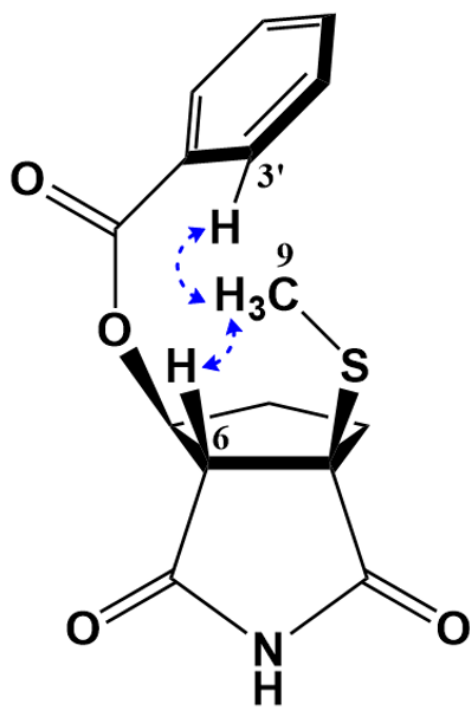
Figure 2.5. Absolute configuration of benzoyl bacillimide

(**a**) Calculated and experimental EDC spectra of benzoyl bacillimide. Based on the optimized structures obtained with TDDFT at the B3-LYP functional, the ECD data were measured. (**b**) Final structure of benzoyl bacillimide

(a)

(b)
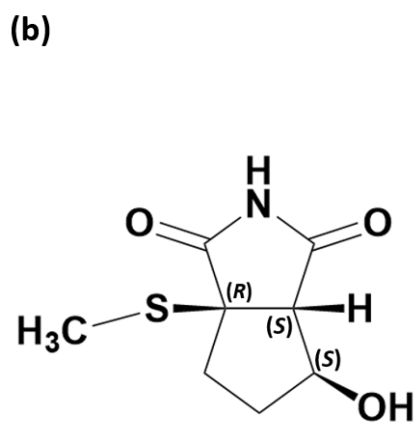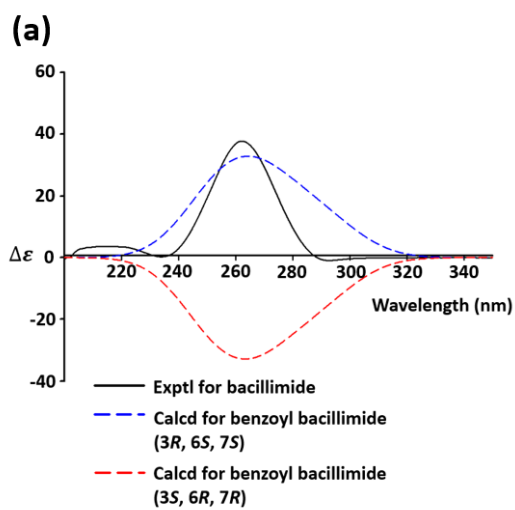
ICL inhibitory activity of isolated compounds

Isolated compounds (**5**-**6**) were tested for inhibitory activity against *C. albicans* ICL based on the methods previously reported (Shin et al., 2005). The IC_{50} values of two compounds and 3-nitropropionate known for a potent ICL inhibitor are shown in Table 2.2. Bacillimide strongly inhibited ICL of *C. albicans* (IC_{50} = 44.24 µM), which is twice higher than IC_{50} value of 3-nitropropionate (IC_{50} = 21.49 µM) (Fig. 2.6a). To confirm the type of inhibition, kinetics analysis was carried out with bacillimide (inhibitor) and DL-isocitric acid (substrate). The Dixon plot showed bacillimide behaved as a mixed inhibitor with an inhibitor constant (Ki) value of 0.42 mM (Fig. 2.6b).

Table 2.2. Inhibitory activity of isolated compounds against the ICL enzyme and growth of *C. albicans* ATCC10231

Compound	ICL IC_{50} (μM)	MIC (μM)
Bacillimide	44.24 ± 1.05	>1273.64
Bacillapyrrole	190.45 ± 3.86	>1280.00
3-Nitropropionate	21.49 ± 0.97	>2149.46
Amphotericin B	Not determined	0.5

3-Nitropropionate and amphotericin B were used as a standard inhibitor of ICL and a representative antifungal drug, respectively.

Figure 2.6. ICL inhibitory activity and inhibitor type of bacillimide

(**a**) Comparison of dose-dependent inhibition curves of the bacillimide and 3-nitropropionate against ICL enzyme of *C. albicans* ATCC10231. Each point represents the mean ± SD (n=3). The data were analyzed using non-linear regression curve fitting in GraphPad Prism ver. 8.0. (**b**) Dixon plot for identifying inhibition type of bacillimide. [S] and V represent the substrate concentration (mM) and reaction velocity (ΔAbsorbace$_{324\ nm}$/sec), respectively. Each data point shows the mean of three independent experiments.

(a)

Bacillaimide

Percentage of inhibition (%) vs Concentration (μM)

$IC_{50} = 44.24 \pm 1.05$ μM

3-Nitroproprionate

Percentage of inhibition (%) vs Concentration (μM)

$IC_{50} = 21.49 \pm 0.97$ μM

(b)

1/V vs 1/[S]

- ▲ 2× MIC μM
- ■ 1× MIC μM
- ● 0 μM

97
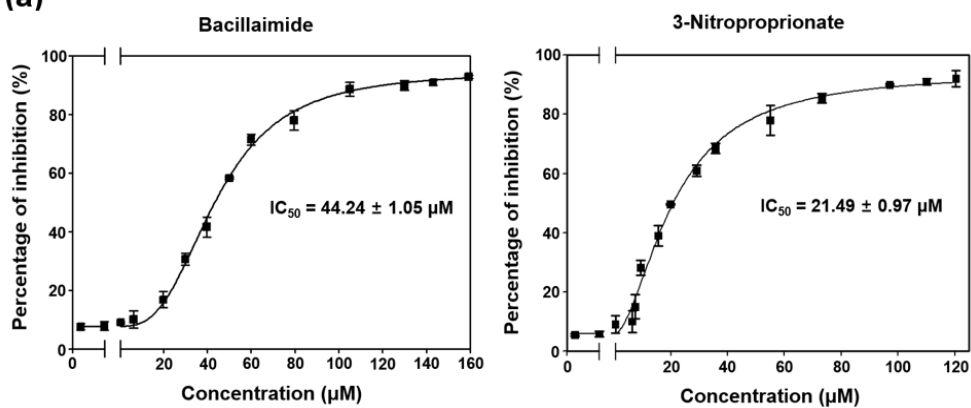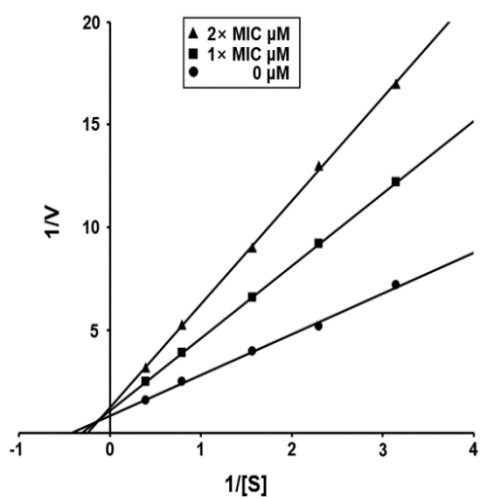
Inhibition of C$_2$ substrate utilization

The glyoxylate cycle is an essential metabolic pathway for virulence in *C. albicans*. When *C. albicans* is phagocytosed by a macrophage, glyoxylate cycle is activated to utilize C$_2$ carbon source such as fatty acid and acetate (McKinney et al., 2000). It was expected that ICL inhibitory compounds would suppress nutrient uptake from C$_2$ carbon sources and survival of the pathogen in the macrophage. To confirm whether bacillimide affects C$_2$ substrate use, five *C. albicans* strains; ATCC10231, ATCC10259, ATCC11006, ATCC18804 and SC5314 were grown in YNB broth containing either 2% glucose or 2% acetate as the only carbon source. Bacillimide inhibited growth of *C. albicans* in acetate at 256 µg/mL while inhibitory effect on cell growth was not monitored in glucose (Table 2.3). These results show that the compound hinders ICL-mediated proliferation under C$_2$-carbon-utilizing conditions.

Table 2.3. Inhibitory effect of bacillimide on five *C. albicans* strains grown in glucose and acetate as a sole carbon source

Strain	MIC (µg/mL)			
	Glucose		Acetate	
	Bacillimide	Amp B[1]	Bacillimide	Amp B[1]
SC5314	>256	0.5	256	0.5
ATCC10231	>256	0.5	256	0.5
ATCC10259	>256	0.5	256	0.5
ATCC11006	>256	1	256	0.5
ATCC18804	>256	1	256	1

C. albicans (2.5×10^3 cfu/mL) were incubated with various concentrations of bacillimide for 2 days at 28°C in YNB broth containing 2% glucose and 2% acetate. [1]Amphotericin B (Amph B) was used as a standard antifungal drug.

Effects of bacillimide on growth phenotype and *icl* expression

To confirm whether bacillimide affects the cell phenotype of wild type and the *icl*-deletion mutant, a growth assay was carried out using *C. albicans* SC5314 (wild-type), *icl*-deletion mutant (MRC10) and *icl*-complementary mutant (MRC11). These strains were streaked onto YNB agar containing 2% glucose or 2% potassium acetate with or without 256 µg/mL of bacillimide. All strains normally grew on both YNB agar plates with glucose and glucose plus the compound. However, MRC10 strain did not grow using acetate as a sole carbon source. Moreover, no cell growth was monitored on the YNB agar plate with acetate plus bacillimide (Fig. 2.7a). To confirm the effects of bacillimide on *icl* expression, semi-quantitative reverse-transcription (RT)-PCR was performed. When SC5314 and MRC11 strains were grown in YNB broth with glucose, *icl*-specific PCR product was not detected in the cultures. However, *icl* expression was strongly monitored when these cells were cultured with acetate. The intensity of PCR band related to *icl* expression reduced with increasing concentrations of bacillimide in the cell cultures (Fig. 2.7b). The expression of GAPDH, house keeping gene in *C. albicans*, was uniformly monitored in all cell cultures regardless of presence of the inhibitory compound. These results indicate that bacillimide inhibits *icl* expression in *C. albicans* under C_2-carbon-utilizing conditions.

Figure 2.7. Analysis of growth phenotypes and *icl* expression in presence of bacillimide

a) *C. albicans* SC5314 (wild-type strain), MRC10 (Δ*icl*) (*icl*-deletion strain) and MRC11 (Δ*icl* + ICL) (*icl*-complementary strain) were cultured on YNB agar plates with 2% glucose or 2% acetate containing 0 µg/mL or 256 µg/mL of bacillimide for 2 days at 28°C. b) Mid-log phase of three *C. albicans* strains in YNB broth containg 2% glucose (Glu) was treated with no bacillimide while those in YNB broth containing 2% acetate (Ace) was treated with various concentrations of bacillimide (C1: 64 µg/mL, C2: 128 µg/mL, C3: 256 µg/mL) and incubated for 4 h at 28°C. Total RNA was extracted from these cells and *icl* expression was analyzed with semi-quantitative RT-PCR. The GAPDH, a house keeping gene was used as a positive control.

(a)

Glucose

Glucose + bacillimide

Acetate

Acetate + bacillimide

Wild-type

Δicl + ICL

Δicl

(b)

	Wild-type					Δicl + ICL					Δicl		
	Glu	Ace	Ace + C1	Ace + C2	Ace + C3	Glu	Ace	Ace + C1	Ace + C2	Ace + C3	Glu	Ace	Ace + C3
GAPDH													
ICL													

C1: 64 µg/mL; C2: 128 µg/mL; C3: 256 µg/mL

103
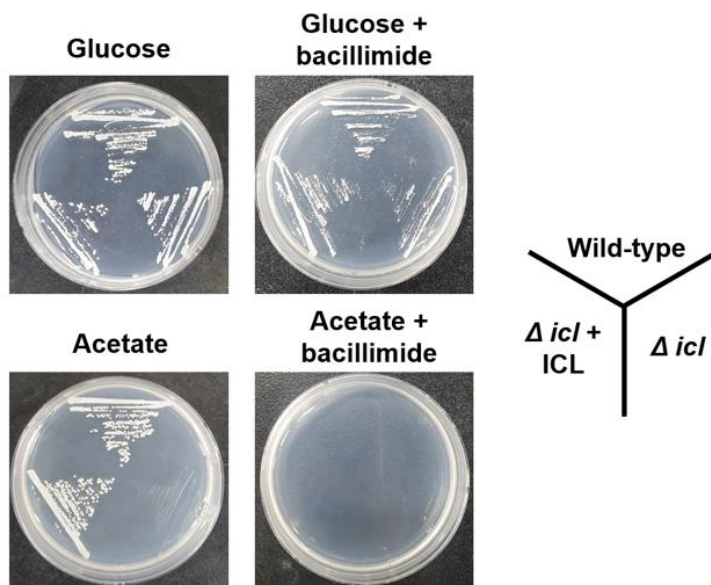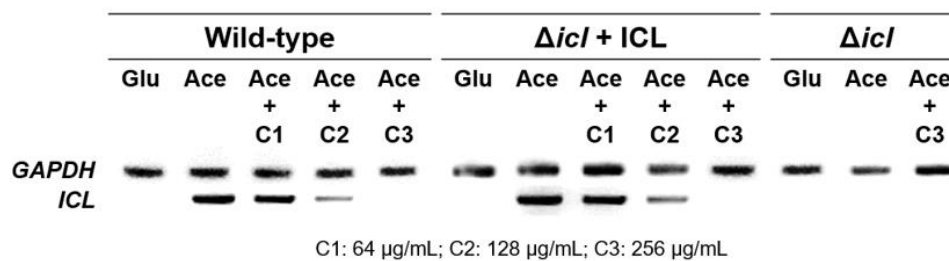
Discussion

The glyoxylate cycle, one of the metabolic pathways in a number of organisms, is catalyzed by two necessary enzymes; ICL and malate synthase. It was reported that various pathogenic microorganisms utilize this cycle for uptake of C_2 carbon source in nutrient-limited environments and to infect host (Kunze et al., 2006; Strijbis and Distel, 2010). Because C_2 carbon sources such as fatty acid are abundant in macrophage phagolysosomes, enzymes related glyoxylate cycle is necessarily up-regulated. The Research on candidiasis in mice has indicated that *icl*-mutant strain lost its virulence and the ability of persistence in host cell was notably reduced (Goldstein and McCusker, 2001; Lorenz and Fink, 2001; Ramirez and Lorenz, 2007). Because the glyoxylate cycle does not exist in mammalian cells, ICL have been evaluated as a promising target of antifungal drugs. Furthermore, inhibitors of ICL have little likelihood to cause resistant strains since ICL enzyme is not essential components in microorganisms. These advantages of ICL as a drug target have increased their value in pharmacological fields. Herein, identified two compounds; bacillimide (**5**) and bacillapyrrole (**6**) showed ICL inhibitory activity. Among two compounds, bacillimide exhibited potential inhibitory activity against toward *C. albicans* ICL as a mixed type inhibitor. Growth assays and semi-quantitative RT-PCR with *icl*-deletion mutants indicated that bacillimide dose-dependently reduced *icl* expression in *C. albicans* under C2-carbon-utilizing conditions.

Alkaloids containing nitrogen atoms in their structure exhibited structural diversity and various pharmacological activities such as anti-tumor, anti-malarial and anti-inflammatory effects. In this study, alkaloid type compounds, bacillimide (**5**) and bacillapyrrole (**6**) were isolated from marine-derived *Streptomyces* MBTC38. Among them, novel compound, bacillimide possesed unprecedented thio-mehtyl

group attached adjacent two five rings. NOESY signals between methyl group proton and H-7, hydroxyl group of bacillimide were not observed because the volume of hydroxyl group of C-6 and H-7 was inadequate for noticeable correlations. Benzoylation for attachment of bulky group at C-6 enabled NOE correlations, which characterized relative configuration of bacillimide. Furthermore, ECD measurement determined the absolute structure of bacillimide (3R, 6S, 7S). Nitrosporeusine A and B which have a similar core structure with bacillimide were previously described with anti-influenza H1N1 virus activitity (Yang et al., 2013). Therefore, in vitro anti-viral assay was carried out with bacillimide and SARS-CoV-2 virus. However, bacillimide exhibited no inhibitory effect against SARS-CoV-2 virus (data not shown). In chemical synthesis of derivatives of nitrosporeusines, the analogue that hydroxyl group at C-6 was substituted with acetoxy group and fluorobenzene was attached thioester bond showed the most significant anti-inflammatory potential (Philkhana et al 2017). Because bacillimide possesses relatively water-soluble functional group such as hydroxyl group at C-6 and methyl group at thioester bond, anti-viral activity of this compound did not exhibited.

The genes encoding enzymes related glyoxylate cycle are required for virulence of microorganisms such as *M. tuberculosis a*nd *C. albicans,* which enabled them to survive inside macrophages (McKinney et al., 2000; Lorenz et al., 2001). Therefore, I hypothesized that inhibitors against enzymes of glyoxylate cycle prevented the uptake of nutrient and reduced the survival rate of these pathogens in macrophages. To identify this assumption, I confirmed the effects of bacillimide on the growth phenotype and ICL transcription of *C. albicans* strains: SC5314 (wild-type), MRC10 (Δ*icl*), and MRC11 (Δ*icl* + ICL). Strains SC5314 and MRC11 did not grown on the YNB agar plate plus acetate and 256 μg/mL of bacillimide. Furthermore, bacillimide reduced mRNA expression of *icl*, which proposed this

105

compound specifically inhibited ICL. The primary target of bacillimide is further studied in that this compound inhibited both ICL and ICL encoding gene, *icl*.

References

Agudelo D, Berube G and Tajmir-Riahi HA (2016a) An overview on the delivery of antitumor drug doxorubicin by carrier proteins. *Int. J. Biol. Macromol*. 88, 354-360.

Agudelo D, Bourassa P, Berube G and Tajmir-Riahi HA (2016b) Review on the binding of anticancer drug doxorubicin with DNA and tRNA: structural models and antitumor activity. *J. Photochem. Photobiol*. *B*. 158, 274-279.

Aminov RI (2010) A brief history of the antibiotic era: lessons learned and challenges for the future. *Front. Microbiol.* 1, 1-7.

Ang KKH, Holmes MJ, Higa T, Hamann MT and Kara UAK (2000) In vivo antimalarial activity of the beta-carboline alkaloid Manzamine A. *Antimicrob. Agents Chemother*. 44, 1645-1649.

Arshad S, Huang V, Hartman P, Perri MB, Moreno D and Zervos MJ (2017) Ceftaroline fosamil monotherapy for methicillin-resistant *Staphylococcus aureus* bacteremia: a comparative clinical outcomes study. *Int. J. Infect. Dis.* 57, 27-31.

Bajaksouzian S, Visalli MA, Jacobs MR and Appelbaum PC (1997) Activities of levofloxacin, ofloxacin, and ciprofloxacin, alone and in combination with amikacin, against acinetobacters as determined by checkerboard and time-kill studies. *Antimicrob. Agents Chemother.* 41(5), 1073-1076.

Barber M and Rozwadowska-Dowzenko M (1948) Infection by Penicillin-Resistant *Staphylococci. Lancet* 641-644.

Blunt JW, Carroll AR, Copp BR, Davis RA, Keyzers RA and Prinsep MR (2018) Marine natural products. *Nat. Prod. Rep*. 35, 8-53.

Bradford M (1976) The Bradford assay. *Anal. Biochem*. 72, 248.

Braña AF, Sarmiento-Vizcaíno A, Pérez-Victoria I, Otero L, Fernández J, Palacios JJ et al. (2017) Branimycins B and C, antibiotics produced by the abyssal actinobacterium *Pseudonocardia carboxydivorans* M-227. *J. Nat. Prod*. 80, 569-573.

Bull AT, Ward AC and Goodfellow M (2000) Search and discovery strategies for biotechnology: the paradigm shift. *Microbiol. Mol. Biol. Rev*. 64, 573-606.

Burlingham BT and Widlanski TS (2003) An intuitive look at the relationship of Ki and IC$_{50}$: a more general use for the Dixon plot. *J. Chem. Educ*. 80(2), 214.

Centers for Disease Control and Prevention (2019) *Antibiotic resistance threats in the United States, 2019*. US Department of Health and Human Services, Centers for Disease Control and Prevention, USA.

Chaudhuri RR, Allen AG, Owen PJ, Shalom G, Stone K and Harrison M (2009) Comprehensive identification of essential *Staphylococcus aureus* genes using transposon-mediated differential hybridisation (TMDH). *BMC Genomics* 10(1), 1-18.

Clark C, Kosowska-Shick K, McGhee P, Dewasse B, Beachel L and Appelbaum PC (2009) Resistance selection studies comparing the activity of razupenem (PTZ601) to vancomycin and linezolid against eight methicillin-resistant and two methicillin-susceptible *Staphylococcus aureus* strains. *Antimicrob. Agents Chemother.* 53, 3118-3121.

Clinical and Laboratory Standards Institute (2018) *Reference method for broth dilution antifungal susceptibility testing of yeasts*, (4th ed.), CLSI, USA.

Clinical and Laboratory Standards Institute (2018) *Methods for Dilution Antimicrobial Susceptibility Test for Bacteria That Grow Aerobically*, (11th ed.), CLSI, USA.

Cordell GA, Quinn-Beattie ML and Farnsworth NR (2001) The potential of alkaloids in drug discovery. *Phytother. Res*. 15(3), 183-205.

Crofton J and Mitchison DA (1948) Streptomycin resistance in pulmonary tuberculosis. *Br. Med. J.* 2(4588), 1009.

Dixon GH and Kornberg HL (1959) Assay methods for key enzymes of the glyoxylate cycle. *Biochem. J.* 72, 3.

Dunn MF, Ramirez-Trujillo JA, Hernández-Lucas I and Dunn M (2009) Major roles of isocitrate lyase and malate synthase in bacterial and fungal pathogenesis. *Microbiology* 155, 3166-3175.

Fang L, Guell M, Church GM and Pfeifer BA (2018) Heterologous erythromycin production across strain and plasmid construction. *Biotechnol. Prog*. 34, 271-276.

Fenical W and Jensen PR (2006) Developing a new resource for drug discovery: marine actinomycete bacteria. *Nat. Chem. Biol. 2*(12), 666-673.

Ferrero L, Cameron B and Crouzet J (1995) Analysis of *gyrA* and *grlA* mutations in stepwise-selected ciprofloxacin-resistant mutants of *Staphylococcus aureus*. *Antimicrob. Agents Chemother.* 39, 1554-1558.

Friedman L, Alder JD and Silverman JA (2006) Genetic changes that correlate with reduced susceptibility to daptomycin in *Staphylococcus aureus*. *Antimicrob. Agents Chemother.* 50, 2137-2145.

Froger A and Hall JE (2007) Transformation of plasmid DNA into *E. coli* using the heat shock method. *J. Vis. Exp*. 6, 253.

Furlan RLA, Garrido LM, Brumatti G, Amarante-Mendes GP, Martins RA, Facciotti MCR et al. (2002) A rapid and sensitive method for the screening of DNA intercalating antibiotics. *Biotechnol. Lett.* 24, 1807-1813.

Goldstein AL and McCusker JH (2001) Development of *Saccharomyces cerevisiae* as a model pathogen: a system for the genetic identification of gene products required for survival in the mammalian host environment. *Genetics* 159, 499.

Grkovic T, Ding Y, Li XC, Webb VL, Ferreira D and Copp BR (2008) Enantiomeric discorhabdin alkaloids and establishment of their absolute configurations using theoretical calculations of electronic circular dichroism spectra. *J. Org. Chem*. 73, 9133-9136.

Gul W and Hamann MT (2005) Indole alkaloid marine natural products: an established source of cancer drug leads with considerable promise for the control of parasitic, neurological and other diseases. *Life Sci*. 78, 442-453.

Hartman BJ and Tomasz A (1984) Low-affinity penicillin-binding protein associated with beta-lactam resistance in *Staphylococcus aureus*. *J. Bacteriol*. 158, 513-516.

Hassanzadeh S, Pourmand MR, Afshar D, Dehbashi S and Mashhadi R (2016) TENT: a rapid DNA extraction method of *Staphylococcus aureus*. *Iran J. Public Health* 45, 1093.

Hautzel R, Anke H and Sheldrick WS (1990) Mycenon, a new metabolite from a *Mycena* species TA 87202 (basidiomycetes) as an inhibitor of isocitrate lyase. *J. Antibiot*. 43, 1240-1244.

Hertweck C, Luzhetskyy A, Rebets Y and Bechthold A (2007) Type II polyketide synthases: gaining a deeper insight into enzymatic teamwork. *Nat. Prod. Rep*. 24, 162-190.

Hu Y and MacMillan JB (2012) A new peptide isolated from a marine derived *Streptomyces bacillaris*. *Nat. Prod. Commun.* 7, 211-214.

Ichinose K, Ozawa M, Itou K, Kunieda K and Ebizuka Y (2003) Cloning, sequencing and heterologous expression of the medermycin biosynthetic gene cluster of *Streptomyces* sp. AM-7161: towards comparative analysis of the benzoisochromanequinone gene clusters. *Microbiology* 149(7), 1633-1645.

Janda JM and Abbott SL (2007) 16S rRNA gene sequencing for bacterial identification in the diagnostic laboratory: pluses, perils, and pitfalls. *J. Clin. Microbiol.* 45, 2761-2764.

Jiang ZK, Guo L, Chen C, Liu SW, Zhang L, Dai SJ et al. (2015) Xiakemycin A, a novel pyranonaphthoquinone antibiotic, produced by the *Streptomyces* sp. CC8-201 from the soil of a karst cave. *J. Antibiot.* 68, 771-774.

Jiang YJ, Zhang DS, Zhang HJ, Li JQ, Ding WJ, Xu CD et al. (2018) Medermycin-type naphthoquinones from the marine-derived *Streptomyces* sp. XMA39. *J. Nat. Prod.* 81, 2120-2124.

Katayama Y, Ito T and Hiramatsu KA (2000) New class of genetic element, *Staphylococcus* cassette chromosome *mec*, encodes methicillin resistance in *Staphylococcus aureus*. *Antimicrob. Agents Chemother.* 44, 1549-1555.

Katz L and Baltz RH (2016) Natural product discovery: past, present, and future. *J. Ind. Microbiol. Biotechnol.* 43, 155-176.

Keatinge-Clay AT (2012) The structures of type I polyketide synthases. *Nat. Prod. Rep.* 29(10), 1050-1073.

Kisgen J and Whitney D (2008) Ceftobiprole, a broad-spectrum cephalosporin with activity against methicillin-resistant *Staphylococcus aureus* (MRSA). *P.T.* 33(11), 631.

Kochanowska-Karamyan AJ, Araujo HC, Zhang X, El-Alfy A, Carvalho P, Avery M et al. (2020) Isolation and synthesis of veranamine, an antidepressant lead from the marine sponge *Verongula rigida*. *J. Nat. Prod.* 83(4), 1092-1098.

Kosowska-Shick K, Clark C, Pankuch GA, McGhee P, Dewasse B, Beachel L et al. (2009) Activity of telavancin against *staphylococci* and *enterococci* determined by MIC and resistance selection studies. *Antimicrob. Agents Chemother.* 53, 4217-4224.

Kunze M, Pracharoenwattana I, Smith SM and Hartig AA (2006) Central role for the peroxisomal membrane in glyoxylate cycle function. *Biochim. Biophys. Acta.* 1763, 1441-1452.

Le TC, Yang I, Yoon YJ, Nam SJ and Fenical W (2016) Ansalactams B-D illustrate further biosynthetic plasticity within the ansamycin pathway. *Org. Lett.* 18, 2256-2259.

Levy SB (1982) Microbial resistance to antibiotics: an evolving and persistent problem. *Lancet 2,* 83-88.

Levy SB (1992) *The Antibiotic Paradox.* Springer, Germany.

Levy SB and Marshall B (2004) Antibacterial resistance worldwide: causes, challenges and responses. *Nat. Med.* 10, S122-S129.

Lineweaver H and Burk D (1934) The determination of enzyme dissociation constants. *J. Am. Chem. Soc.* 56, 658-666.

Liu QY, Zhou T, Zhao YY, Chen L, Gong MW, Xia QW et al. (2015) Antitumor effects and related mechanisms of penicitrinine A, a novel alkaloid with a unique spiro skeleton from the marine fungus *Penicillium citrinum*. *Mar. Drugs* 13(8), 4733-4753.

Lorenz MC and Fink GR (2001) The glyoxylate cycle is required for fungal virulence. *Nature* 412, 83.

Lown JW (1983) The mechanism of action of quinone antibiotics. *Mol. Cell. Biochem.* 55(1), 17-40.

McKinney JD, Zu Bentrup KH, Muñoz-Elías EJ, Miczak A, Chen B, Chan WT et al. (2000) Persistence of *Mycobacterium tuberculosis* in macrophages and mice requires the glyoxylate shunt enzyme isocitrate lyase. *Nature* 406, 735-738.

Nass NM, Farooque S, Hind C, Wand ME, Randall CP, Sutton JM et al. (2017) Revisiting unexploited antibiotics in search of new antibacterial drug candidates: the case of γ-actinorhodin. *Sci. Rep.* 7, 1-11.

Naught M, Wilkinson A, Nic M, Jirat J, Kosata B and Jenkins A (2006) *Compendium of chemical terminology* (2nd ed.). IUPAC, UK.

Ng EY, Trucksis M and Hooper DC (1996) Quinolone resistance mutations in topoisomerase IV: relationship to the *flqA* locus and genetic evidence that topoisomerase IV is the primary target and DNA gyrase is the secondary target of fluoroquinolones in *Staphylococcus aureus*. *Antimicrob. Agents Chemother.* 40, 1881-1888.

Nomoto K, Okabe T, Suzuki H and Tanaka N (1988) Mechanism of action of lactoquinomycin A with special reference to the radical formation. *J. Antibiot.* 41, 1124-1129.

Okabe T, Nomoto K, Funabashi H, Okuda S, Suzuki H and Tanaka N (1985) Lactoquinomycin, a novel anticancer antibiotic. II. physico-chemical properties and structure assignment. *J. Antibiot.* 38(10), 1333-1336.

O'Neill J (2016) *Tackling drug-resistant infections globally: final report and recommendations*. Government of the United Kingdom, UK.

Osterman IA, Komarova ES, Shiryaev DI, Korniltsev IA, Khven IM, Lukyanov DA et al. (2016) Sorting out antibiotics' mechanisms of action: a double fluorescent protein reporter for high-throughput screening of ribosome and DNA biosynthesis inhibitors. *Antimicrob. Agents Chemother.* 60, 7481-7489.

Osterman IA, Wieland M, Maviza TP, Lashkevich KA, Lukianov DA, Komarova ES et al. (2020) Tetracenomycin X inhibits translation by binding within the ribosomal exit tunnel. *Nat. Chem. Biol.* 16, 1071-1077.

Pagmadulam B, Tserendulam D, Rentsenkhand T, Igarashi M, Sawa R, Nihei CI et al. (2020) Isolation and characterization of antiprotozoal compound-producing *Streptomyces* species from Mongolian soils. *Parasitol. Int.* 74, 101961.

Pan HQ, Zhang SY, Wang N, Li ZL, Hua HM, Hu JC et al. (2013) New spirotetronate antibiotics, lobophorins H and I, from a South China Sea-derived *Streptomyces* sp. 12A35. *Mar. Drugs* 11, 3891-3901.

Philkhana SC, Verma AK, Jachak GR, Hazra B, Basu A and Reddy DS (2017) Identification of new anti-inflammatory agents based on nitrosporeusine natural products of marine origin. *Eur. J. Med. Chem.* 135, 89-109.-

Procópio REDL, Silva IRD, Martins MK, Azevedo JL and Araújo JMD (2012) Antibiotics produced by *Streptomyces*. *Braz. J. Infect. Dis.* 16(5), 466-471.

Ramirez MA and Lorenz MC (2007) Mutations in alternative carbon utilization pathways in *Candida albicans* attenuate virulence and confer pleiotropic phenotypes. *Eukaryot. Cell* 6, 280.

Roberts MF and Margaret F (1998) *Alkaloids: biochemistry, ecology, and medicinal applications*, Springer, USA.

Sharma V, Sharma S, Zu Bentrup KH, McKinney JD, Russell DG, Jacobs WR et al. (2000) Structure of isocitrate lyase, a persistence factor of *Mycobacterium tuberculosis*. *Nat. Genet*. 7, 663-668.

Shepard TL (2007) Nature Publishing Group, All natural. *Nat. Chem. Biol*, *3*, 351.

Shimizu Y, Ogata H and Goto S (2017) Type III polyketide synthases: functional classification and phylogenomics. *Chembiochem* 18, 50-65.

SHIN DS, KIM S, YANG HC and OH KB (2005) Cloning and expression of isocitrate lyase, a key enzyme of the glyoxylate cycle, of *Candida albicans* for development of antifungal drugs. *J. Microbiol. Biotechnol*. 15(3), 652-655.

Song Y, Li Q, Liu X, Chen Y, Zhang Y, Sun A et al. (2014) Cyclic hexapeptides from the deep South China Sea-derived *Streptomyces scopuliridis* SCSIO ZJ46 active against pathogenic gram-positive bacteria. *J. Nat. Prod*. 77, 1937-1941.

Strijbis K and Distel B (2010) Intracellular acetyl unit transport in fungal carbon metabolism. *Eukaryot. Cell* 9, 1809-1815.

Sugiyama Y, Watanabe K and Hirota A (2009) Surugapyrroles A and B, two new *N*-hydroxypyrroles, as DPPH radical-scavengers from *Streptomyces* sp. USF-6280 strain. *Biosci. Biotechnol*. *Biochem*. 73(1), 230-232.

Takano S, Hasuda K, Ito A, Koide Y, Ishii F, Haneda I et al. (1976) A new antibiotic, medermycin. *J. Antibiot*. 29(7), 765-768.

Tanaka N, Okabe T, Isono F, Kashiwagi M, Nomoto K, Takahashi M et al. (1985) Lactoquinomycin, a novel anticancer antibiotic. I. taxonomy, isolation and biological activity. *J. Antibiot.* 38, 1327-1332.

Tenover FC, McDougal LK, Goering RV, Killgore G, Projan SJ, Patel JB et al. (2006) Characterization of a strain of community-associated methicillin-resistant *Staphylococcus aureus* widely disseminated in the United States. *J. Clin. Microbiol.* 44(1), 108-118.

Toral-Barza L, Zhang WG, Huang X, McDonald LA, Salaski EJ, Barbieri LR et al. (2007) Discovery of lactoquinomycin and related pyranonaphthoquinones as potent and allosteric inhibitors of AKT/PKB: mechanistic involvement of AKT catalytic activation loop cysteines. *Mol. Cancer Ther.* 6(11), 3028-3038.

Tortorella E, Tedesco P, Palma Esposito F, January G, Fani R, Jaspars M et al. (2018) Antibiotics from deep-sea microorganisms: current discoveries and perspectives. *Mar. Drugs* 16(10), 355.

Tse WC and Boger DL (2004) A fluorescent intercalator displacement assay for establishing DNA binding selectivity and affinity. *Acc. Chem. Res.* 37, 61-69.

Tsuji BT, Yang JC, Forrest A, Kelchlin PA and Smith PF (2008) In vitro pharmacodynamics of novel rifamycin ABI-0043 against *Staphylococcus aureus*. *J. Antimicrob. Chemother.* 62, 156-160.

Turner NA, Sharma-Kuinkel BK, Maskarinec SA, Eichenberger EM, Shah PP, Carugati M et al. (2019) Methicillin-resistant *Staphylococcus aureus*: an overview of basic and clinical research. *Nat. Rev. Microbiol.* 17(4), 203-218.

Tyler PA (2003) *Ecosystems of the deep oceans* (1st ed.). Elsevier Science, Amsterdam.

Van Hal SJ, Jensen SO, Vaska VL, Espedido BA, Paterson DL and Gosbell IB (2012) Predictors of mortality in *Staphylococcus aureus* bacteremia. *Clin*. *Microbiol*. *Rev*. 25, 362-386.

Vanni P, Giachetti E, Pinzauti G and McFadden BA (1990) Comparative structure, function and regulation of isocitrate lyase, an important assimilatory enzyme. *Comp*. *Biochem*. *Physiol*. *B*. 95(3), 431-458.

Wahaab F and Subramaniam K (2018) Bioprospecting marine actinomycetes for multidrug-resistant pathogen control from Rameswaram coastal area, Tamil Nadu, India. *Arch. Microbiol.* 200, 57-71.

Wang J, Zhang R, Chen X, Sun X., Yan Y, Shen X et al. (2020) Biosynthesis of aromatic polyketides in microorganisms using type II polyketide synthases. *Microb. Cell Fact.* 19, 1-11.

Watanabe T (1963) Infective heredity of multiple drug resistance in bacteria. *Bacteriol.Rev.* 27(1), 87.

Williamson RT, McDonald LA, Barbieri LR and Carter GT (2002) In support of the original medermycin/lactoquinomycin A structure. *Org. Lett.* 4(26), 4659-4662.

Wilson DN (2014) Ribosome-targeting antibiotics and mechanisms of bacterial resistance. *Nat. Rev. Microbiol*. 12, 35-48.

Wright PC, Westacott RE and Burja AM (2003) Piezotolerance as a metabolic engineering tool for the biosynthesis of natural products. *Biomol. Eng*. 20, 325-331.

Wu M and Hancock RE (1999) Interaction of the cyclic antimicrobial cationic peptide bactenecin with the outer and cytoplasmic membrane. *J. Biol. Chem.* 274, 29-35.

Yang A, Si L, Shi Z, Tian L, Liu D, Zhou D et al. (2013) Nitrosporeusines A and B, unprecedented thioester-bearing alkaloids from the Arctic *Streptomyces nitrosporeus*. *Org. Lett.* 15(20), 5366-5369.

Zaman SB, Hussain MA, Nye R, Mehta V, Mamum KT and Hussain N (2017) A review on antibiotic resistance: alarm bells are ringing. *Cureus* 9, 1-9.

Zhu F and Lin Y (2006) Marinamide, a novel alkaloid and its methyl ester produced by the application of mixed fermentation technique to two mangrove endophytic fungi from the South China Sea. *Chin. Sci. Bull.* 51(12), 1426-1430.

Ziegler J and Facchini PJ (2008) Alkaloid biosynthesis: metabolism and trafficking. *Annu. Rev. Plant Biol*. 59, 735-769.

Zotchev SB (2012) Marine actinomycetes as an emerging resource for the drug development pipelines. *J. Biotechnol.* 158(4), 168-175.

Supplementary Materials

Supplementary Figure 1. HRESIMS (positive mode) data of compound 1

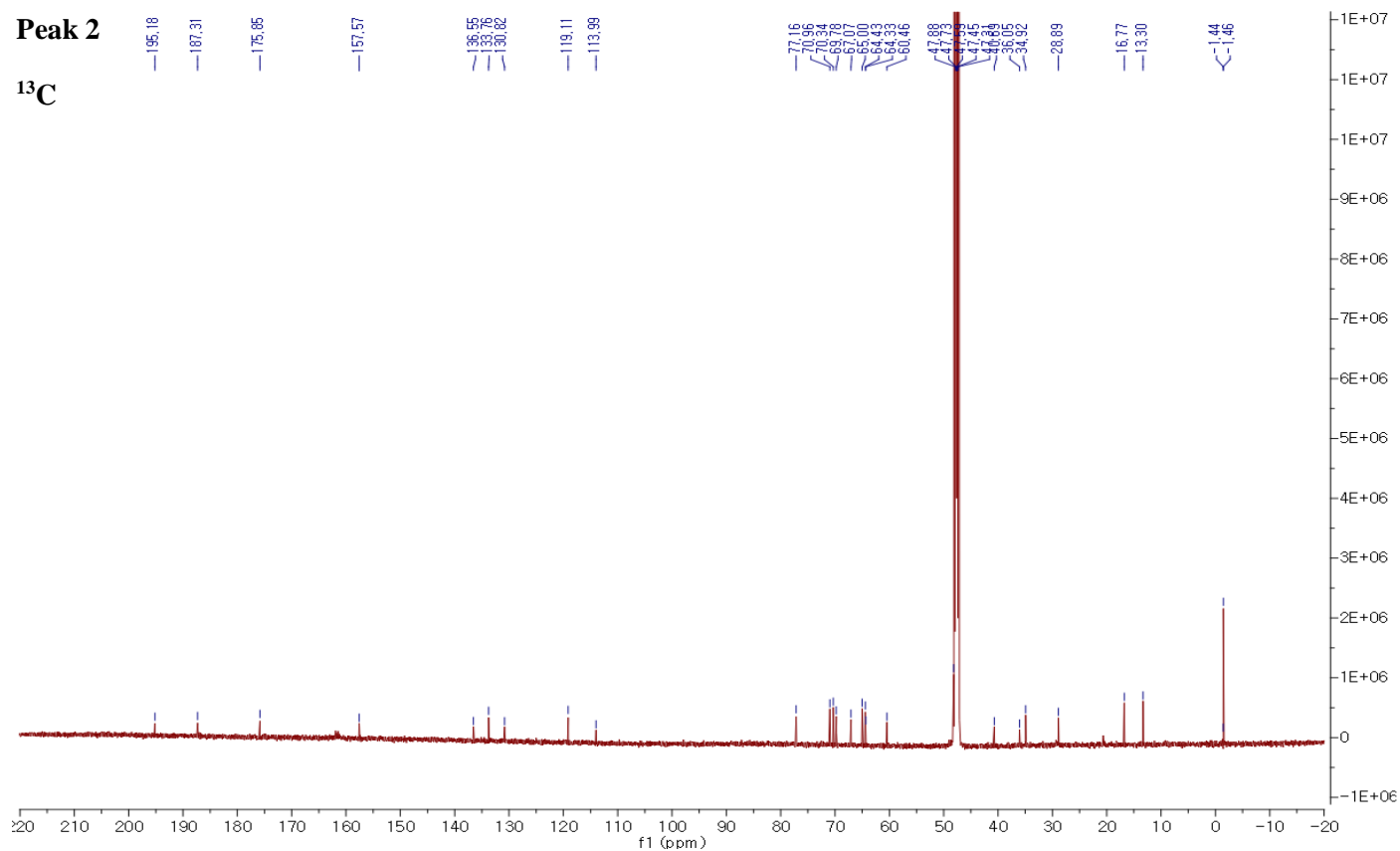Spectrum from LQM_A.wiff (sample 1) - LQM_A, Experiment 1, +TOF MS (100 - 2000) from 0.392 min

Supplementary Figure 2. ¹H NMR data of compound 1 in methanol-d_4

Peak 1

¹H NMR

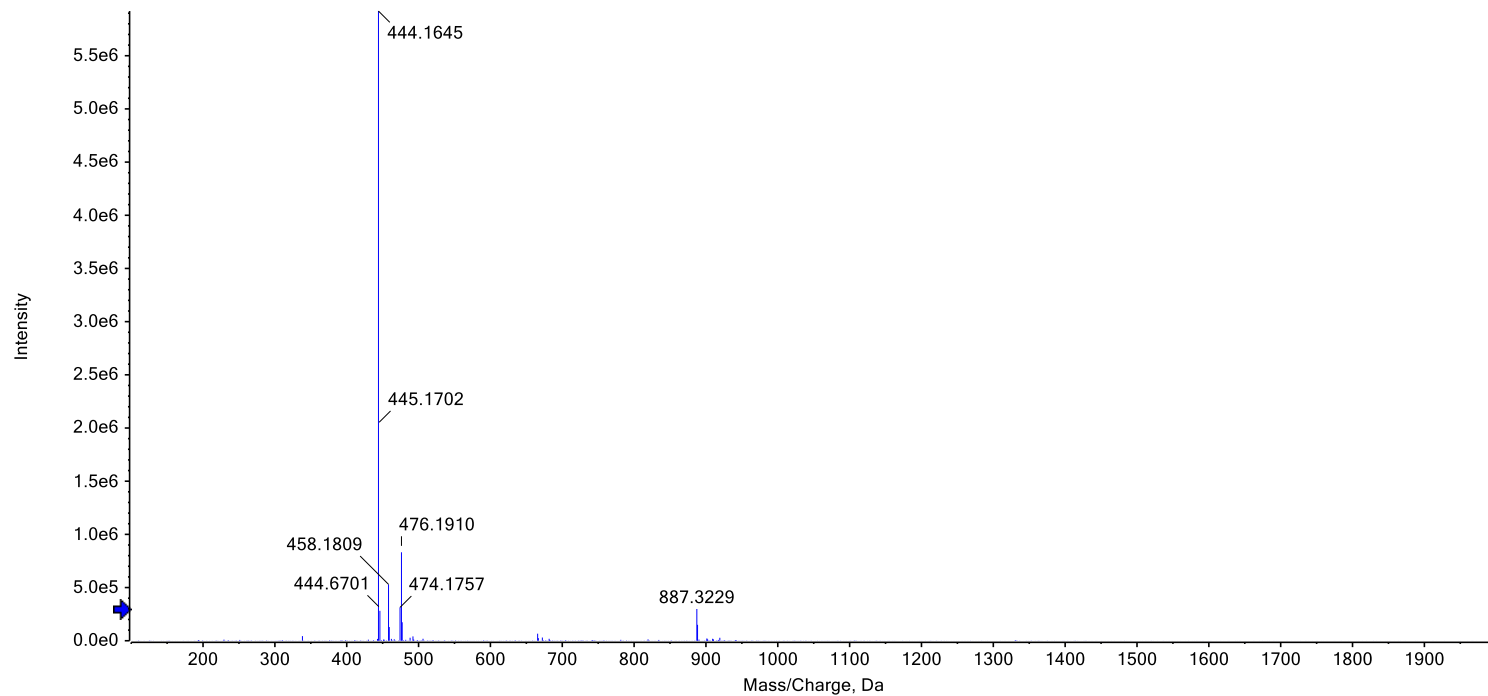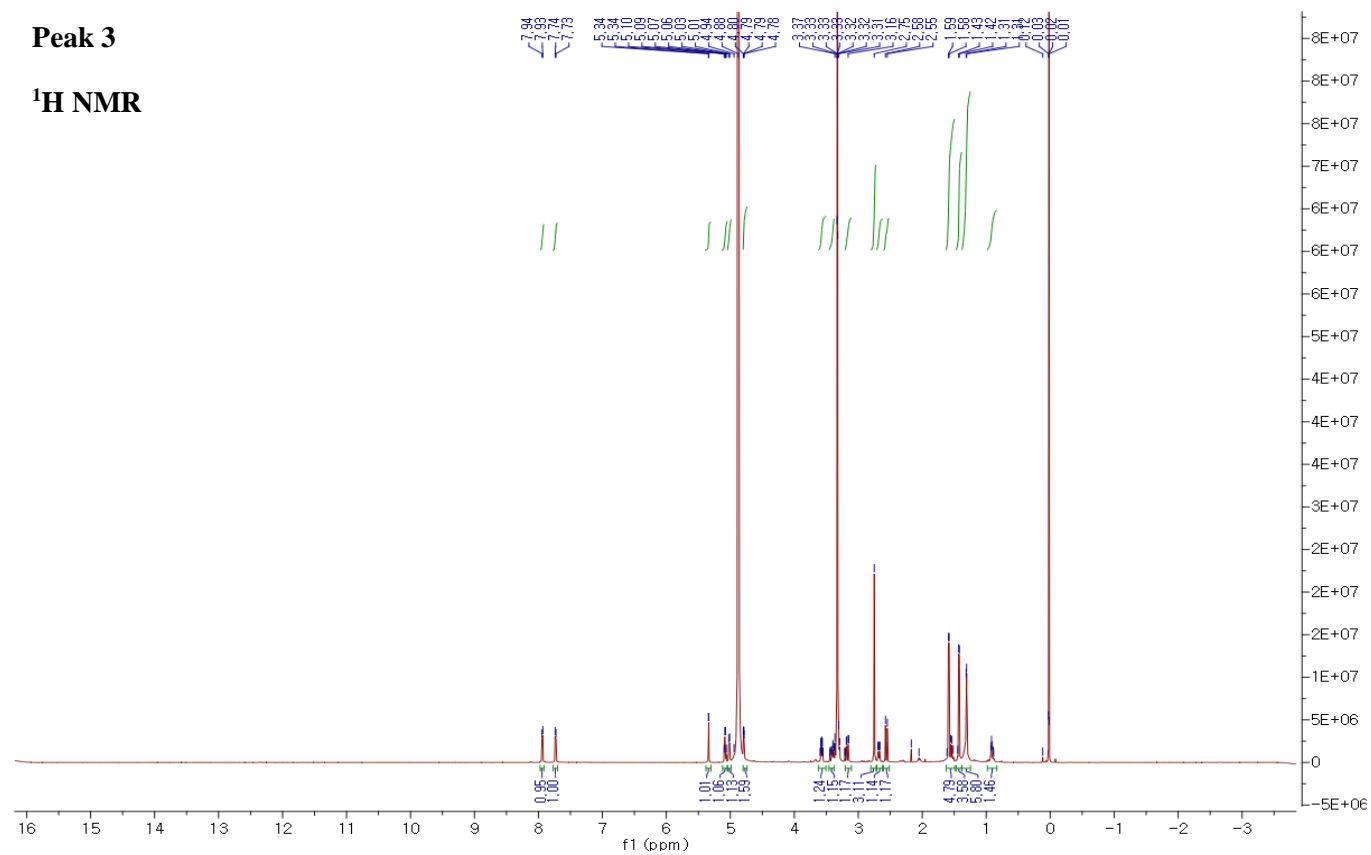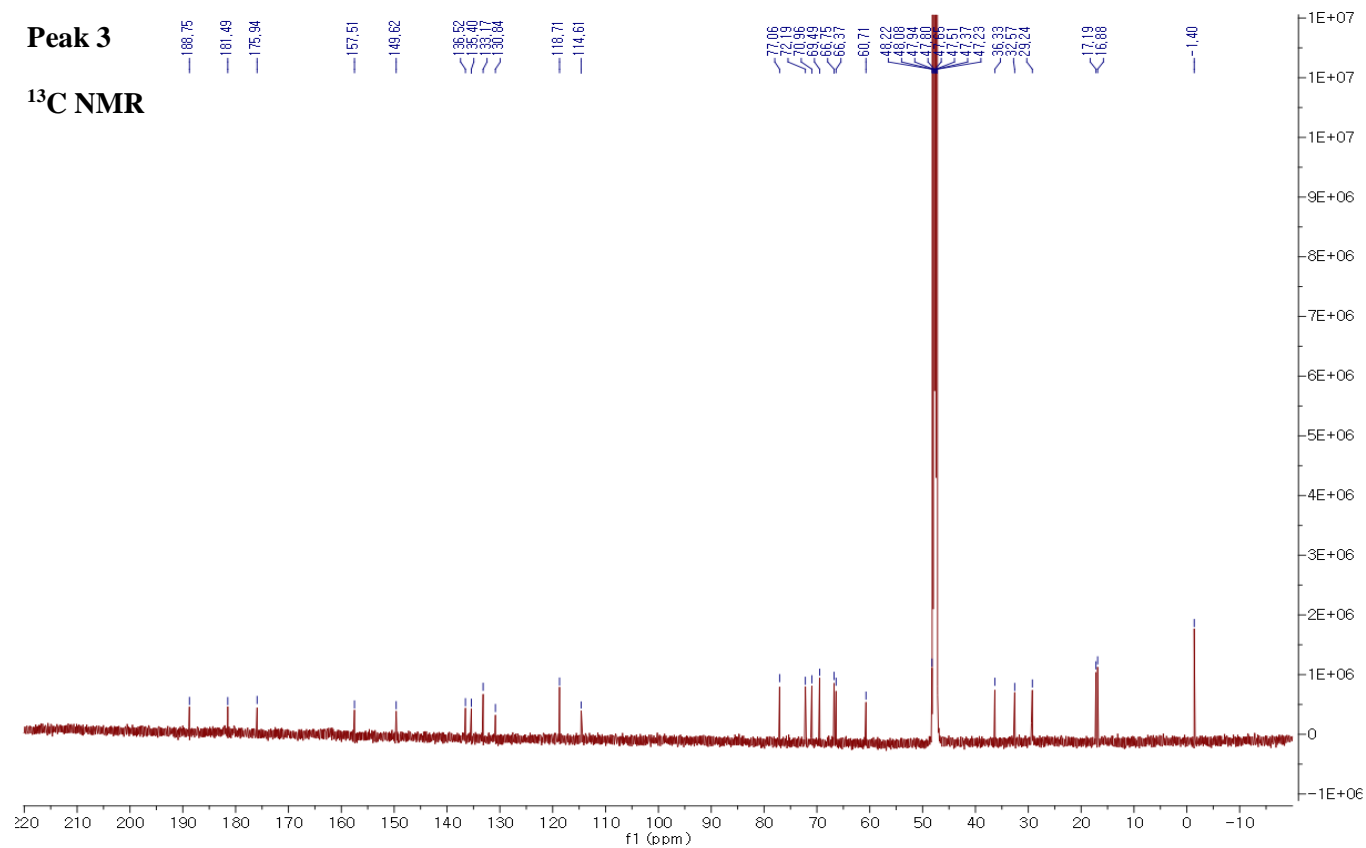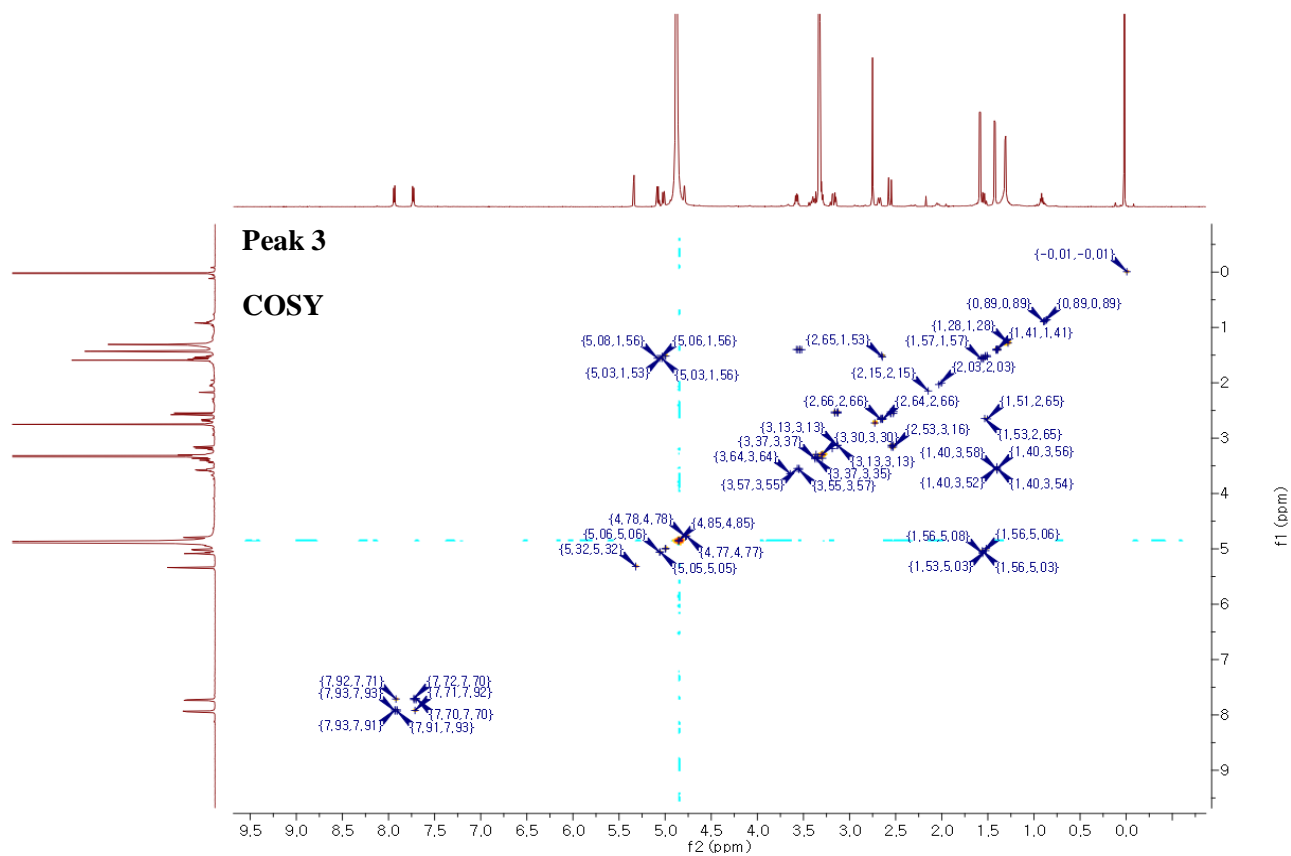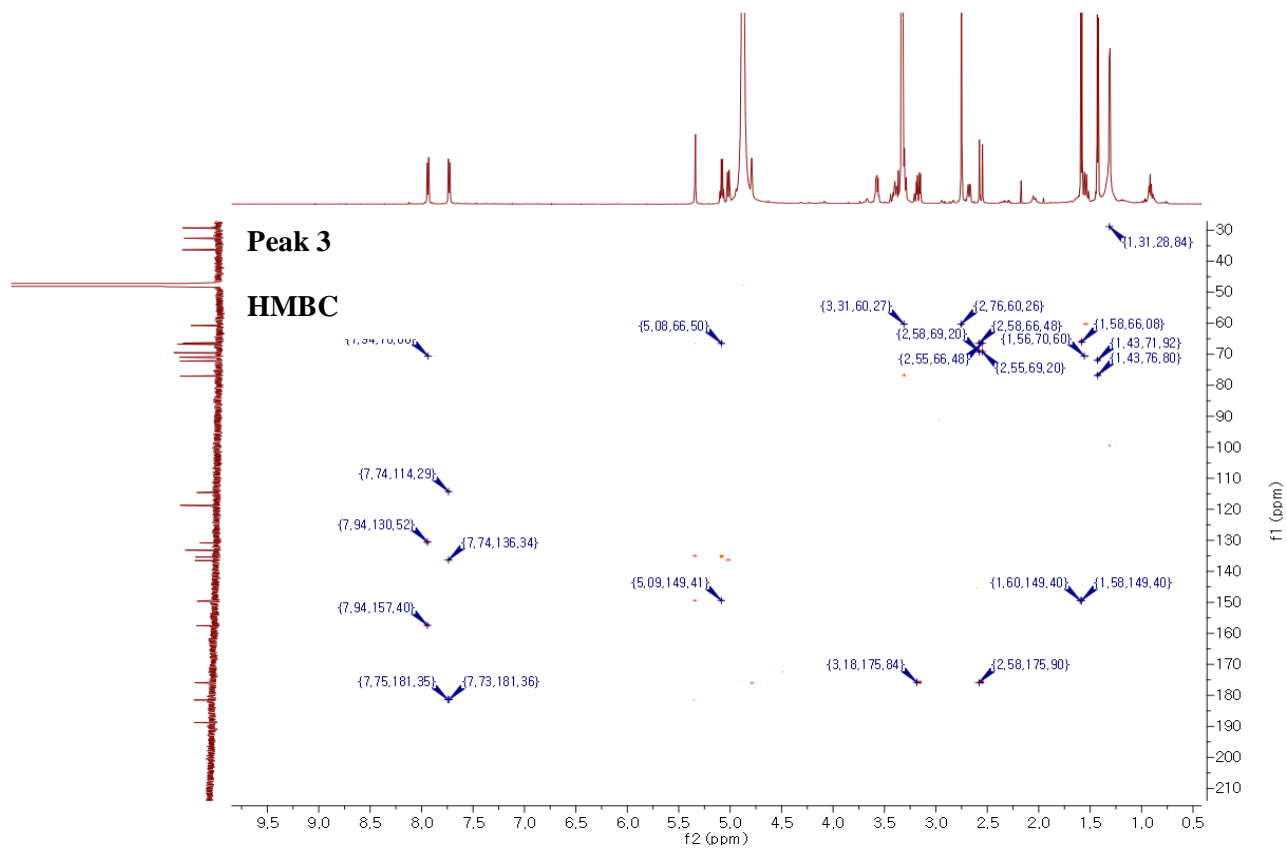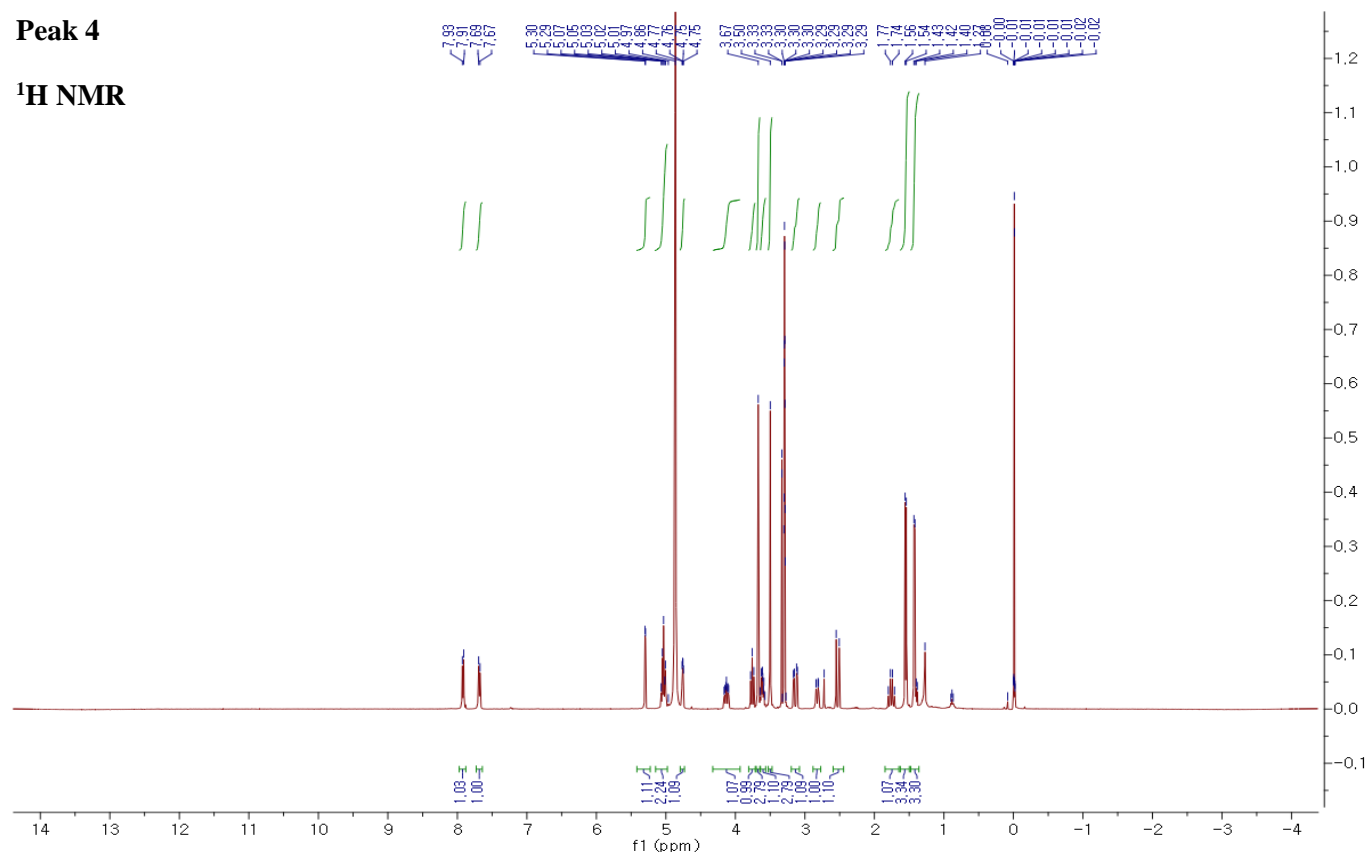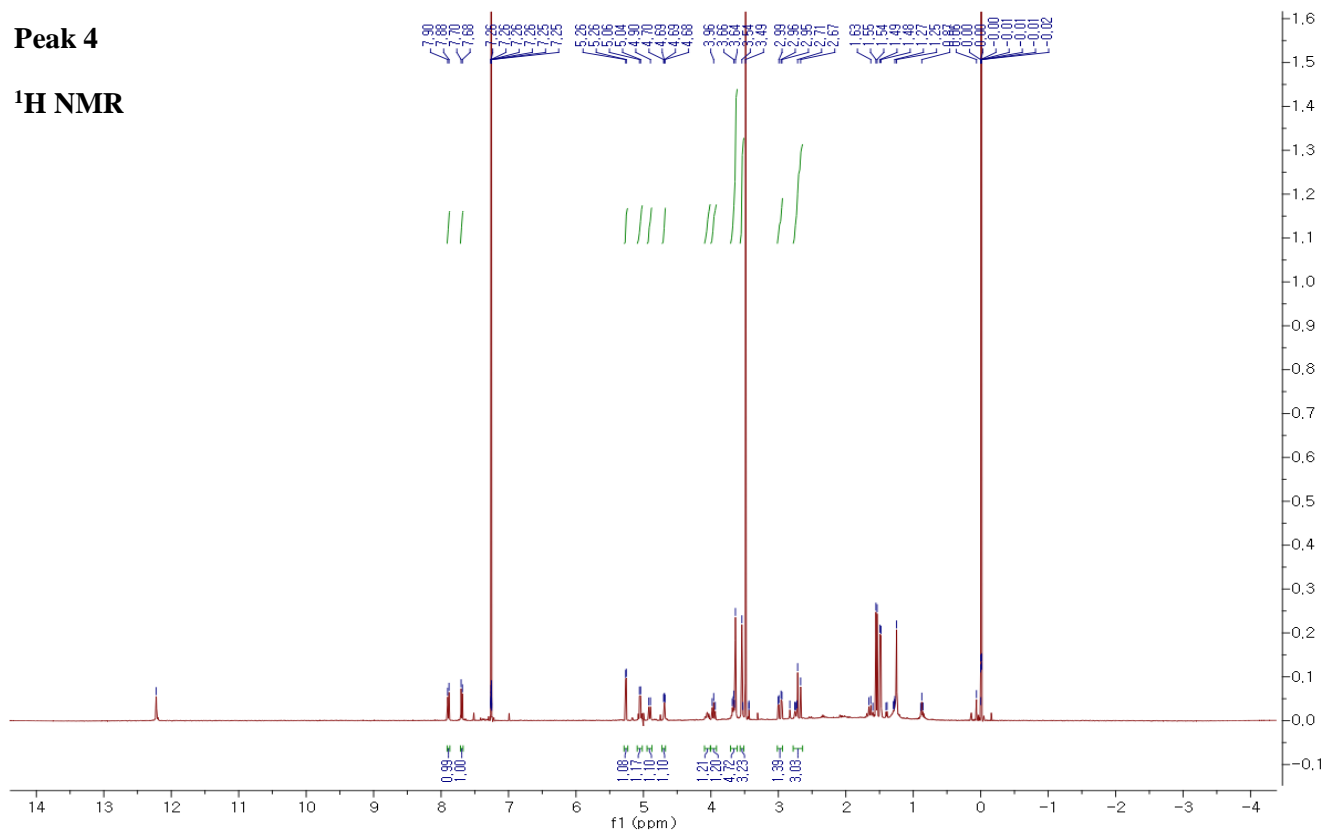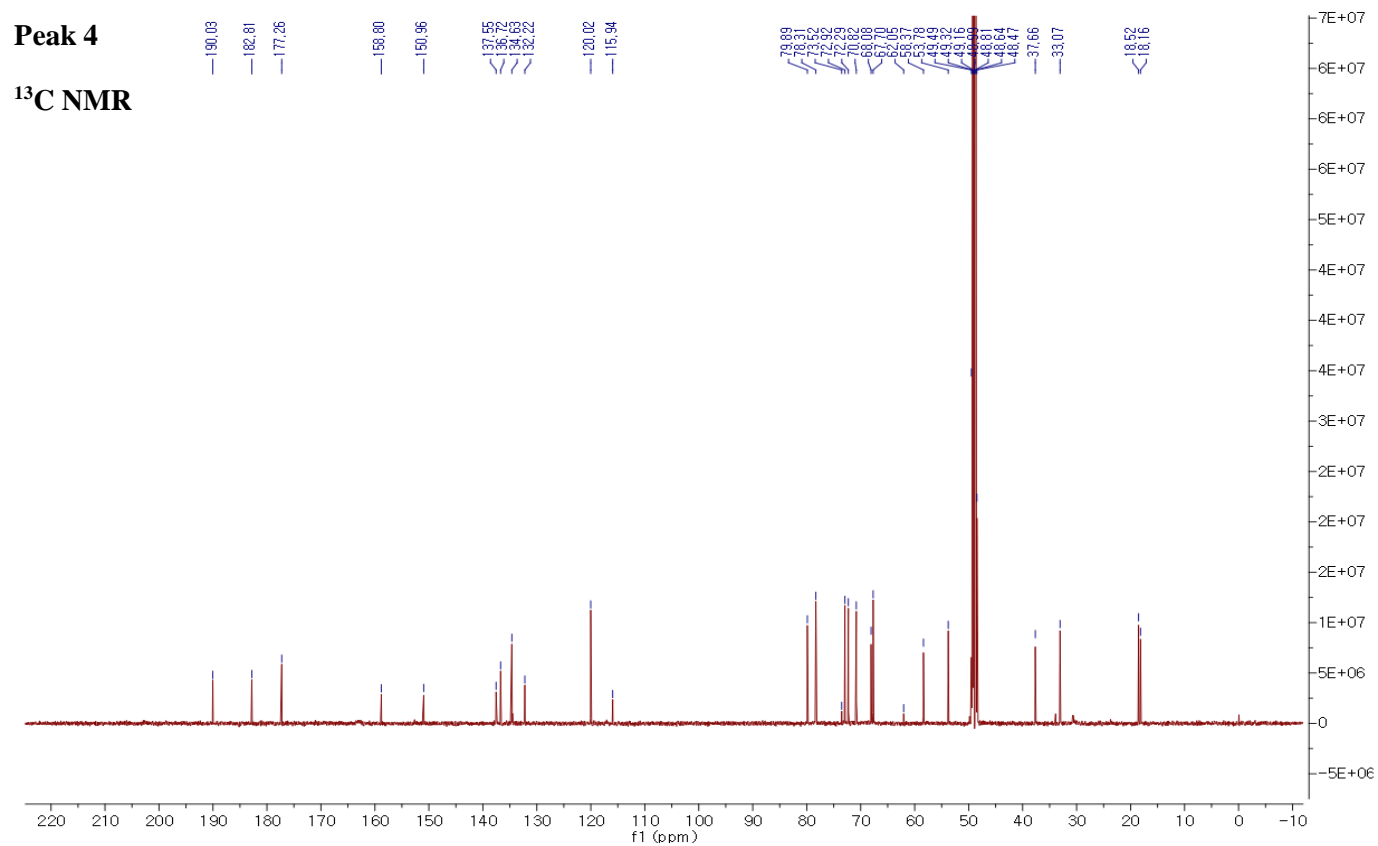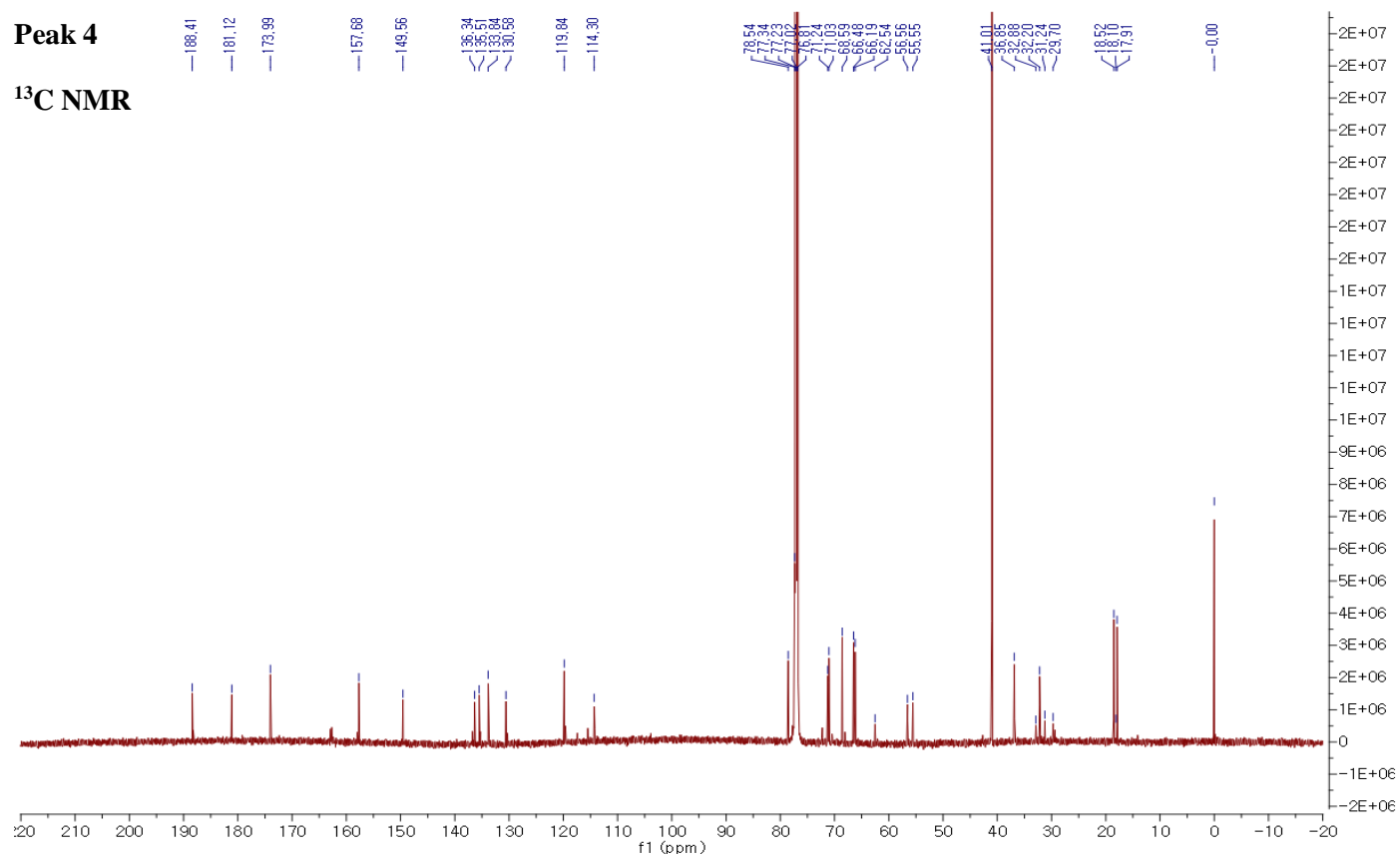**Supplementary Figure 3. ^{1}H NMR data of compound 1 in chloroform-*d***

Peak 1

^{1}H NMR

Supplementary Figure 4. ^{13}C NMR data of compound 1 in methanol-d_4
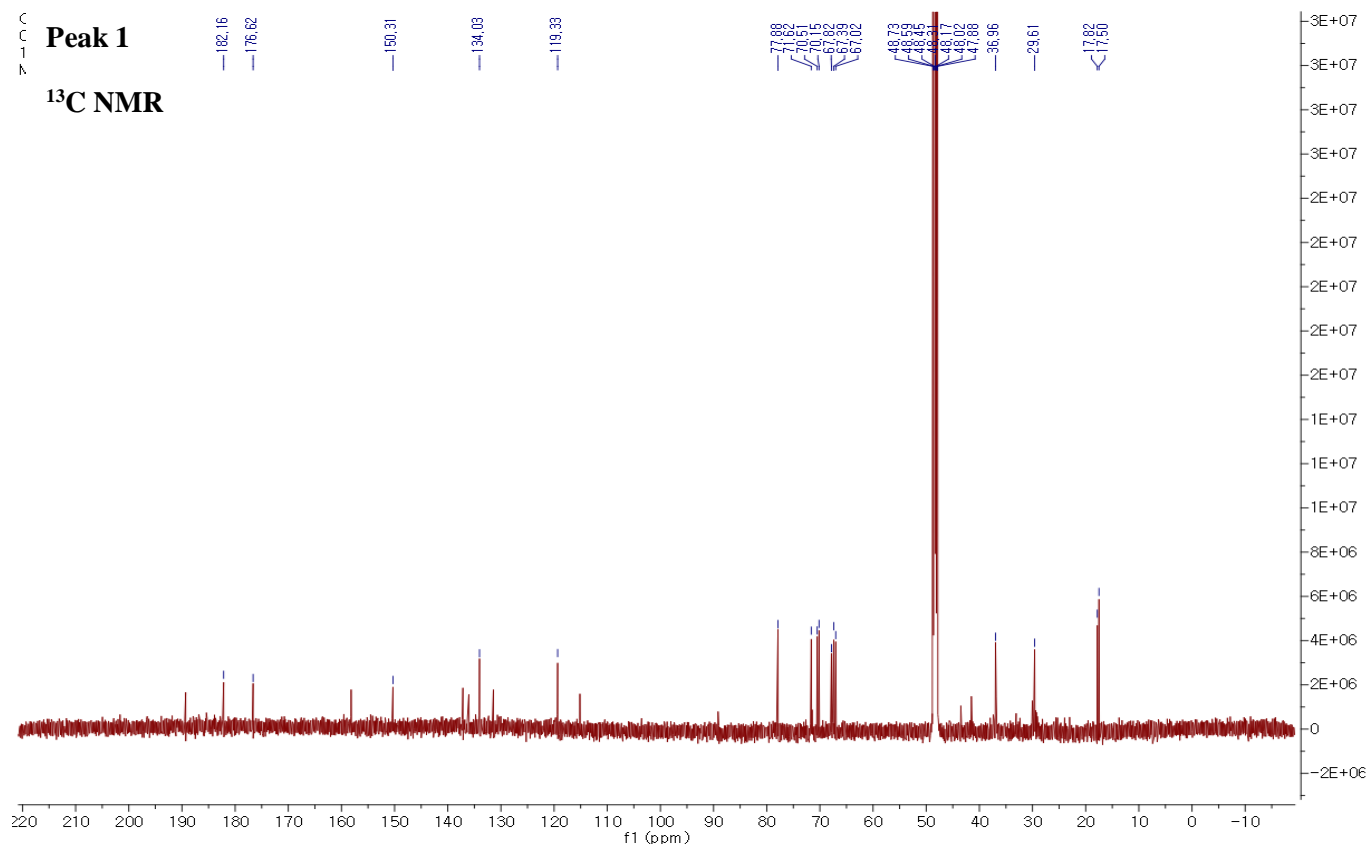
Supplementary Figure 5. ^{13}C NMR data of compound 1 in chloroform-*d*
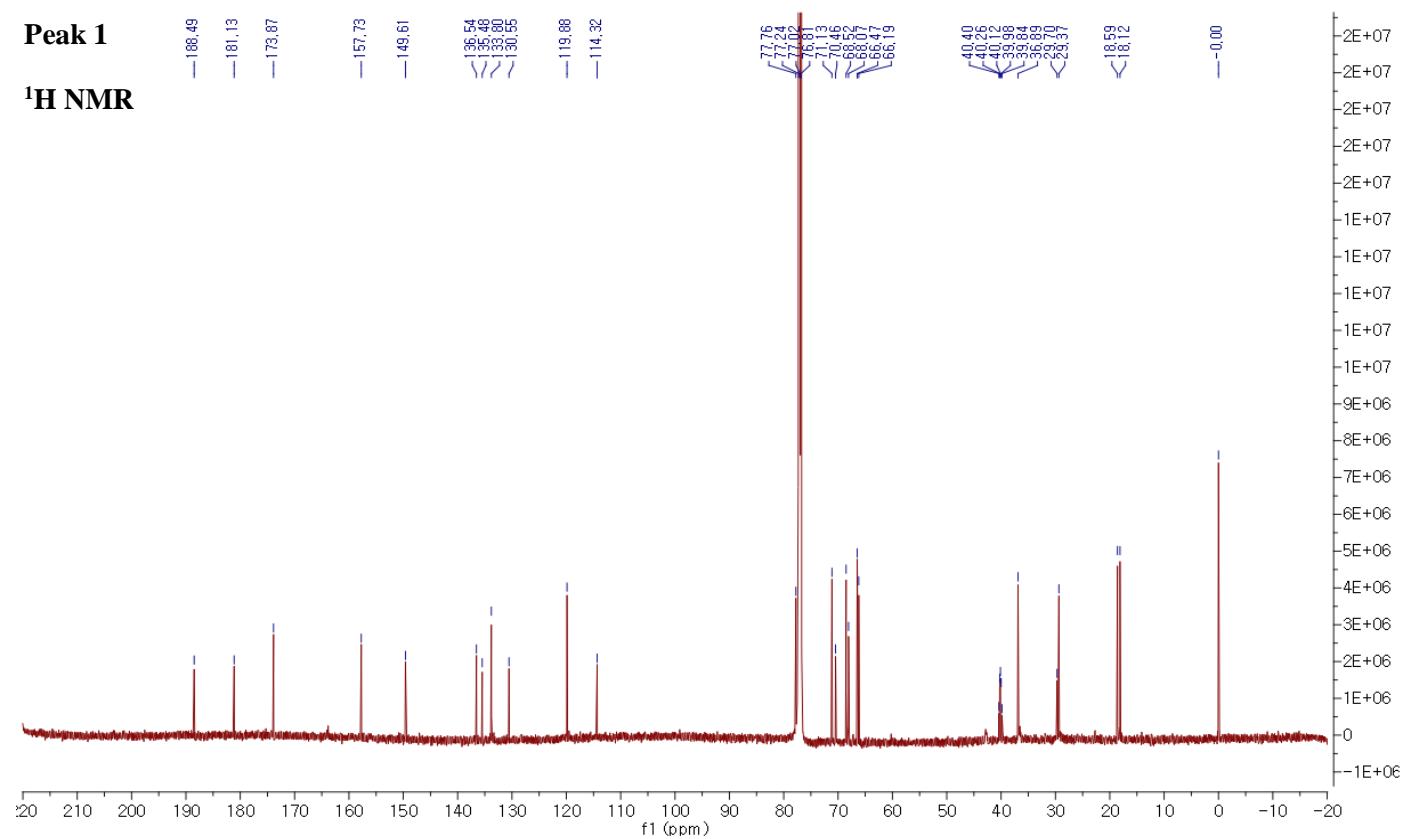
Supplementary Figure 6. COSY NMR data of compound 1 in methanol-d_4

Peak 1

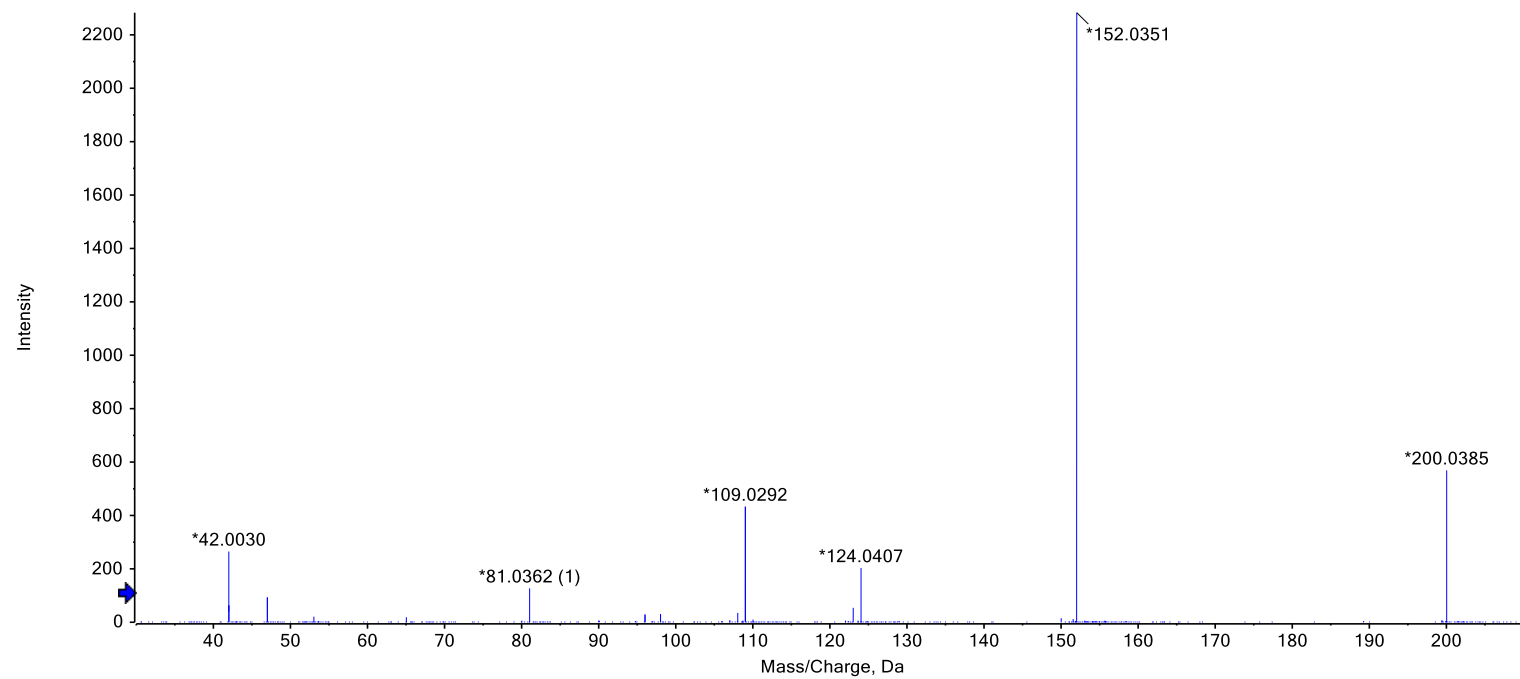COSY
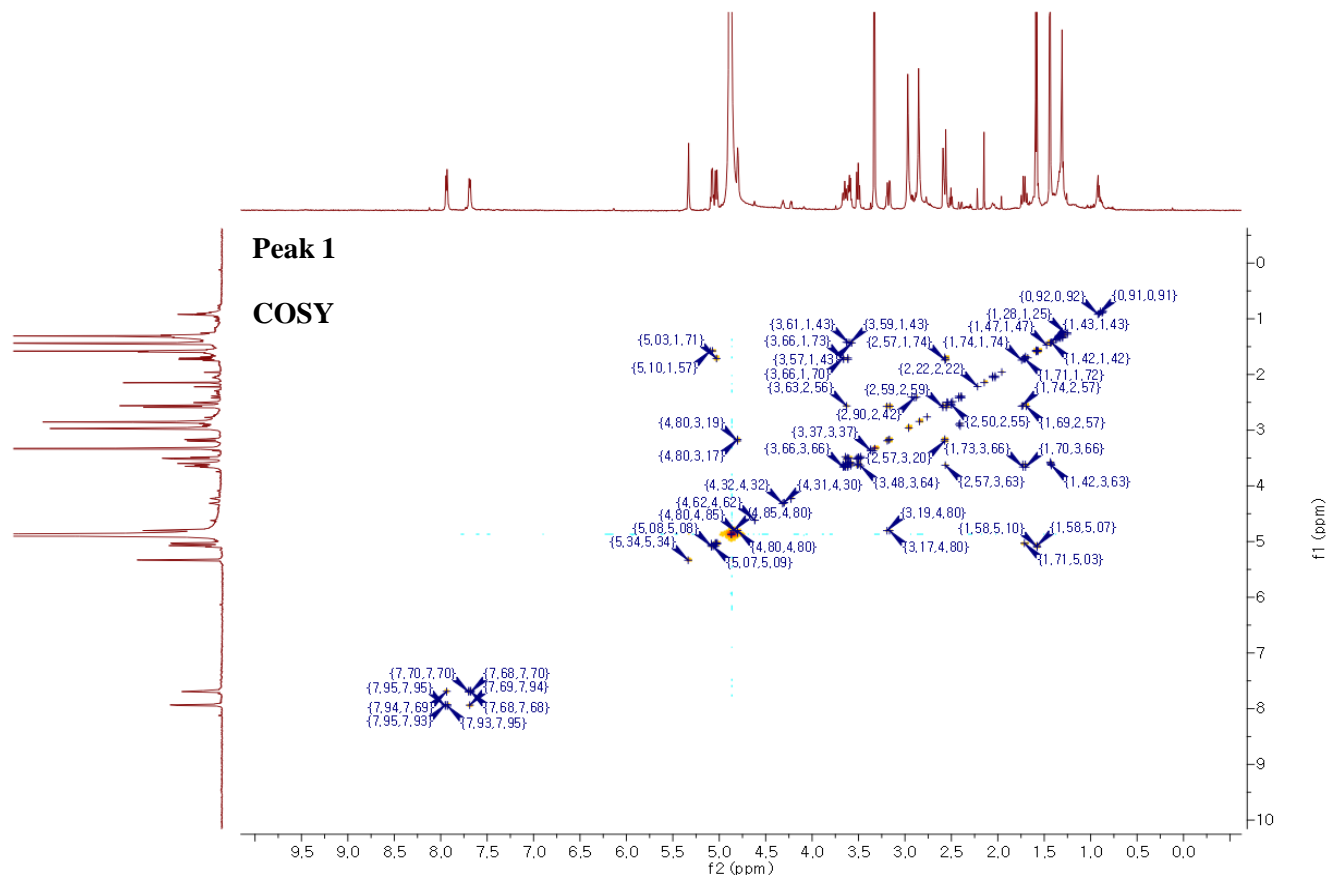
Supplementary Figure 7. HMBC NMR data of compound 1 methanol-d_4

123
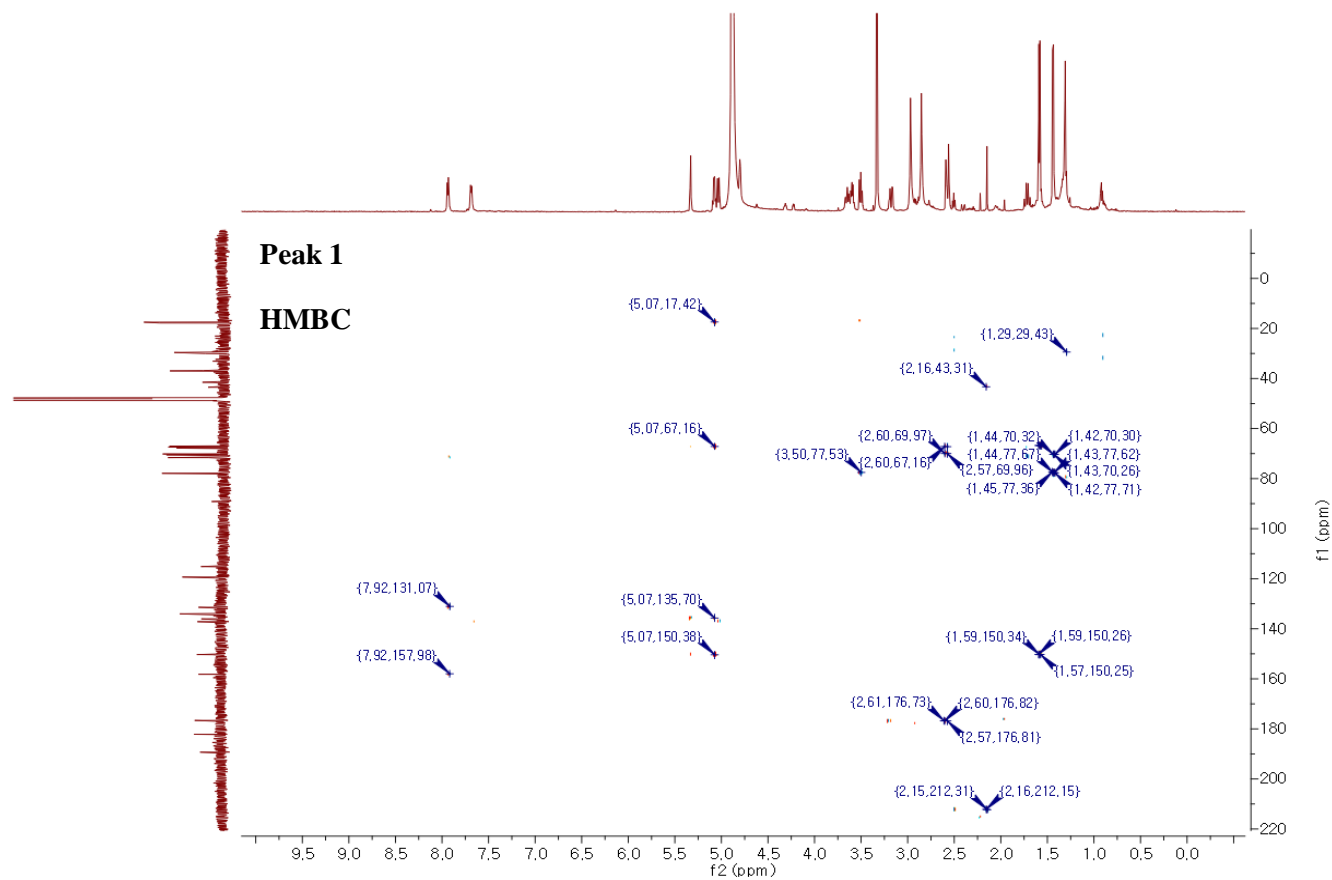
Supplementary Figure 8. HSQC NMR data of compound 1 methanol-*d₄*

124
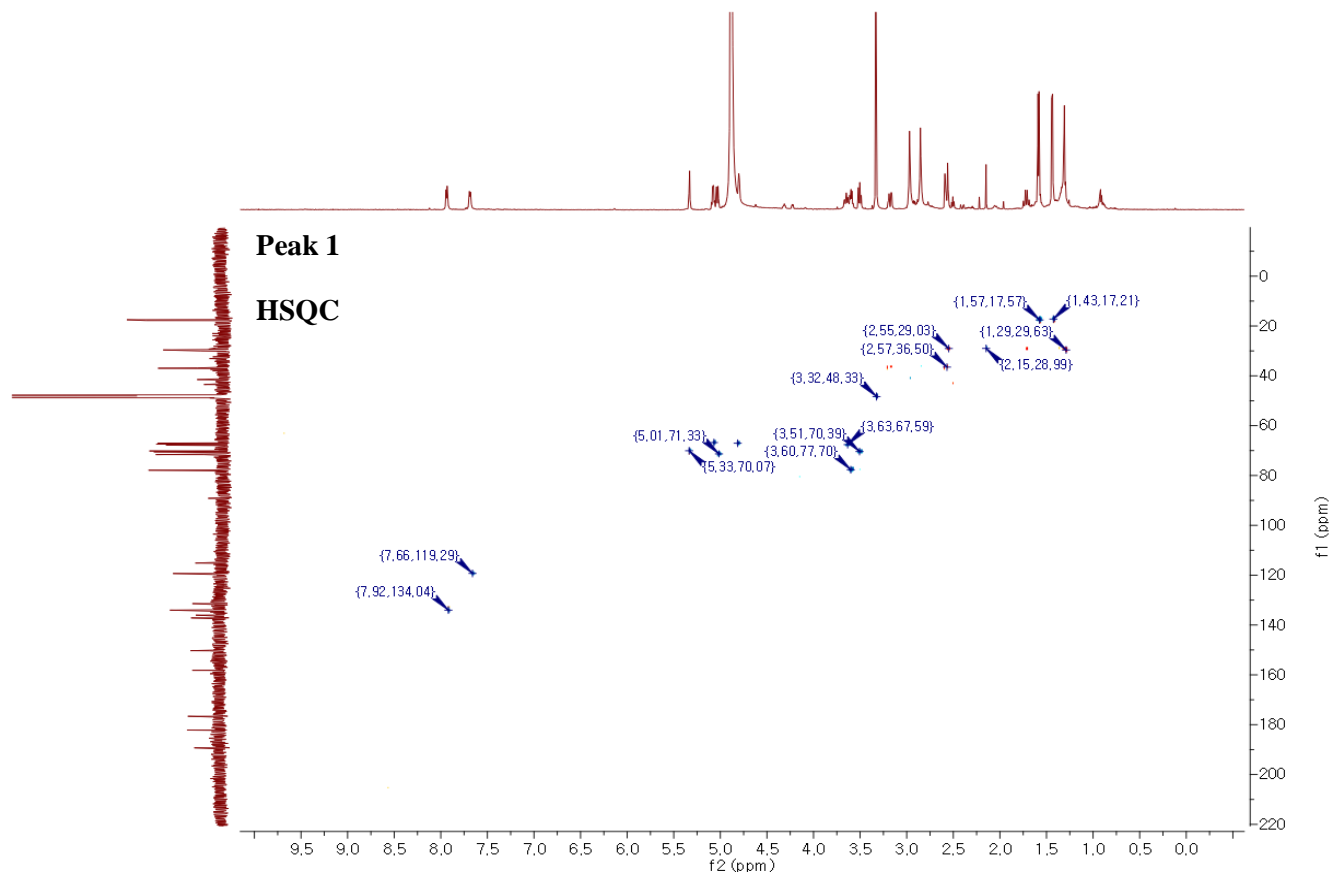
Supplementary Figure 9. HRESIMS (positive mode) data of compound 2

Spectrum from LQM_B.wiff (sample 1) - LQM_B, Experiment 1, +TOF MS (100 - 2000) from 0.400 min
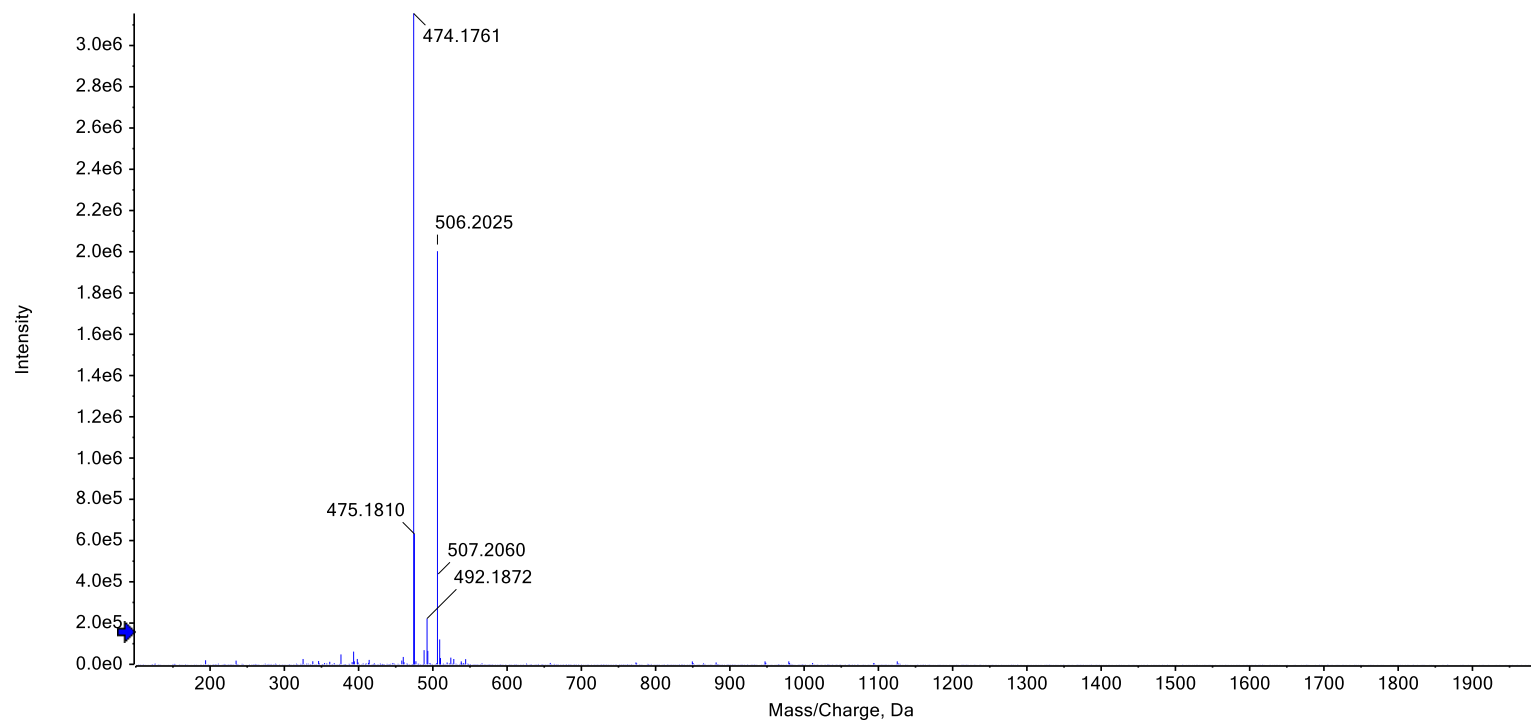
Supplementary Figure 10. ¹H NMR data of compound 2 in methanol-d_4

Peak 2

¹H NMR
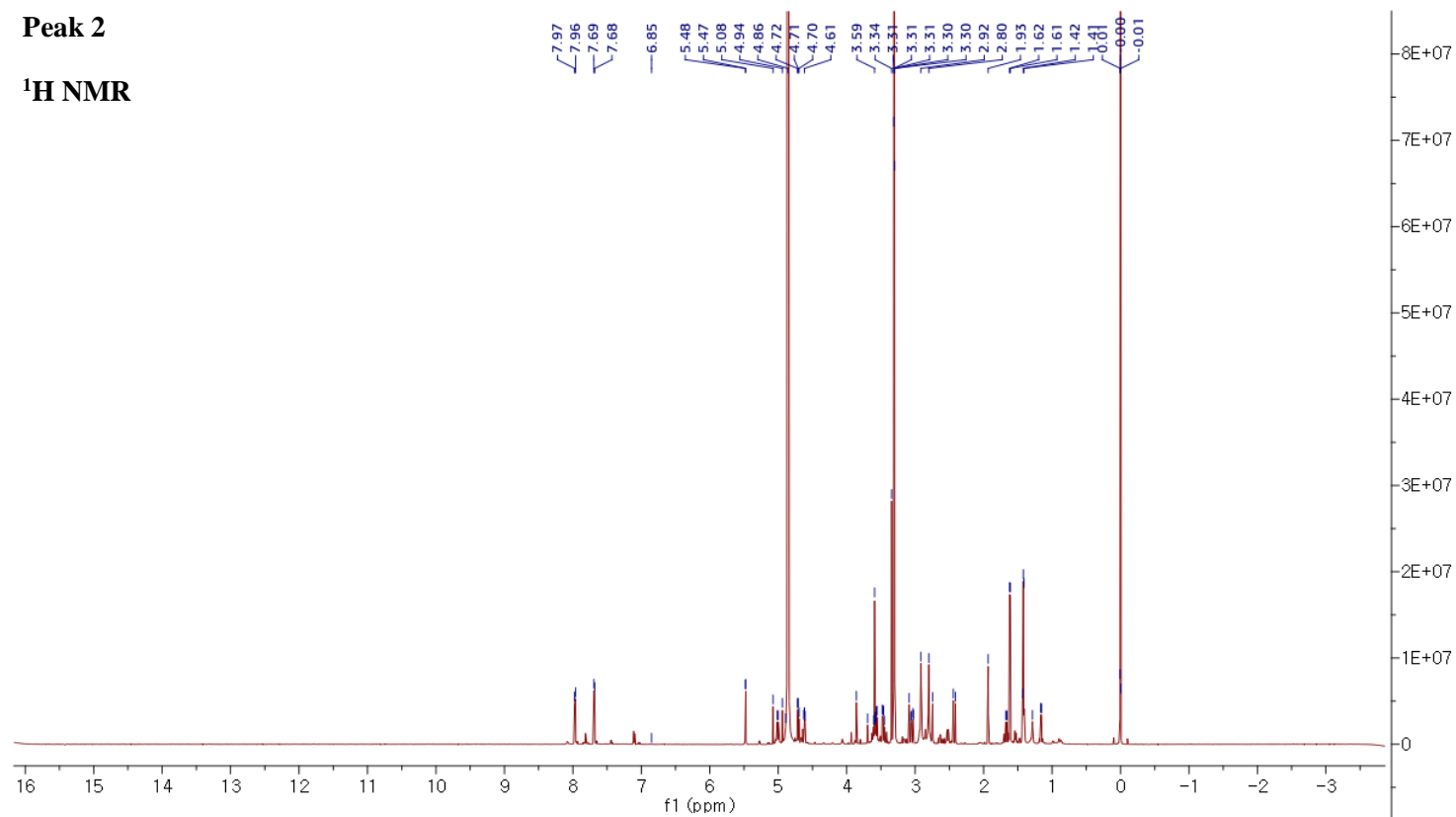
Supplementary Figure 11. ^{13}C NMR data of compound 2 in methanol-d_4

Supplementary Figure 12. HRESIMS (positive mode) data of compound 3

Spectrum from N_LQM_A.wiff (sample 1) - N_LQM_A, Experiment 1, +TOF MS (100 - 2000) from 0.394 min

128

Supplementary Figure 13. ¹H NMR data of compound 3 in methanol-d_4

Peak 3

¹H NMR

129

Supplementary Figure 14. ^{13}C NMR data of compound 3 in methanol-d_4

Peak 3

^{13}C NMR

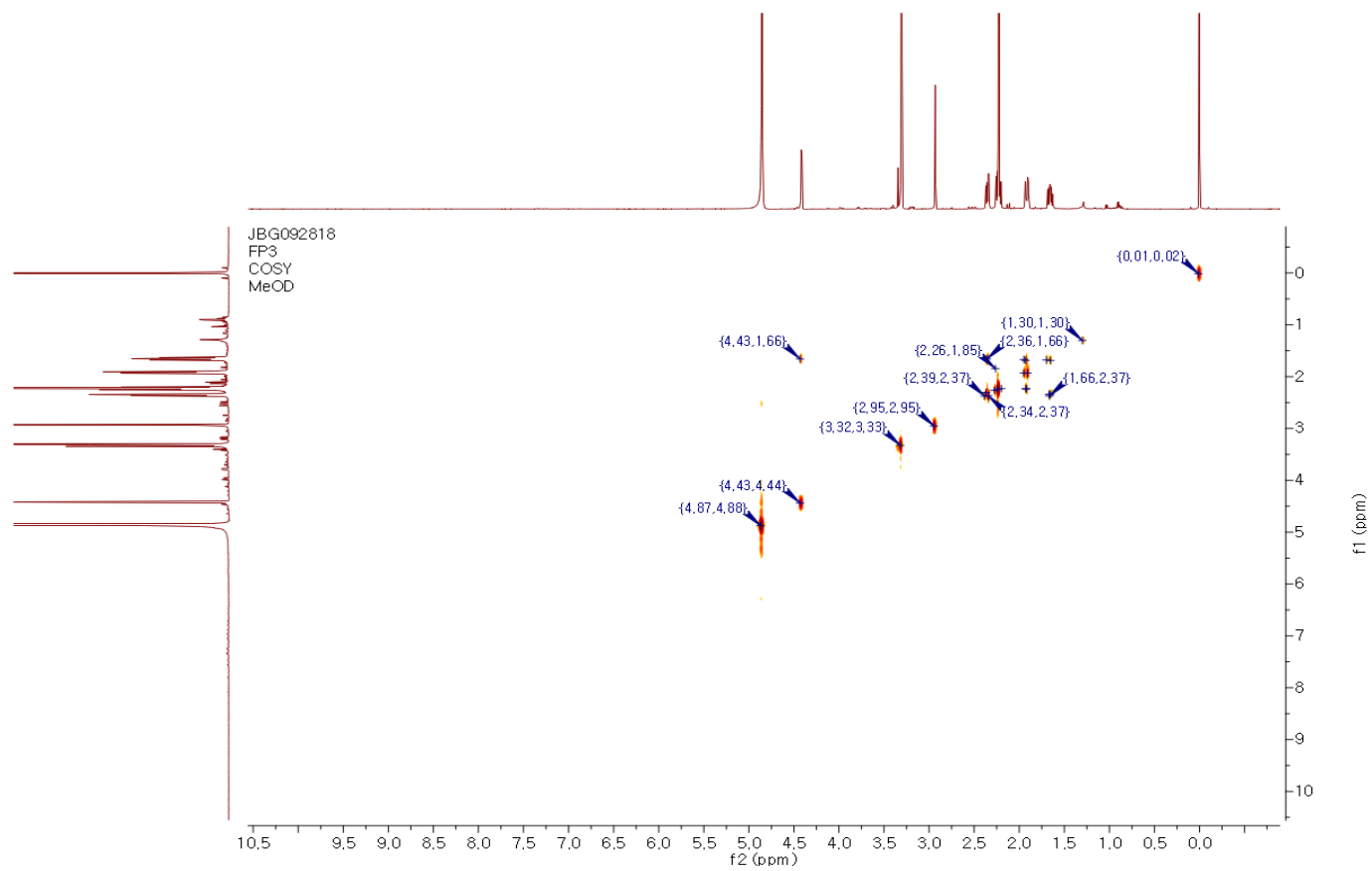**Supplementary Figure 15. COSY NMR data of compound 3 methanol-*d₄***

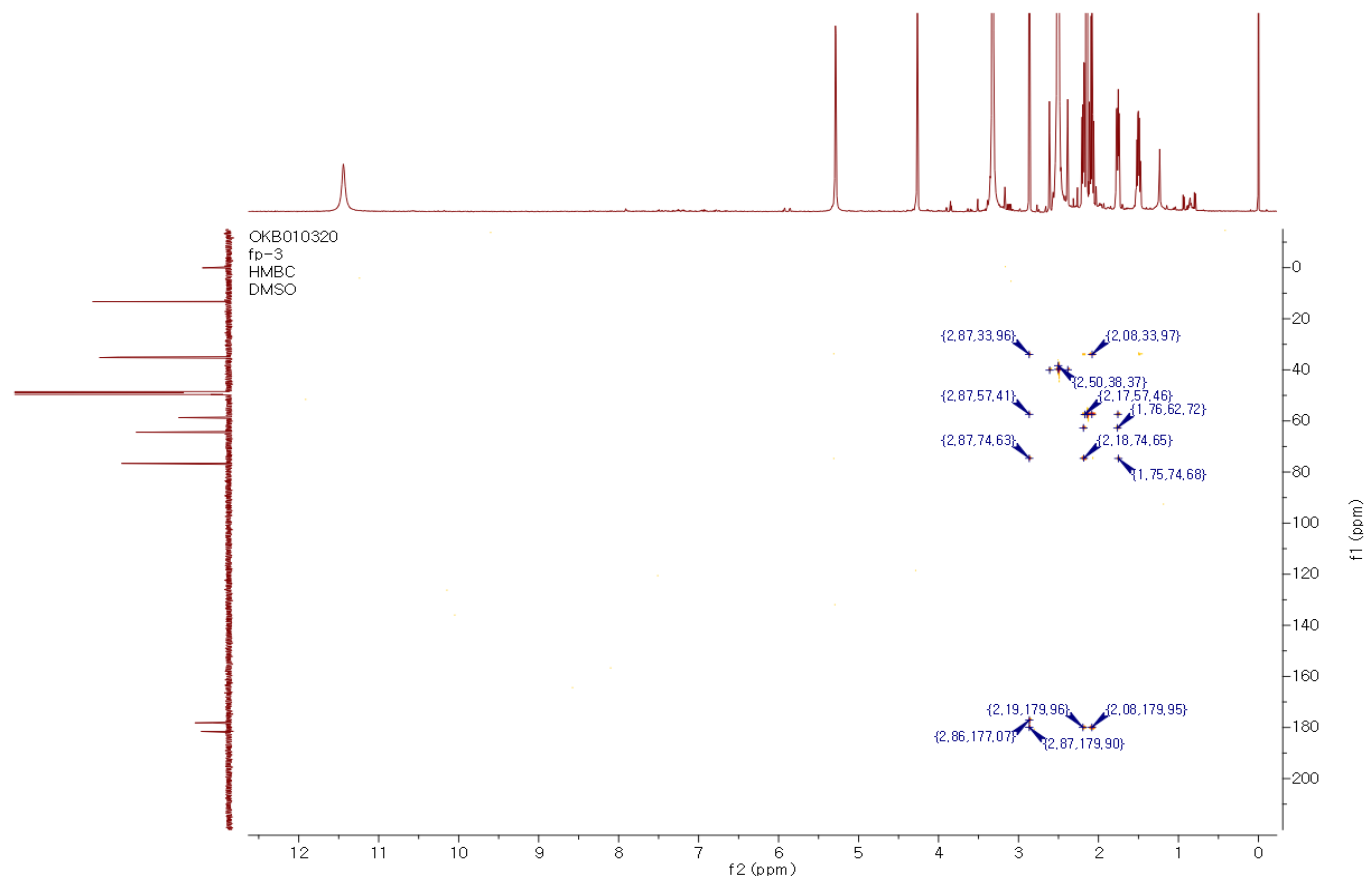**Supplementary Figure 16. HMBC NMR data of compound 3 methanol-d_4**

Supplementary Figure 17. HSQC NMR data of compound 3 methanol-*d₄*
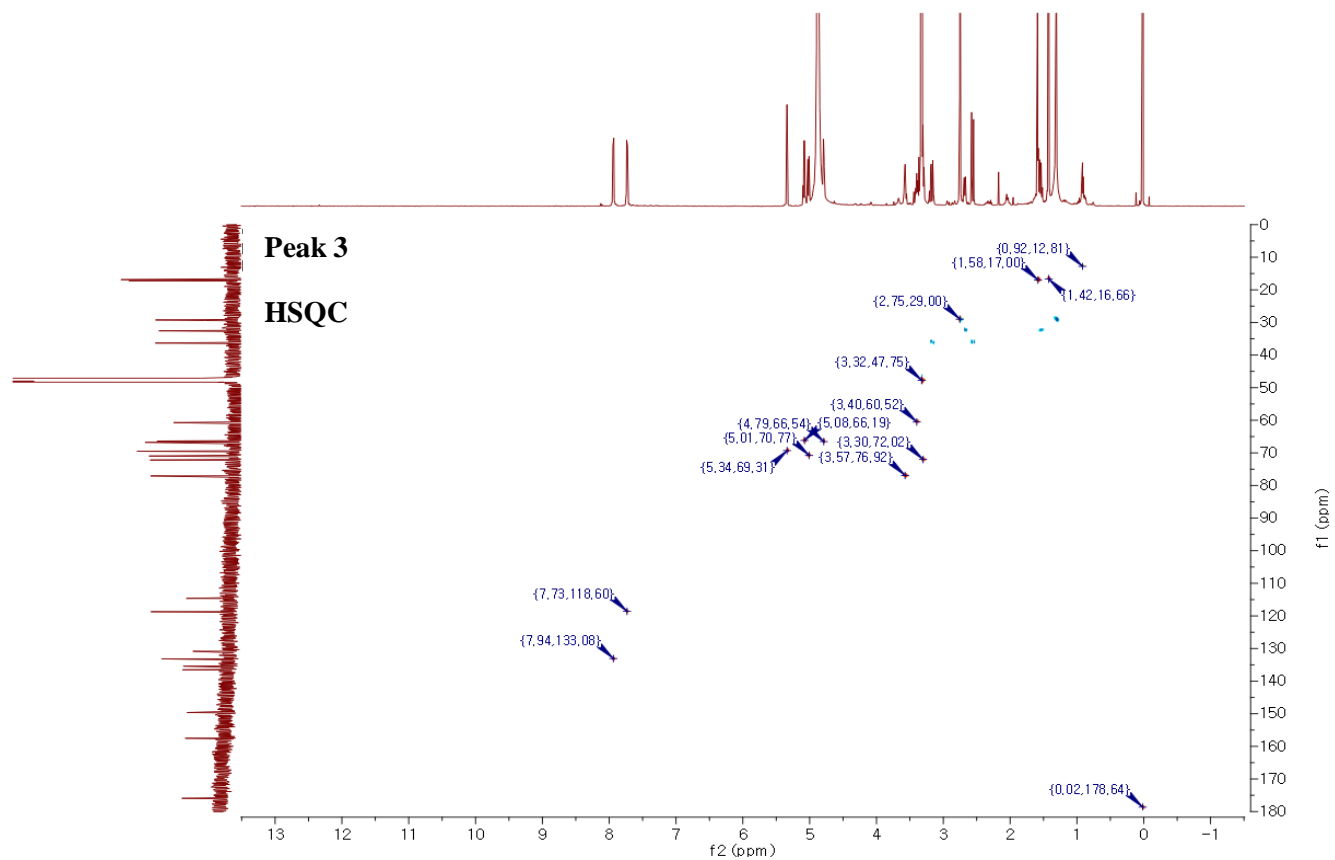
Supplementary Figure 18. HRESIMS (positive mode) of compound 4

Spectrum from MNY_A.wiff (sample 1) - MNY_A, Experiment 1, +TOF MS (100 - 2000) from 0.301 min
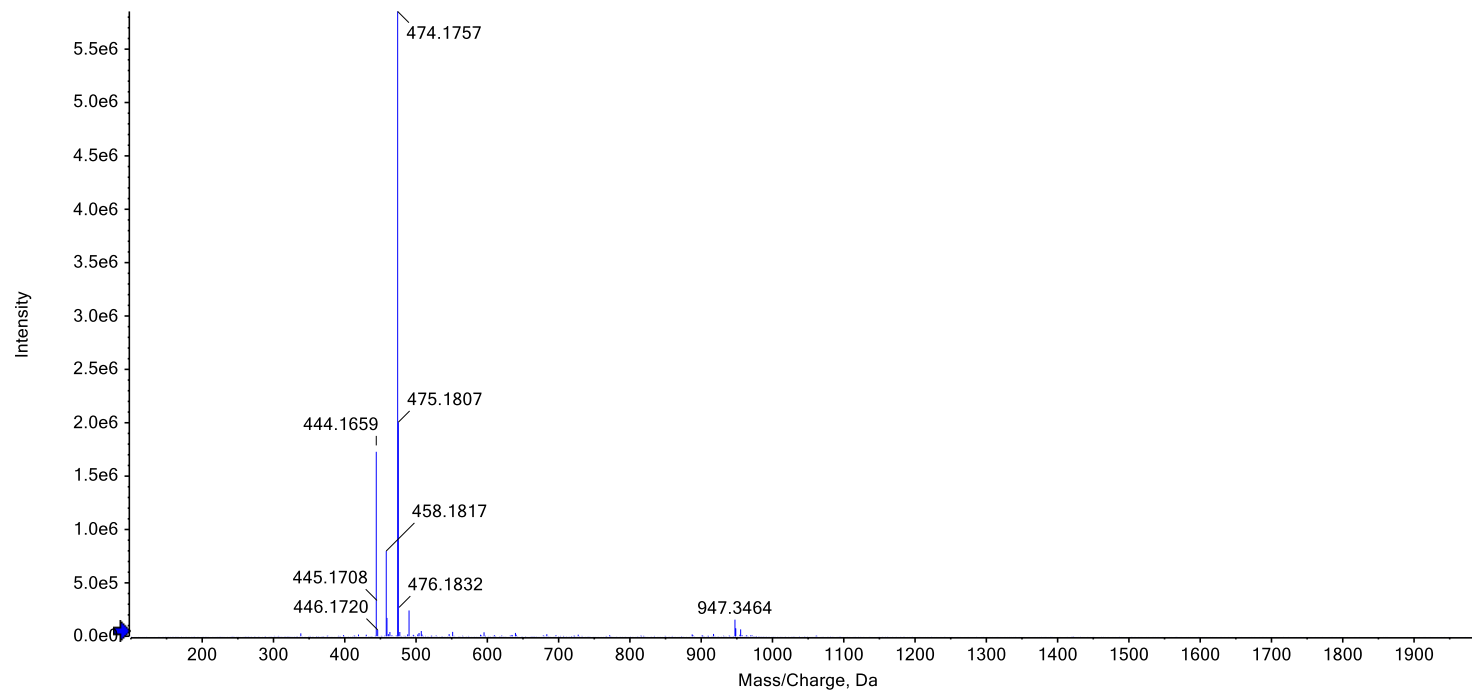
Supplementary Figure 19. ^{1}H NMR data of compound 4 in methanol-d_4

Peak 4

^{1}H NMR

Supplementary Figure 20. ¹H NMR data of compound 4 in chloroform-*d*

Peak 4

¹H NMR

Supplementary Figure 21. ^{13}C NMR data of compound 4 in methanol-d_4

Peak 4

^{13}C NMR

Supplementary Figure 22. ^{13}C NMR data of compound 4 in chloroform-*d*

Peak 4

^{13}C NMR

Supplementary Figure 23. HRESIMS (negative mode) data of compound 5

Spectrum from FP3_Negative.wiff (sample 1) - FP3_Negative, Experiment 2, -TOF MS^2 (30 - 1000) from 0.589 min
Precursor: 200.0 Da

Supplementary Figure 24. ^{13}C NMR data of compound 5 in methanol-*d4*
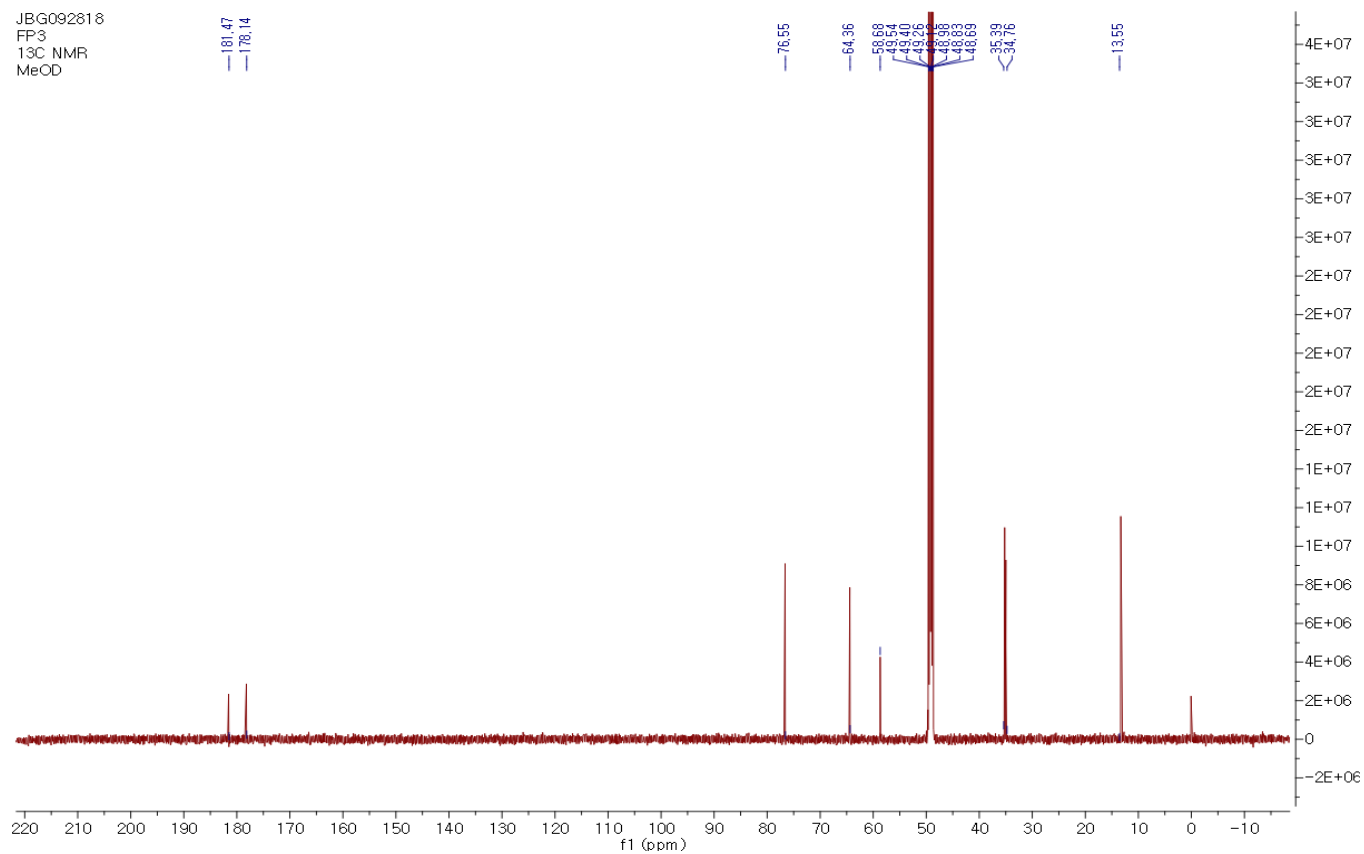
Supplementary Figure 25. ¹H NMR data of compound 5 in DMSO-*d6*
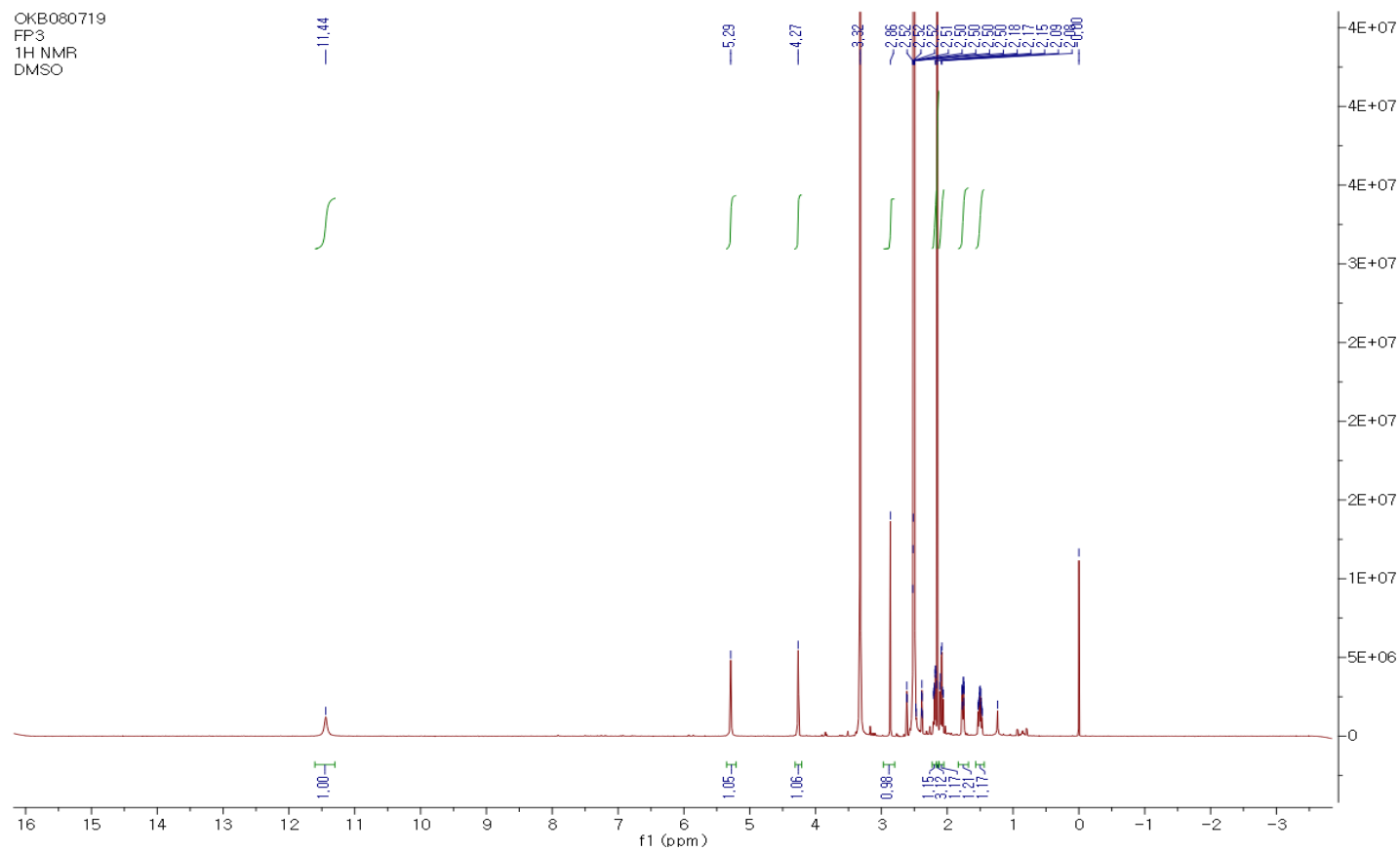
Supplementary Figure 26. HSQC NMR data of compound 5 in methanol-*d4*
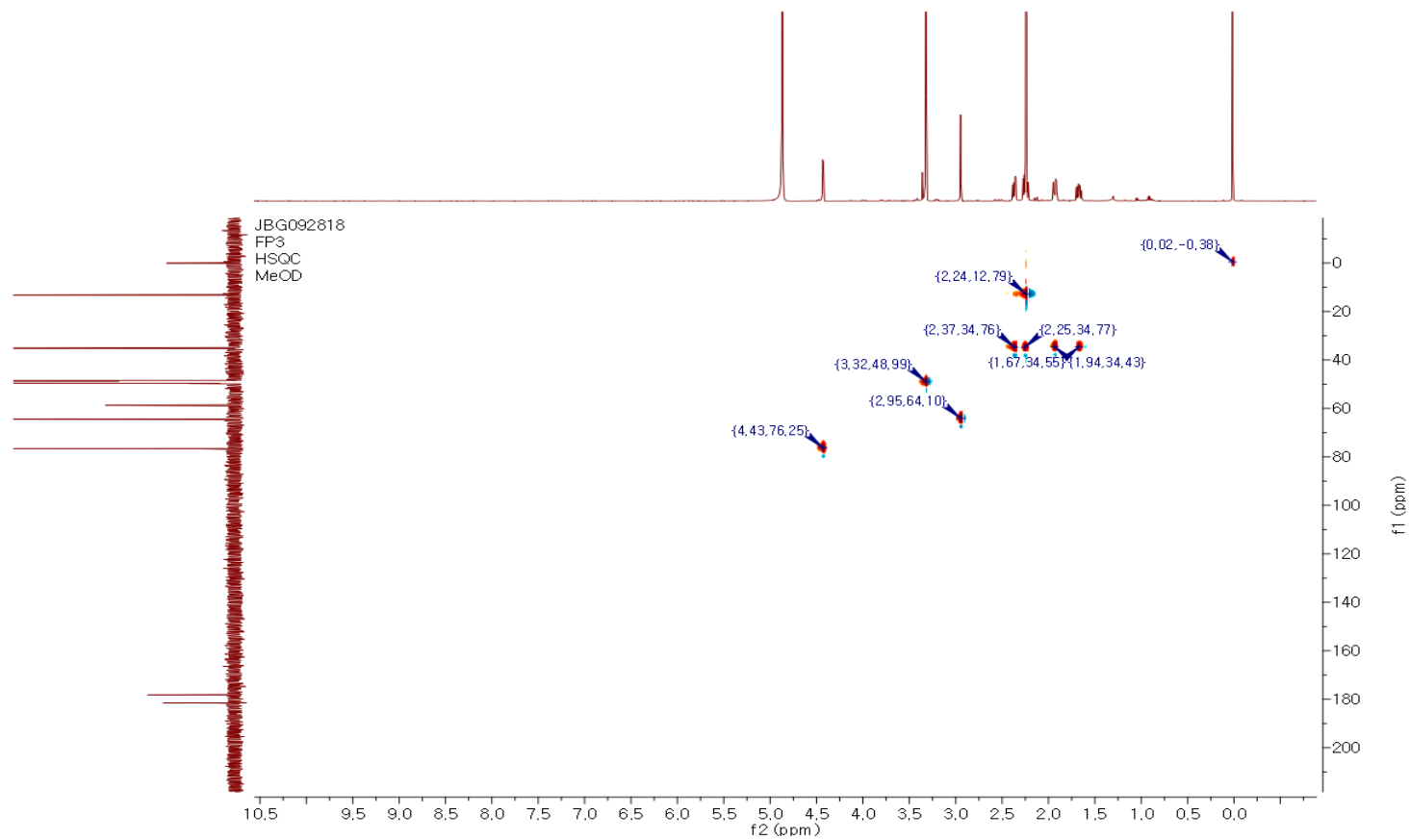
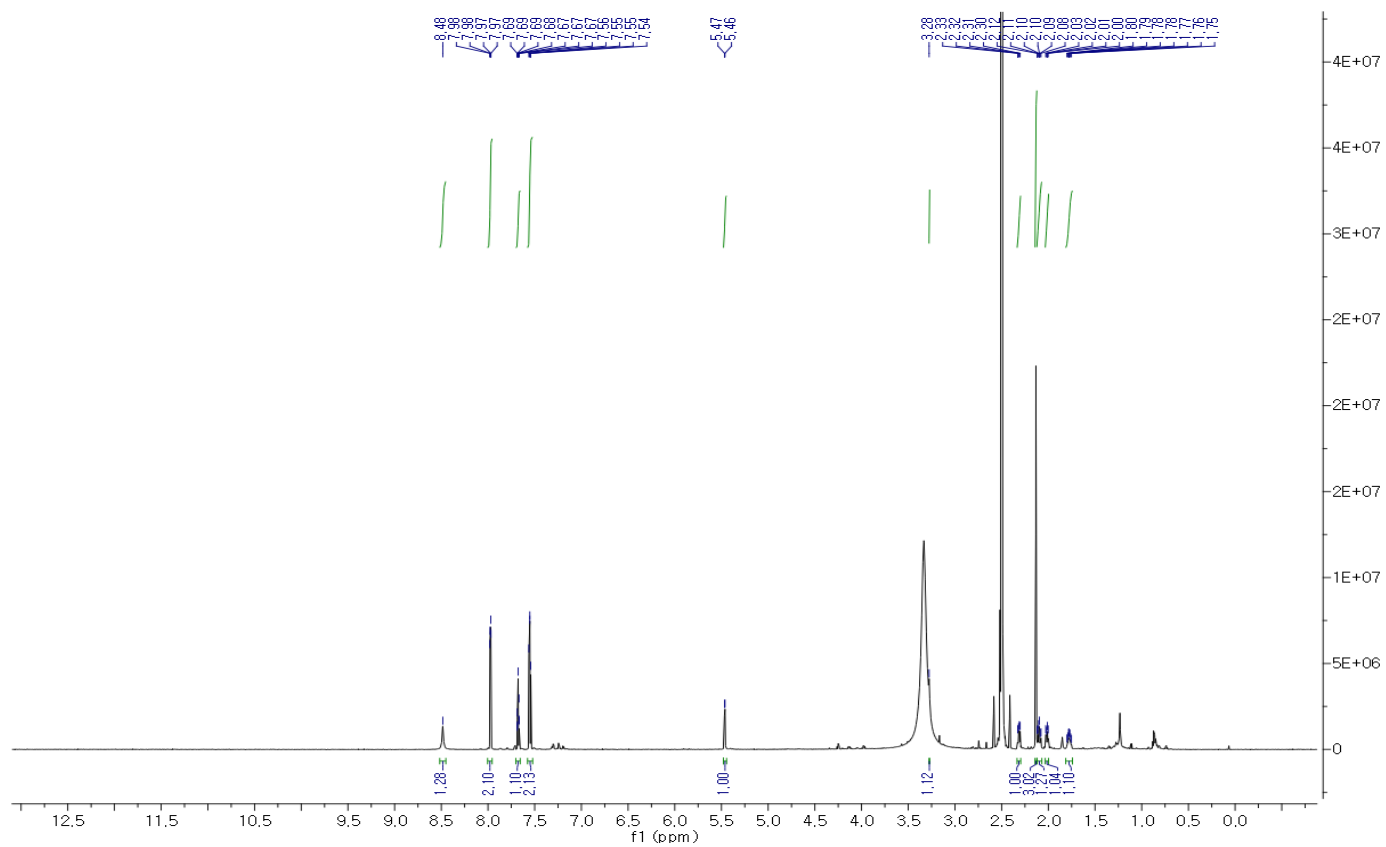**Supplementary Figure 27. COSY NMR data of compound 5 in methanol-*d4***

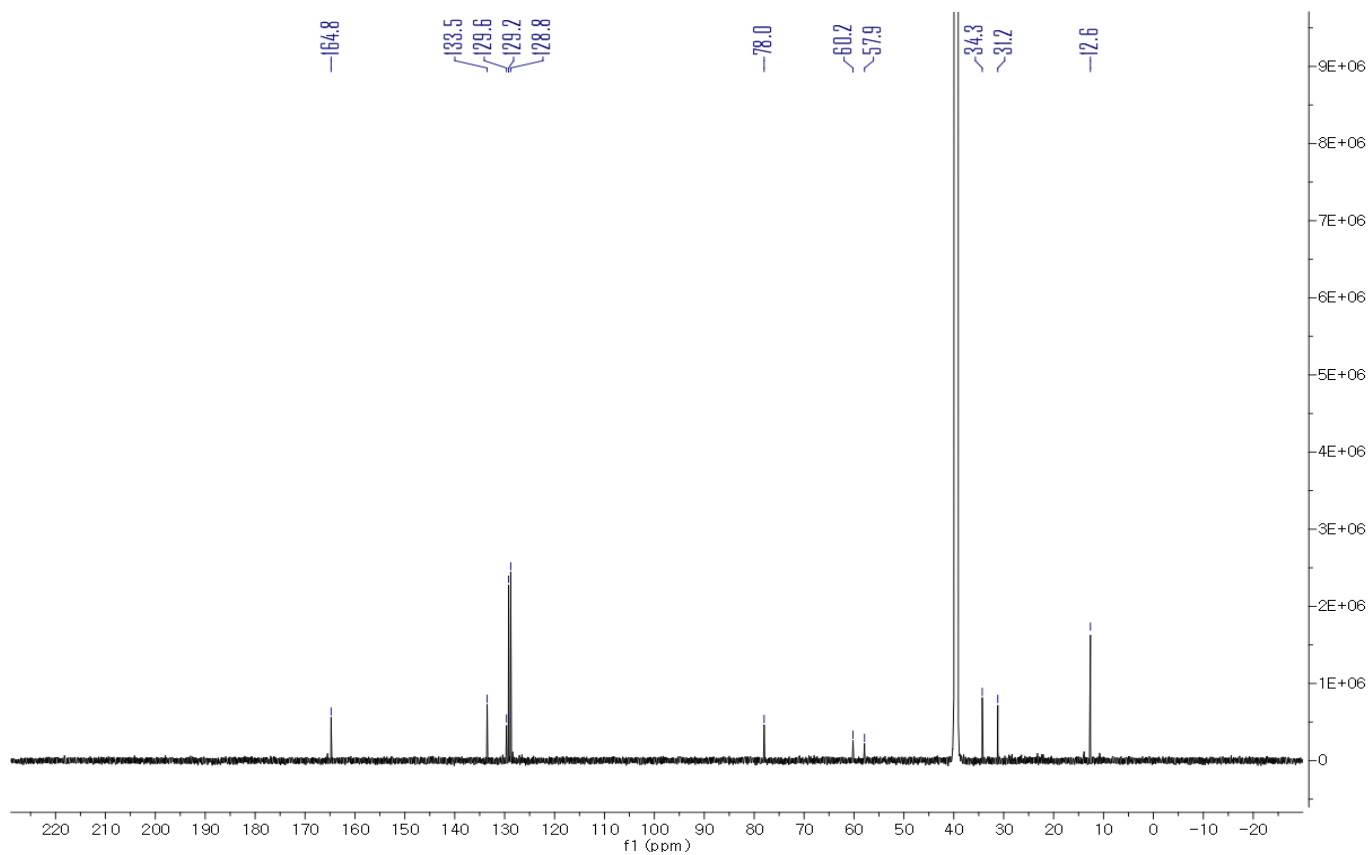**Supplementary Figure 28. HMBC NMR data of compound 5 in DMSO-*d6***

144

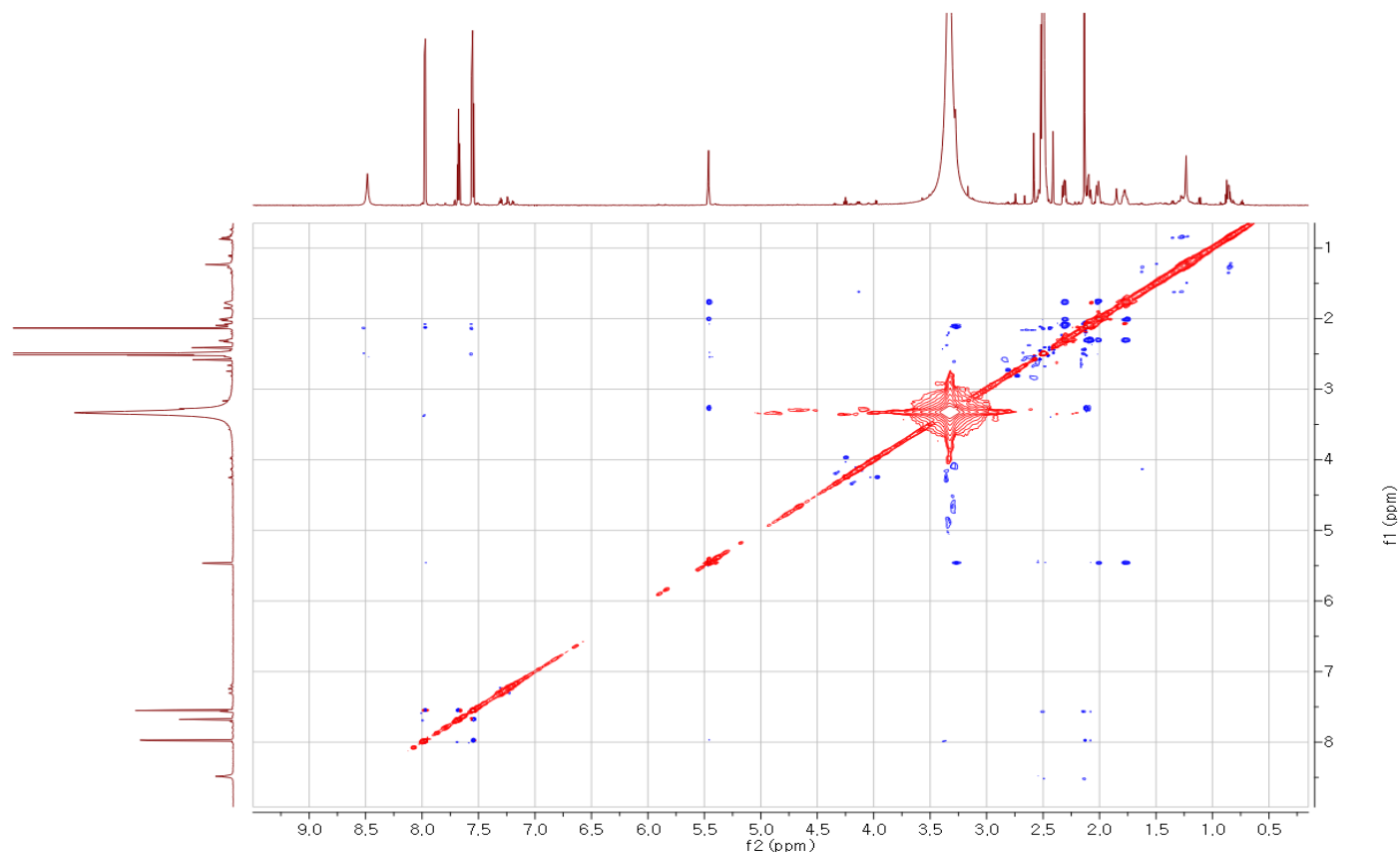**Supplementary Figure 29. NOESY NMR data compound 5 in DMSO-*d6***
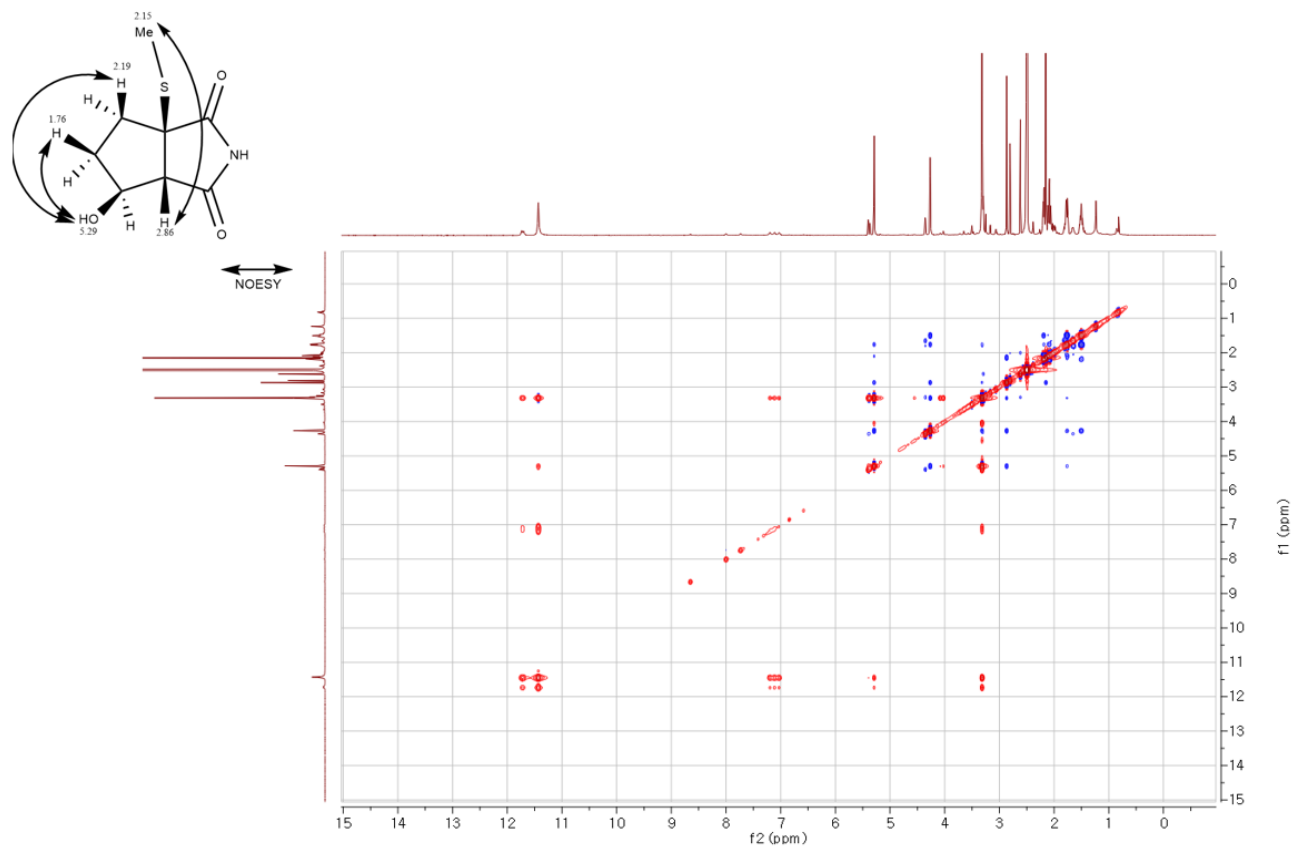
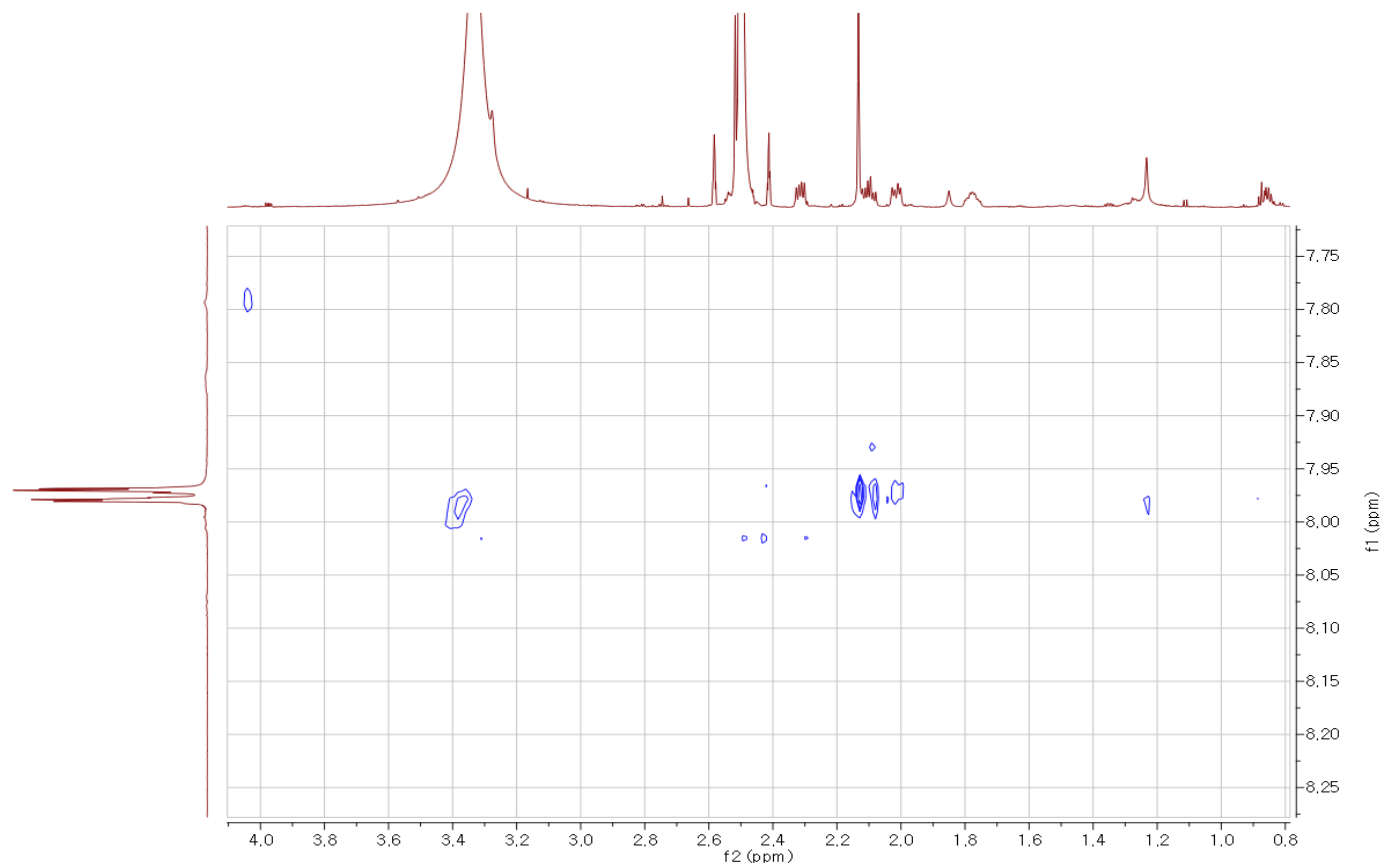**Supplementary Figure 30. ^{1}H NMR data of benzoyl derivative in DMSO-*d6***

Supplementary Figure 31. ¹³C NMR data of benzoyl derivative in DMSO-*d6*

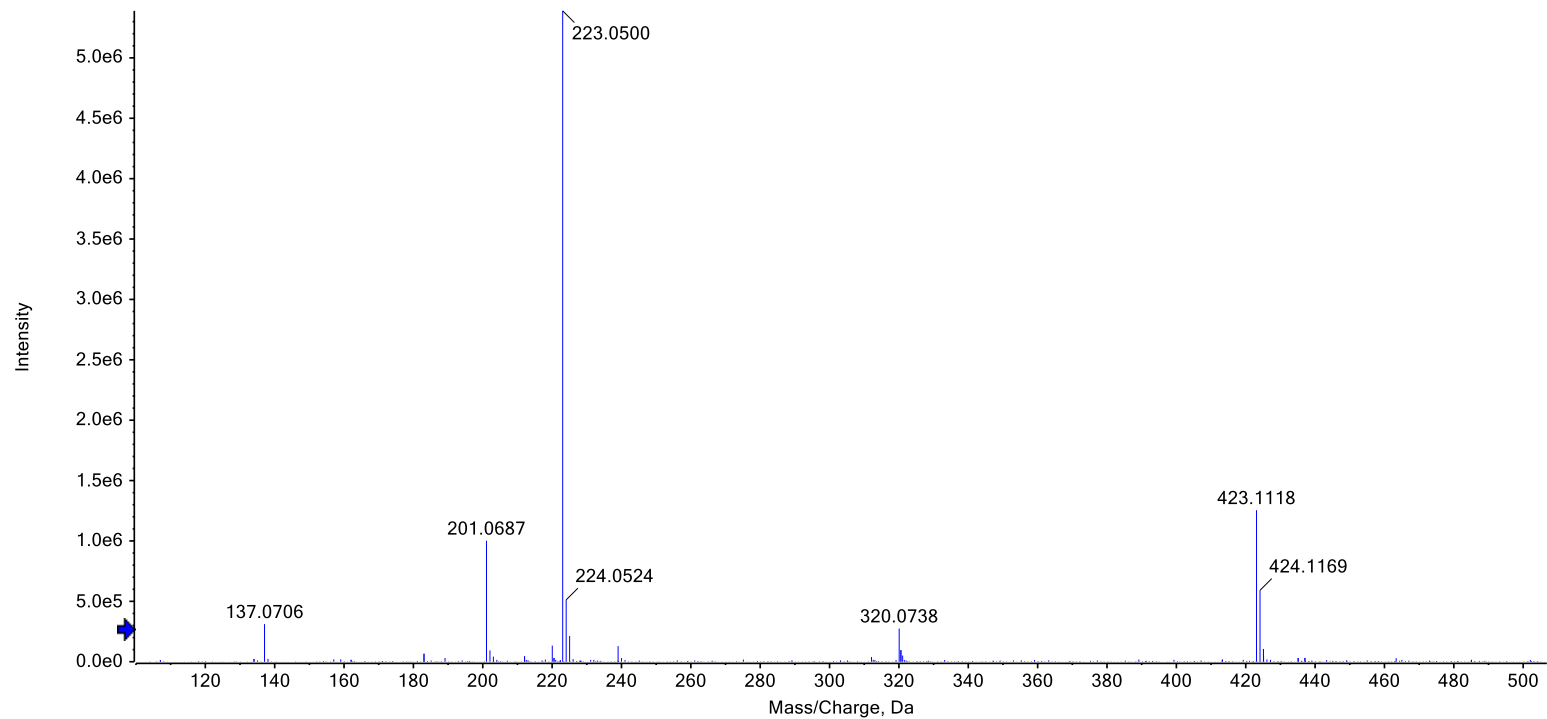**Supplementary Figure 32. NOESY correlations of benzoyl derivative in DMSO-*d6***

148

Supplementary Figure 33. Expanded NOESY correlations of benzoyl derivative in DMSO-*d6*
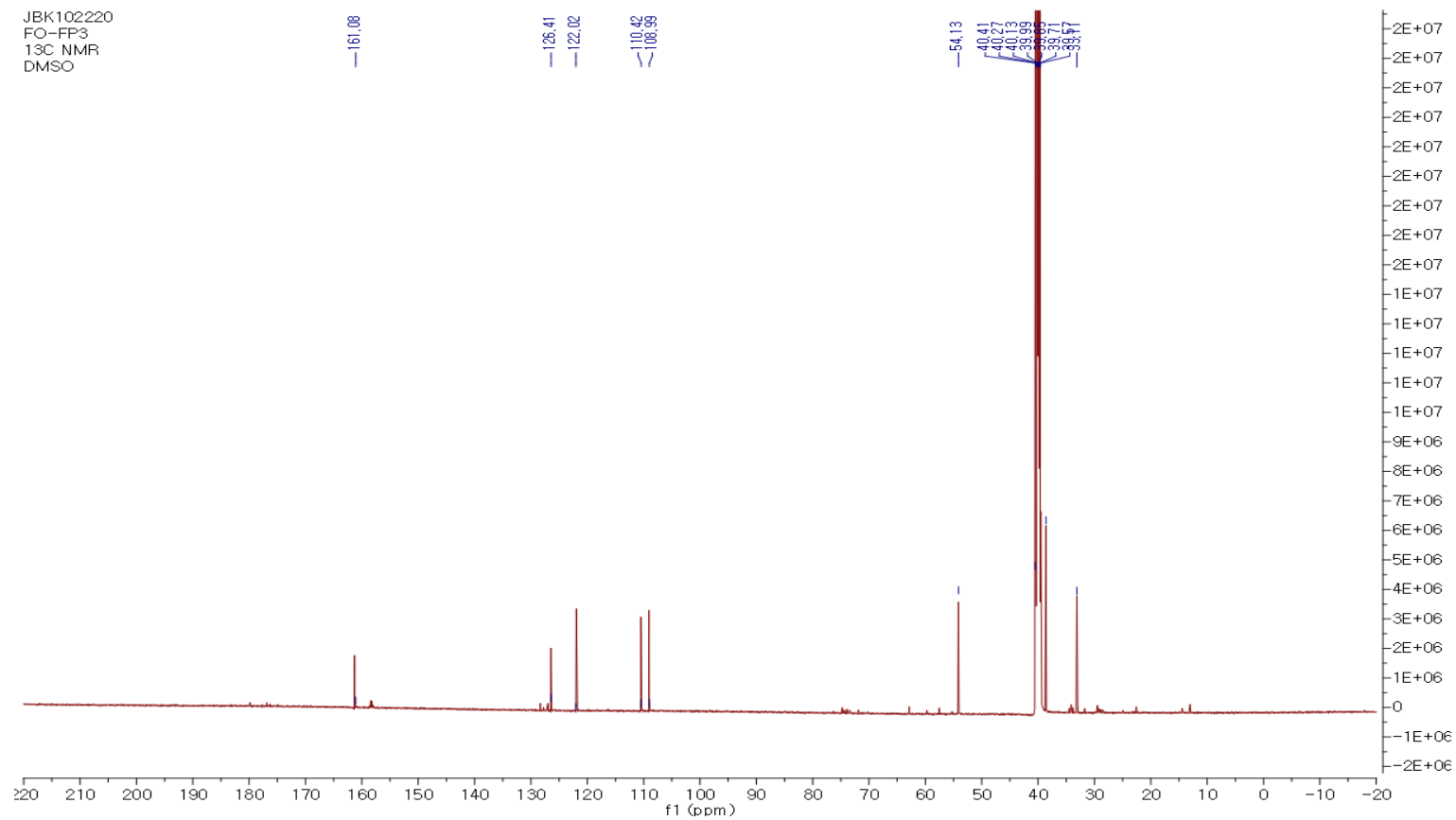
Supplementary Figure 34. HRESIMS (positive mode) data of compound 6

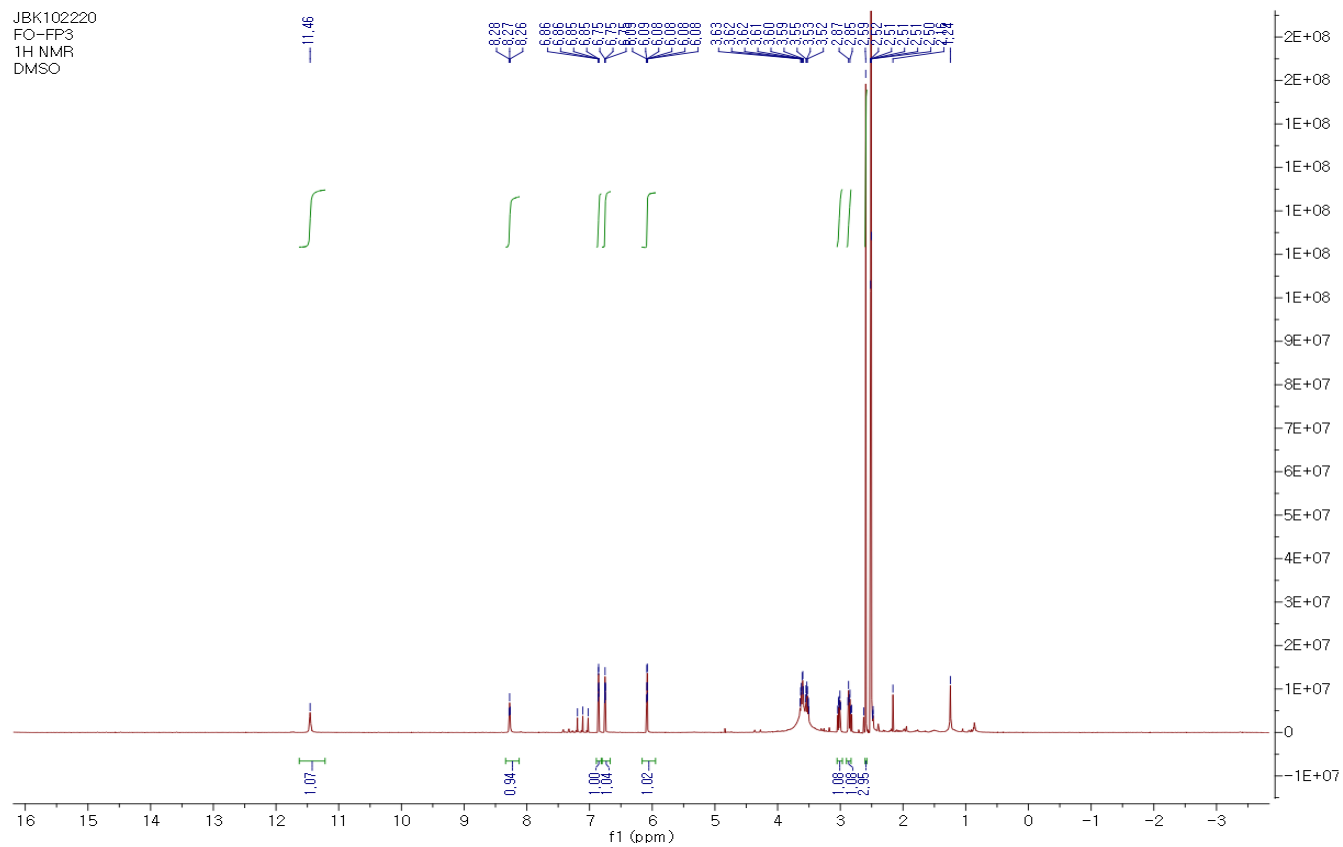Spectrum from FOFP3.wiff (sample 1) - FOFP3, Experiment 1, +TOF MS (100 - 2000) from 0.451 min

150

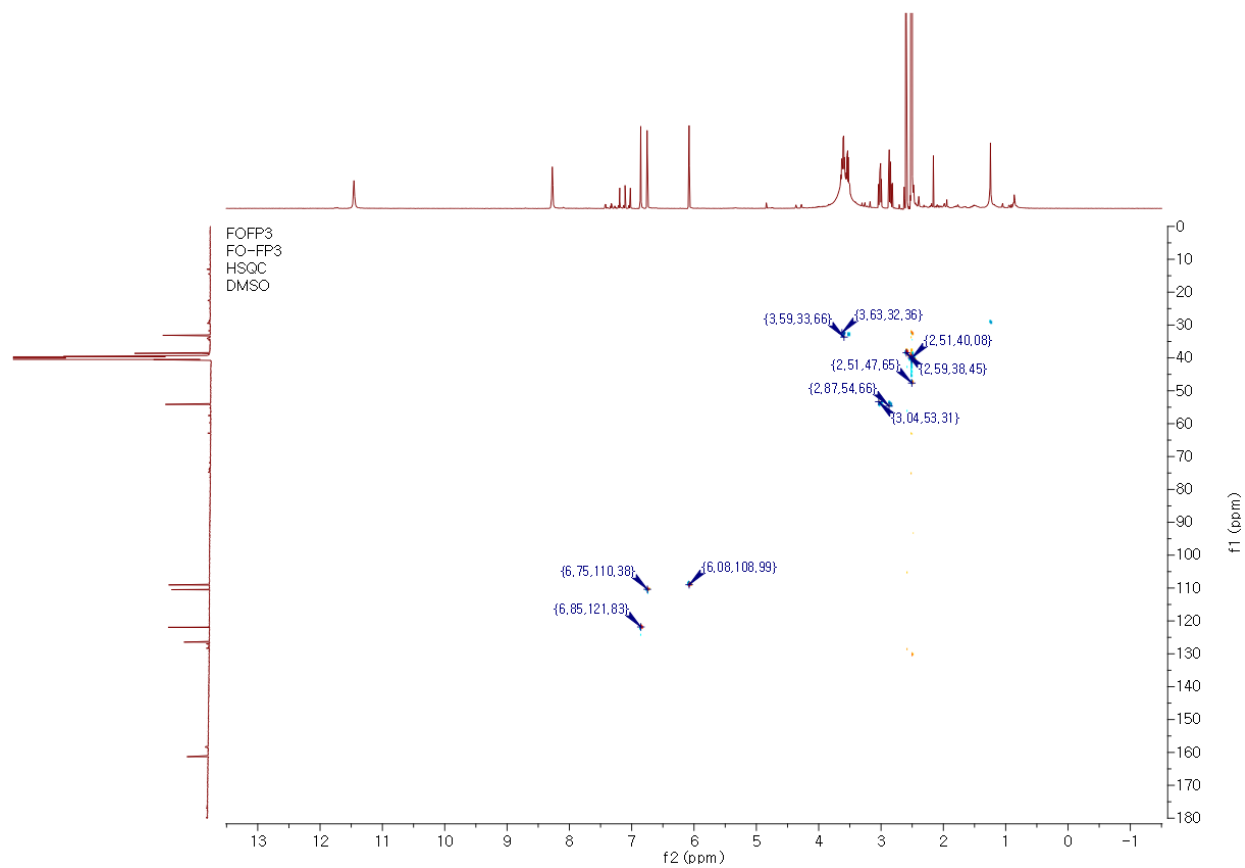**Supplementary Figure 35. ^{13}C NMR data of compound 6 in DMSO-*d6***

Supplementary Figure 36. ^{1}H NMR data of compound 6 in DMSO-*d6*

Supplementary Figure 37. HSQC NMR data of compound 6 in DMSO-*d6*

FOFP3
FO-FP3
HSQC
DMSO

{3,59,33,66} {3,63,32,36}
{2,51,40,08}
{2,51,47,65} {2,59,38,45}
{2,87,54,66}
{3,04,53,31}

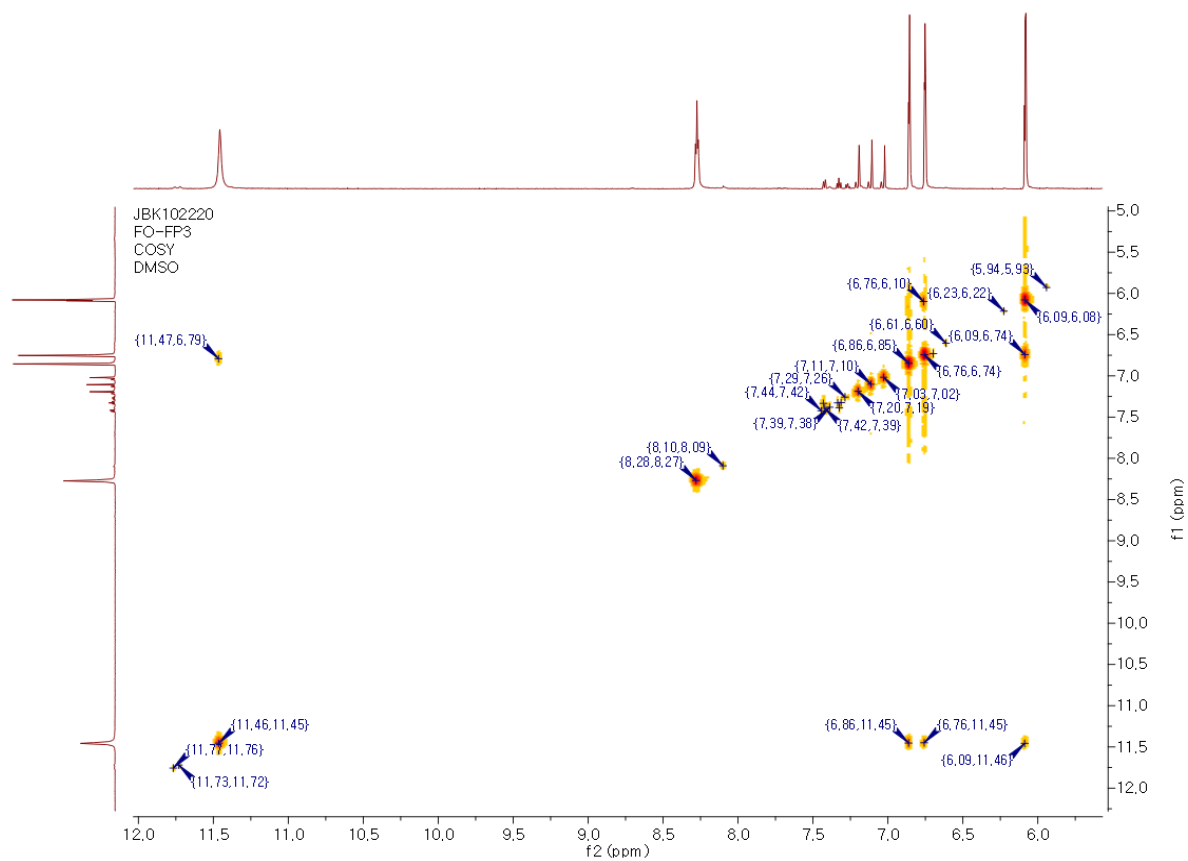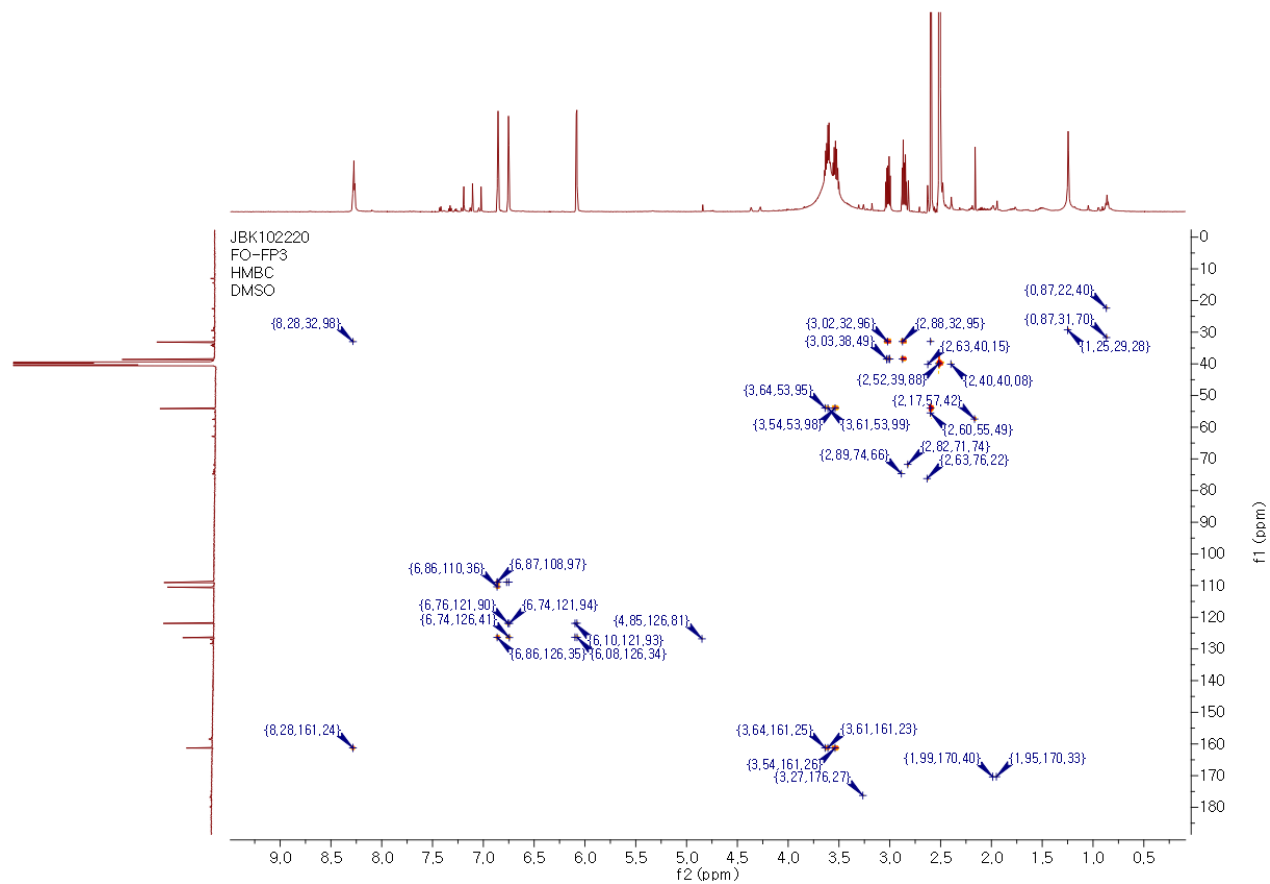{6,75,110,38} {6,08,108,99}
{6,85,121,83}

f1 (ppm)

f2 (ppm)

Supplementary Figure 38. COSY NMR data of compound 6 in DMSO-*d6*

154

Supplementary Figure 39. HMBC NMR data of compound 6 in DMSO-*d6*

155

Abstract in Korean

서울대학교 대학원

농생명공학부 응용생명화학전공

정범구

Actinobacteria 는 우수한 생리 활성을 가지는 2 차 대사물질을 생산하는 매력적인 미생물이다. 해양 환경은 낮은 산소농도, 적은 양의 빛 그리고 높은 압력 등과 같은 독특한 환경적 요소들을 가지고 있다. 이 때문에 해양 유래의 actinobacteria 는 새로운 구조와 작용 기전을 가지는 대사물질들의 생산 주체로서 주목받고 있다. 본 연구는 해양 방선균 유래 천연물의 생리활성을 평가하고 그에 대한 작용 기전을 탐색하는 내용을 담고 있다.

첫번째 파트는 분리된 4 개의 lactoquinomycin 계열 물질들의 항세균 효과를 탐색하고 그 작용 기전을 탐색하는 연구를 다루고 있다. Lactoquinomycin A (LQM-A, 물질 **1**)와 3 개의 유사체 (물질 **2-4**)는 그람 양성 세균에 대해서 우수한 저해능을 보이는 것으로 나타났다. 특히 LQM-A 는 대표적인 항생제 저항성 균주인 methicillin-resistant *Staphylococcus aureus* 에 대해서 뛰어난 활성을 보임과 동시에 저항성 균주를 유발하지 않는 것으로 확인되었다. 구조적 유사성을 기반으로 제작된 dual-reporter 실험을 통하여 LQM-A 는 번역을 저해하기 보다는 DNA 에 손상을 주는 기전을 갖는 것으로 확인되었다. 이는 ethidium bromide displacement 실험을 통하여 LQM-A 가 DNA 이중가닥에 끼임으로서 DNA 손상이 유발하는 것으로 나타났다. 또한 LQM-A 는 DNA 에 끼어들면서 황색 포도상 구균의 필수 유전자인 *grlA* 와 *grlB* 의

발현을 상당히 억제하는 함으로써 항세균 효과를 갖는 것으로 확인되었다.

두번째 파트는 *Candida albicans* 가 숙주에 감염 시 또는 병원성을 띄는데 있어 필수 효소인 isocitrate lyase (ICL)에 저해 활성을 갖는 물질을 규명하고 저해 활성을 확인하는 연구를 담고 있다. 분광학적 정보를 토대로 분리된 두 물질에 대한 구조를 동정하였고 bacillimide (물질 **5**)와 bacillapyrrole (물질 **6**)로 명명하였다. 신규 물질인 bacillimide 의 절대 구조 (3R, 6S, 7S)는 NOESY 와 ECD 분석을 이용하여 결정하였다. 두 물질은 모두 ICL 효소에 대해서 저해능을 보이는 것으로 확인되었다. 그 중 bacillimide 는 ICL 저해제로 알려진 3-nitropropionate 에 비해서 활성은 낮지만 매우 뛰어난 활성을 보였으며 Dixon plot 을 이용하여 저해 방식을 살펴본 결과 혼합형의 형태를 보이는 것으로 나타났다 (IC$_{50}$ = 44.24 μM). ICL 발현을 담당하는 유전자(*icl*)가 삭제된 또는 보완된 돌연변이를 이용한 생장 실험을 통하여 bacillimide 는 ICL 을 저해함으로써 탄소 2 개로 이루어진 영양소의 섭취를 어렵게 하는 것으로 나타났다. 이는 *icl* 의 전사를 억제함으로써 이루어진다는 것을 역전사 중합효소반응을 통해 입증하였다.

주요어: 해양 유래 방선균, 2 차 대사물질, 메티실린 저항성 황색 포도상구균, 락토퀴노마이신, 알칼로이드, 아이소시트르산 분해효소

학번: 2014-21903

Acknowledgement

박사 학위를 받는데 짧지 않은 시간이 걸렸습니다. 대학교에 처음 입학했을 때가 생각납니다. '너는 졸업하고 무엇을 할 생각이니?' 라는 질문에 저는 대학원에 가고 싶다는 말을 입에 달고 살았던 것 같습니다. 어떤 구체적인 계획이 있었다기 보다는 과학자가 되고 싶었던 어렸을 때의 꿈이 첫번째 이유였고 전문대학원에 진학하는 친구들에게 우리 과 대학원도 충분히 메리트가 있다는 걸 보여주고 싶었던 게 두번째 이유였던 것 같습니다. 돌이켜 보았을 때 대단한 성과를 낸 것도 아니고 아쉬웠던 점들도 많았지만 후회없이 학위과정을 수행한 것 같아서 뿌듯한 마음이 듭니다. 동시에 제가 박사 학위를 취득하는데 있어 도움을 주신 분들에게 고마움을 전하려고 합니다.

먼저 지도 교수님인 오기봉 교수님께 감사의 말씀을 전합니다. 교수님에게 혼이 나서 서운했던 적도, 교수님과 실험과 관련된 디스커션 과정에서 언쟁을 벌였던 적도 있지만 항상 인생 선배로서 지도해주신 점 너무 감사하게 생각하고 있습니다. 학위 기간 동안 교수님께 배웠던 것들과 교수님과 함께 했던 추억 모두 오래도록 가지고 가도록 하겠습니다. 건강 하세요! 그리고 미생물 생물공학실에서 함께 생활했던 선후배들, 완기형, 우영누나, 소형누나, 찬홍이형, 하영누나, 수현이, 재호, 새연이, 정윤이 특히 불성실하게 졸업 실험에 임했던 저에게 화 한번 내지 않고 하나하나 꼼꼼하게 가르쳐 주신 사수였던 희규형과 1 년 후배지만 옆자리에서 배울 점이 참 많다고 느꼈고 학위 기간 내내 의지가 되어줬던 은지에게 고맙다는 말을 전합니다.

저희 연구실과 공동연구를 하며 천연물 구조 동정에 있어 도움을 주신 약학대학 신종헌 교수님과 연구실 분들에게도 감사의 인사를 전합니다. 교수님의 구조 동정 강의를 들으면서 학문에 대한 열정과

박학다식함을 느낄 수 있었던 것 같습니다. 더불어 제 물질의 구조 분석에 도움을 주신 김창권, 박성철, 권오석 박사님도 고생하셨습니다. 감사합니다. 제가 연구를 함에 있어 가장 중요한 균주 제공에 도움을 주시고 학위 발표에 심사위원으로 참석해주신 KIOST 이희승 박사님께도 감사의 인사를 전합니다.

학부 생활을 포함하여 11 년이 넘는 시간 동안 저를 지도해 주신 응용생명화학 전공 교수님들께도 감사의 인사를 드립니다. 학부 시절 참 공부도 안하고 수업시간에 잠만 자던 그런 학생이었는데, 포기하지 않고 끌고 와주셔서 지금 이 자리에 제가 있을 수 있지 않나 생각합니다. 작고하신 김수언 교수님을 비롯하여 생각하며 연구를 해야한다는 깨달음을 주신 최양도 교수님, 수업에서 늘 좋은 얘기를 많이 해주셨던 노희명 교수님, 동아리 지도교수님으로 복도에서 만날 때마다 허심탄회하게 많은 얘기를 나눴던 이상기 교수님, 항상 반갑게 먼저 인사해 주시는 김민균 교수님, 속은 누구보다 따뜻하신 배의영 교수님, 학문에 대한 열정을 느낄 수 있었던 신찬석 교수님 그리고 새로 부임하신 권용훈, 송영훈 교수님 감사합니다. 특히 농업생명과학대학 홍보대사단 칼시안을 하면서 가깝게 지냈고 다른 실험실 학생임에도 실험에 필요한 기계들을 언제든 사용할 수 있게 허락해주신 김정한 교수님께 특별히 감사하다는 말씀을 전합니다. 또한 학위과정을 하면서 힘든 일이 있을 때마다 든든한 버팀목이 되어주었던 7 층의 다른 연구실 분들에게도 고마운 마음을 전합니다. 특히 동기의 소중함을 알게 해줬던 용호형, 윤미누나 그리고 은지에게 고맙습니다. 언제가는 다시 뭉칠 날이 있으면 참 좋을 것 같아요! 힘든 일이 있을 때 언제든 커피 한잔, 술 한잔 기울이며 얘기를 들어준 지호형, 아름누나, 민우, 유진이, 서현이에게도 감사하다는 말을 이 자리를 빌어 전합니다. 그리고 이번에 같이 박사 졸업 준비를 하면서 실험을 비롯한 여러 측면에서 많은 도움을 준 은영이와 상훈이형에게도 고마움을 전합니다. 마지막으로

과사에 찾아가면 항상 밝게 맞이해 주신 전공 조교님들, 수정누나, 소영누나 그리고 긴 학위 기간을 함께 해서 정말 고마웠던 정민누나에게도 감사의 말씀을 드립니다.

결코 짧지 않는 기간을 묵묵히 기다려준 저희 가족들에게도 고맙습니다. 제가 제일로 존경하는 저희 아버지, 하고 싶은 일 계속 하시면서 사셨으면 좋겠고 아들로서 더 잘하도록 하겠습니다. 건강하세요! 미워할 수 없는 엄마, 학위 기간 동안 참 많은 일이 있었지만 그런 일들을 통해서 많이 성장하고 배웠던 것 같아요. 아프지 마시고 오래오래 함께 해요. 사랑합니다. 마지막으로 동생 경환이, 어렸을 때는 참 많이 싸우고 그랬던 것 같은데 이제 와서는 너만큼 의지 되는 사람이 없는 것 같아 고맙다. 새로 분사한 회사에서도 하고 싶은 일 하면서 건강하게 지냈으면 좋겠다! 모두 감사하고 사랑합니다.